JAIST Repository
https://dspace.jaist.ac.jp/

Title	固相抽出法を集積化した高感度液体電極プラズマ発光分析法の開発
Author(s)	Do, Van Khoai
Citation	
Issue Date	2015-09
Type	Thesis or Dissertation
Text version	ETD
URL	http://hdl.handle.net/10119/12970
Rights	
Description	Supervisor:高村　禅，マテリアルサイエンス研究科，博士

JAIST
JAPAN
ADVANCED INSTITUTE OF
SCIENCE AND TECHNOLOGY

Japan Advanced Institute of Science and Technology

Development of highly sensitive liquid electrode plasma optical emission spectrometry with integrated solid phase extraction

DO VAN KHOAI

Japan Advanced Institute of Science and Technology

Doctoral Dissertation

Development of highly sensitive liquid electrode plasma optical emission spectrometry with integrated solid phase extraction

DO VAN KHOAI

Supervisor: Professor Dr. Yuzuru Takamura

School of Materials Science

Japan Advanced Institute of Science and Technology

September, 2015

Referee in Chief:	**Prof. Yuzuru Takamura**
	Japan Advanced Institute of Science and Technology
Referees	**Prof. Goro Mizutani**
	Japan Advanced Institute of Science and Technology
	Prof. Masahiko Tomitori
	Japan Advanced Institute of Science and Technology
	Prof. Yuichi Hiratsuka
	Japan Advanced Institute of Science and Technology
	Prof. Akitoshi Okino
	Tokyo Institute of Technology

Abstract

Liquid electrode plasma optical emission spectrometry (LEP OES) is a novel analytical method employing the micro-discharge plasma generated in a liquid channel as an excitation source. LEP OES has advantages, for instance, no nebulizer required, battery-operated device, compactness and portability. However, LEP OES is not sufficiently sensitive to detect directly metal in low-concentration samples (ex. tap water and drinking water). Solid phase extraction (SPE) is a preconcentration method, which is used to increase analyte concentration prior to the detection. The analyte is firstly retained on a solid phase, and then is extracted to a mobile eluent in more concentrated form for quantitative determination. In the study, to improve sensitivity, LEP OES is combined with SPE. Accordingly, a SPE column is integrated on a LEP chip. The LEP is generated using direct current (DC) and alternating current (AC), which are named as DC LEP and AC LEP, respectively. Chip designs, performance protocols, data acquisition and data processing were proposed based on the investigated properties of each type of plasma sources. Lead was chosen as analyte of interest.

The chip for SPE-LEP combination containing a SPE column and a LEP channel was made by polydimethylsiloxane (PDMS) utilizing basic photolithography. The SPE resin was manually stuffed into the column using a syringe. Preconcentration was carried out with optimized parameters (sample volume and sample flow-rate). Then the eluent (ethylenediaminetetraacetate - EDTA 0.03 M) was applied through the resin to extract the ions of interest and transport them to LEP detection.

For SPE – DC LEP combination, a flow control technique with a pneumatic micropump was developed for fluid actuation. The design and fabrication of the pump were modified to be suitable with the integration. The pump is capable of providing an equalized volume of eluent for each LEP measurement cycle. Discharge volume of the pump is 90 nL with a relative error of 2%. Each small divided eluent requires a plasma generation and gives an emission spectrum. The emission intensities were fitted with exponential modified Gaussian (EMG) model. The fit curves are elution curves. The areas of the fit curves are proportional to the analyte amount that presents in the sample, thus they were used for quantitative determination of analyte (lead). With the proposed method, limit of detection (LOD) for lead was achieved as 0.4 µg/L (part per billion – ppb), 50 times improved compared to conventional LEP using quart chip. Sample volume used was 1 mL, and eluent volume was as small as 20 µL. The elution time was 40 minutes. The precision was improved compared to the method using syringe pump.

AC LEP has been developed for the first time in our study. Unlike DC LEP, AC LEP is capable of generating gently in the LEP channel at low flow-rate. Thus SPE – AC LEP were performed continuously. A buffer, the mixture of 0.1 M nitric acid and 5% v/v formic acid, was capable of maintaining the plasma for long time. During plasma generation, the eluent was introduced into the plasma by a syringe pump. The emission signals were obtained continuously, and then were fitted with EMG model. Similarly, the EMG fit curves were used to determine lead in the samples. LOD was obtained to be 0.5 µg/L (ppb) similarly with SPE – DC LEP. Sample volume used was 2 mL, and eluent volume was as small as 20 µL. The elution time was 8 minutes.

In conclusion, the integration of SPE into liquid electrode plasma for highly sensitive detection of lead has been successfully developed. Two types of LEP (DC LEP and AC LEP) were characterized. From the investigated characteristics, suitable chip layouts, fluid actuation techniques and data acquisition for the best combination LEP and SPE have been proposed. Generally, the sensitivity was improved about 50 times. SPE – DC LEP may offer a precise and sensitive method, while SPE – AC LEP offers a more simple and rapid method.

Keywords: Liquid electrode plasma, Solid phase extraction, Elemental analysis.

Acknowledgement

First of all I would like to express the deepest sense of gratitude to my main supervisor, *Professor Yuzuru Takamura*, for his kind support, enlightening suggestions and effective discussion throughout my Ph.D course. I would like to thank *Professor Yoshiaki Ukita* and *Professor Phan Trong Tue* who are always willing to help and discuss about my research. My sincere thankfulness is extended to *Dr. Tamotsu Yamamoto*, CEO of Micro Emission Ltd., *Mr. Syuji Tatsumi*, and other members of Micro Emission Ltd. for their kind help and instrumentation.

I would like to thank the thesis examination committee, *Professor Goro Mizutani*, *Professor Tatsuo Kaneko*, *Professor Yuichi Hiratsuka*, *Professor Masahiko Tomitori* and *Professor Akitoshi Okino* for their helpful comments and valuable suggestions.

I would like to thank my second supervisor, *Professor Masahiro Takagi*, and my advisor for minor research, *Professor Takahiro Hohsaka* for the time they spent for me.

I also take this chance to express my sincere gratitude to *Japan Advanced Institute of Science and Technology* for generous financial support that enabled me to pursue the Ph.D program to a successful end.

I would like to thank all of my friends and all members of Takamura Laboratory at School of Materials Science (JAIST) for their kind help, their smiles and understanding.

And last but not the least; I am particularly grateful to my parents, my wife *Nguyen Thi Duyen An* and my son *Do Khang*, who are always behind and encourage me unconditionally. I would like to dedicate the dissertation to them.

Japan, Autumn 2015.

Do Van Khoai

Contents

Chapter 1
General Introduction

1.1. Introduction to plasma and liquid micro-plasma sources for elemental analysis

1.1.1. Plasma

Plasma in nature is one of the four fundamental states of matter, the others being solid, liquid, and gas. Basically, plasma is a partially ionized gas consisting of equal numbers of positive and negative charges, and a different number of un-ionized neutral molecules [1,2]. The term “plasma” was first introduced by Langmuir in 1928 to describe a state which contains balanced charges of ions and electrons which make it electro-conductive.

Plasmas occur in the nature but also can be artificially created by lab-instruments and in industry. It has been exploited for numerous applications, including thermonuclear synthesis, electronics, lasers, fluorescent lamps, and many others.

Plasma offers **three major features** essential for applications in chemistry and related fields [1]:

1. Temperatures of at least some plasma components and energy density can significantly exceed those in conventional chemical technologies,
2. Plasma is able to contain very high concentrations of energetic and chemically active species (e.g., electrons, ions, atoms and radicals, excited states, and photons),

3. Plasma can exist at non-thermal equilibrium which has heavy particles (ions, radicals, neutrals, etc.) at much lower temperature than electrons. Some non-thermal plasmas have bulk temperature as low as the room temperature.

Various plasma sources including natural and artificial occur over a wide range of pressures, electron temperatures, and electron densities as shown Fig 1.1, which is reported by Frigman [1].

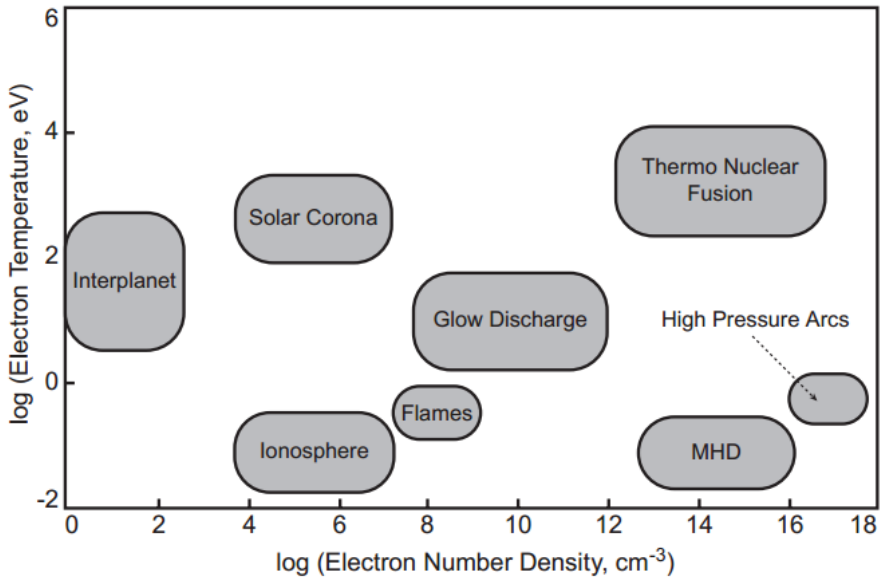

Figure 1.1 Plasma temperatures and densities [Extracted from Ref.1].

1.1.2. Liquid discharge micro-plasmas for elemental analysis

For elemental analysis in laboratory, plasma is often generated through electrical discharges, including glow discharges, arc discharges, radiofrequency and microwave discharges, non-thermal atmospheric pressure discharges, and other types of micro-discharges [1]. In the elemental analysis field, the well-known powerful laboratory methods are inductively coupled plasma optical emission

spectrometry (ICP OES), atomic absorption spectrometry (AAS), and inductively coupled plasma mass spectrometry (ICP MS). However these methods requires a high power supplier and supporting equipment (especially a nebulizer), which make the methods not feasible for on-site analysis. In addition, their operation and maintenance costs are relatively high, which is not economic for continuous monitoring. Thus, the need of miniaturized plasma sources, which are more versatile in generation, require less power, and are capable of onsite performance, is raised. For this purpose, liquid discharge micro-plasma might be a good candidate.

This thesis has mainly discussed on plasma that is generated by the electrical liquid discharge and utilized as an excitation source for optical detection of metal ions. The plasmas are generated in a gap between a liquid sample and an electrode or in between two liquid electrodes by an application of a high voltage at the atmospheric pressure. With the discharge plasmas, the atomic lines of metallic ions in the sample solution are obtained in the emission spectrum. Thus, the metallic ions in the solution can be qualitatively and quantitatively determined. Fig. 1.2 shows the principle of emission spectrum appearance. A nucleus is surrounded by electron orbitals with different energy levels. At unexcited state or initial state, electrons are at initial basic level. Once an atom is excited by photons or external electrons through applied energy, electrons are moved to the higher energy-level. If the excited electrons return to the initial state (relaxation), photons with characteristic wavelengths are released. The intensity of emission light is proportional to the number of the excited atoms, thus is proportional to concentration of the analyzed element. The principle of optical emission

spectrometry has been widely applied for qualitative determination (through characteristic wavelengths) and quantitative determination (through intensity of emission lights).

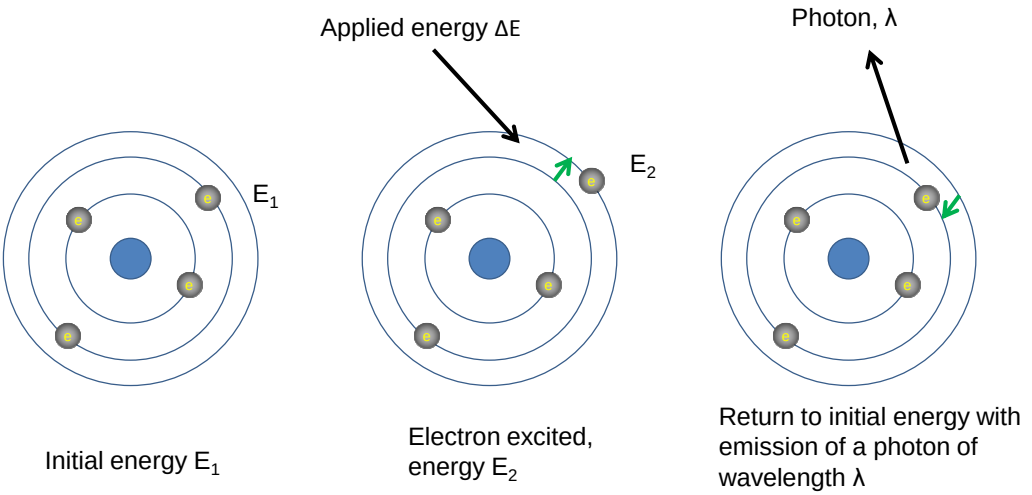

Figure 1.2 Mechanism of photon generation of specific wavelength in optical emission spectrometry.

Several reviews have also summarized the design of different discharge configurations with fundamental processes and characteristics, which can be found in ref. [3-7]. In following part, some typical liquid electrode discharge sources are summarized. They are divided based on types of electrical sources that is used for discharge generation: direct current (DC) and alternating current (AC) driven liquid electrode discharges.

1.1.2.1. Electrolyte as cathode atmospheric glow discharge (ELCAD)

The ELCAD invented more than 20 years ago is an excitation source for optical detection toxic heavy metals in liquid samples [8]. Cserfalvi investigated

that the glow discharge could be produced between liquid sample surfaces in ambient air and a metal cathode surfaces; thus, the plasma spectrum contained the atomic lines of the metals dissolved in the sample [9]. Then his group investigated a unique analytical source for the direct analysis of many metals in aqueous solutions in the 1–50 mg/L concentration range without sample preparation [5]. Recently, Gyorgy has applied ELCAD to AAS with the arrangement as described in Fig. 1.3, and its side view was presented as in Fig. 1.4. The work may improve the strength of ELCAD. In addition, table 1.1 reported limits of detection (LODs) of elements (calculated by 3SD of intensities of the blank sample) obtained with different electrolyte cathode discharge (ELCAD) systems (presented in mg/L - ppm) [10].

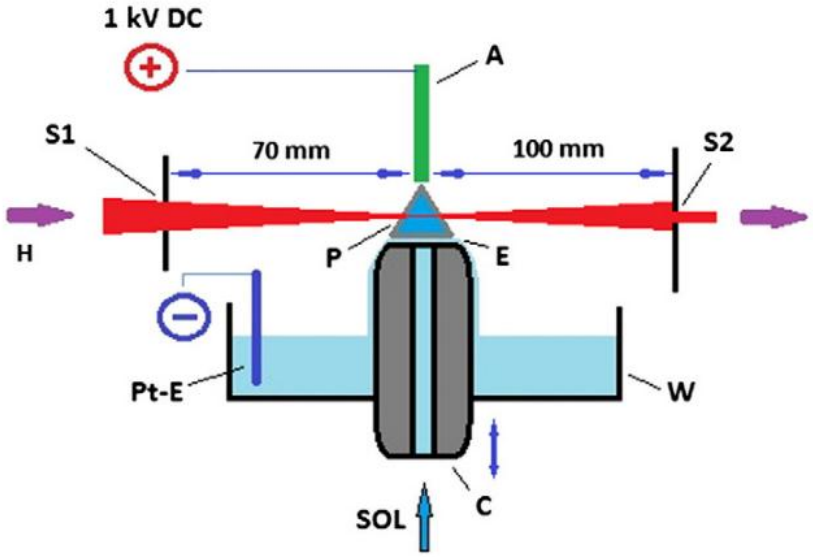

Figure 1.3 Schematic representation of the ELCAD-AAS experimental arrangement; A – W-rod anode, C – capillary with adjustable height, E – electrolyte cathode (surface), H – monochromatic, chopped beam from the HCL of the AA spectrometer, P – plasma, Pt-E – Pt-contact electrode, S1 – exit slit of the AA spectrometer, S2 – diaphragm (d = 0.5 mm) fixed in front of the entrance slit of the detector of AA spectrometer, SOL – sample/plasma (blank) solution from pump, W – waste (solution) reservoir [introduced by Gyorgy et al. ref. 10].

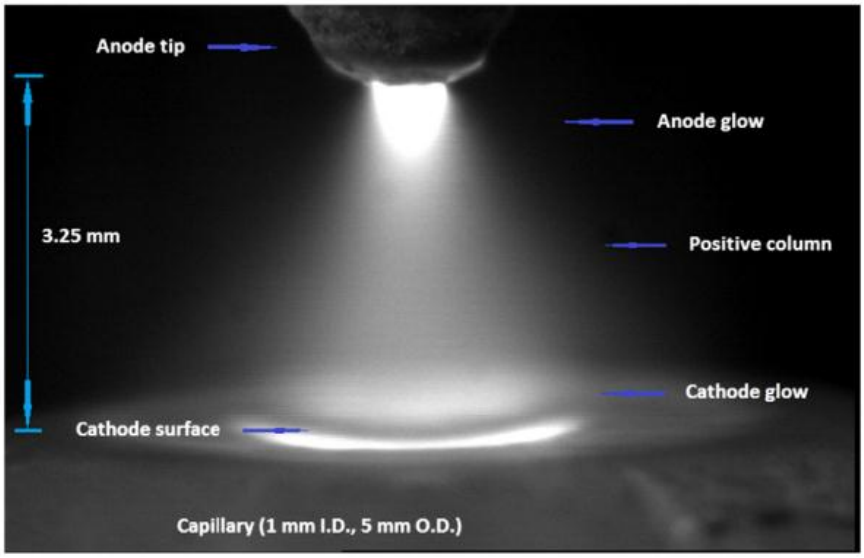

Figure 1.4 Side view of the ELCAD [observed by Gyorgy et al. ref.67]

Shekhar developed an ELCAD system with a new configuration. Plasma fluctuations owing to the variations in the gap between solid anode and liquid cathode were effectively eliminated by a V-groove to the glass capillary. The modified configuration enabled a stable plasma even at low flow-rates (0.96 mL min^{-1}). The LODs of Ca, Cu, Cd, Pb, Hg, Fe, and Zn were found to be 17, 11, 5, 45, 15, 28, and 3 ng/mL (ppb), respectively [11]. Recently, Shekhar improved the sensitivity of this modified ELCAD-AES system by the addition of a few percent of acetic acid for mercury determination. The addition enabled a significant enhancement in emission signal of mercury. As a result, LOD for inorganic mercury was about 8 times improved, to be 2 ng/mL (ppb) [12]. Other ELCAD systems with different designs can be found in the following references [13-26].

Table 1.1 Limits of detection (LODs) of various metal elements (3SD of intensities of the blanks) obtained by (ELCAD) systems with different configurations (presented in mg/L-ppm) (Ref. number in the table is referred in ref. [3])

Element	Ref.																
	[9][a]	[10]	[15]	[16]	[17]	[18][c]	[20]	[21]	[22][a,c]	[23]	[32]	[33]	[34]	[35][c]	[37]	[47][d]	[51][e]
Ag						0.002		0.005		0.0003							
Al				0.3													
Au								0.078									
Ca	0.4				0.020		0.09	0.023			0.3	0.017					
Cd	0.1		0.03	0.7	0.010	0.015	0.05	0.009	0.014	0.002		0.005					0.090
Cr		0.2		0.9													
Cs								0.211									
Cu	0.06	0.01	0.01	0.3	0.030	0.024	0.08	0.031	0.022	0.004	0.65	0.011					
Fe		0.02									0.1	0.028					
Hg			0.08	1		0.270		0.349		0.022		0.015	0.015, 0.010[c]	0.002		0.0007, 0.0012[c]	
K	0.2		0.001				0.004	0.013									
Li						0.0002	0.002	0.008		0.00006							
Mg	0.8, 1.5[b]					0.001	0.04	0.019		0.0002							
Mn	0.4, 0.7, 0.8[b]	0.03		0.1		0.011	0.1	0.030									
Na	0.06		0.001		0.0008	0.0004	0.002	0.0008		0.0001					0.003		0.040
Ni	0.4	0.02						0.110	0.034								
Pb	0.8	0.03	0.01	0.3	0.080	0.060		0.082	0.028	0.006		0.045					
Rb							0.04										
Sr								0.049									
Zn	0.1	0.6					0.1	0.042	0.016		0.7	0.003					

[a] 2σ of the blank criterion is used.
[b] Different analytical lines are taken.
[c] A multiple sample loading in the FI mode is applied.
[d] Used as a sample introduction unit for ICP.
[e] Alternating current electrolyte atmospheric liquid discharge (ac-EALD) is used.

1.1.2.2. Solution cathode glow discharge (SCGD)

Webb et al. first proposed a simplified ELCAD design, which they named as solution-cathode glow discharge (SCGD) [27-29]. Fig. 1.5 illustrates the mechanism of the SCGD method. The solution was introduced to the cell through a serological pipette that had been bent upwards. The solution sprayed out with typical flow of 3.5 mL/min from the tip into a reservoir which contains a grounded graphite electrode. Other reports of SCGD can be found in the ref. [30-33].

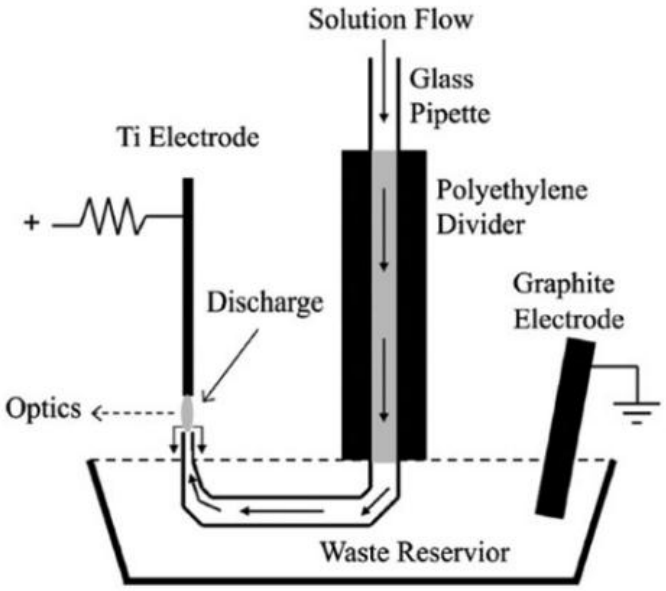

Figure 1.5 Diagrammatic representation of solution-cathode glow discharge (SCGD) (proposed by Webb et al. [27])

1.1.2.3. Liquid sample atmospheric pressure glow discharge (LS-APGD)

Compared with ELCAD, LS-APGD is quite simpler in construction and required components. It was introduced for the first time by Marcus and Davis [34]. The representation is shown in Fig. 1.6. LS-APGD is typically generated between

the surface of the solution flowing from a stainless steel or glass capillary and an opposite counter electrode (made by Cu, Ni, or stainless steel). Both electrodes are fully opened to the ambient air. The proposed LS-APGD runs stably at flow rates of 0.5-1.5 mL/min and also permits direct injection of analyte solution introduction. LODs for Na, Fe and Pb were 12, 12, and 14 ppm (mg/L), respectively [34].

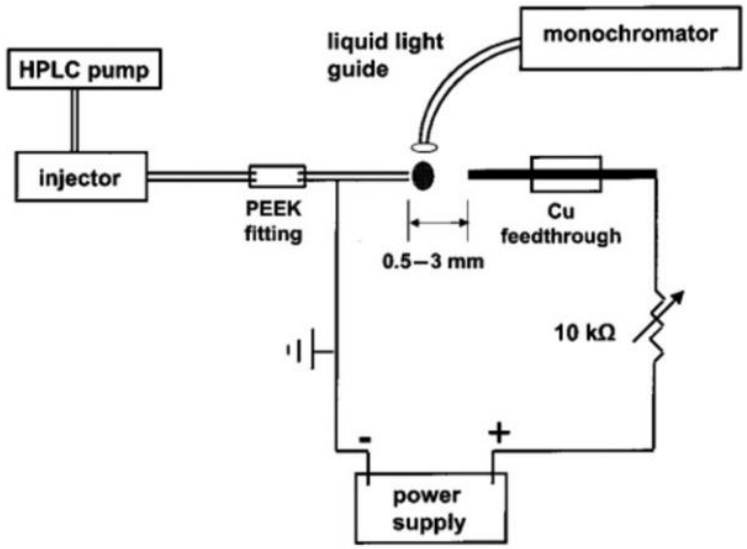

Figure 1.6 Diagrammatic representation of the liquid sampling atmospheric pressure glow discharge (LS-APGD) apparatus introduced by Marcus and Davis in Ref. [34].

1.1.2.4. Dielectric barrier discharge DBD

The electrical discharge developed due to high voltage in the gap between two electrodes, and at least one of the two electrodes is covered with a dielectric is called as dielectric barrier discharge (DBD) [35]. Fig. 1.7 shows the common configurations of DBD.

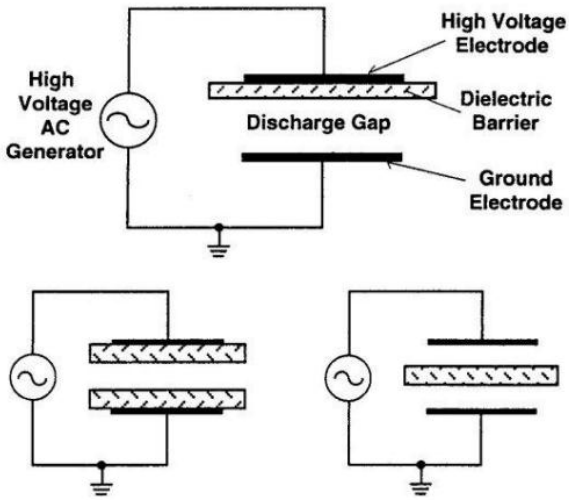

Figure 1.7 Common configurations of dielectric barrier discharge [35]

With DBD, direct solution analysis is very challenging. This is partly because DBD system cannot provide sufficient power for complete evaporation of electrolyte. Direct analysis of metal ions in liquid sample by using a specially designed capillary DBD at atmospheric pressure was first demonstrated by Tombrink [36]. The experimental arrangement of dielectric capillary barrier discharge was illustrated in Fig. 1.8. The DBD is powered by a radio-frequency generator. The advantage of the method was the very low sample flow rate (about 1 μL/min) leading to small sample size required and the low power consumption. More recently, Krahling modified the former DBD system called as liquid electrode dielectric barrier discharge (LE-DBD) with higher working flow rates. LODs for K and Ba were obtained to be 0.02 mg/L (ppm) and 6.9 mg/L (ppm), respectively, at flow rate of 20 μL/min [37].

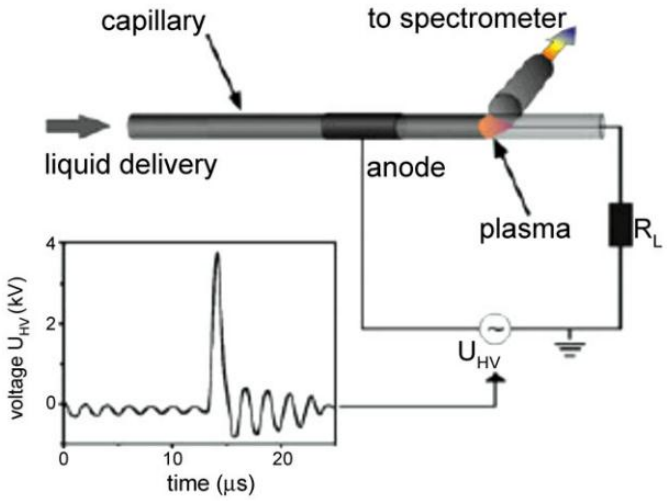

Figure 1.8 Dielectric capillary barrier discharge set-up proposed by Tombrink [36].

In other study, Huang developed atmospheric-pressure liquid discharge plasma driven by an AC power supply and the electrolyte solution played as one electrode (ac-AELD) [38]. The configuration of the ac-AELD is presented in Fig. 1.9. With the applications of ac voltage, the plasma was self-ignited. The ac-electrolyte atmospheric liquid discharge could be maintained at low flow rate of 0.2 mL/min and low discharge power (≤18 W) supply. LODs for sodium and cadmium were 0.04 and 0.09 mg/L (ppm), respectively.

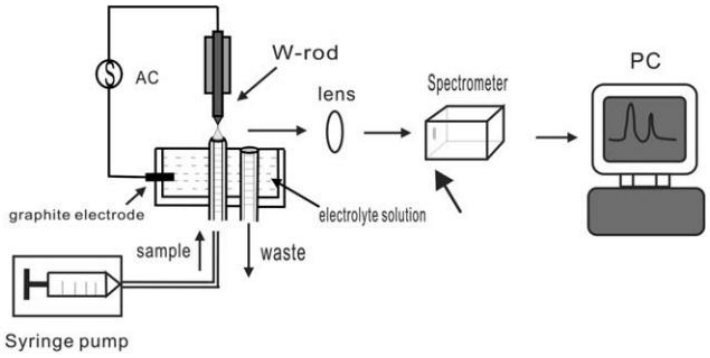

Figure 1.9 Schematic diagram of the experiment setup of ac-EALD developed by Huang [38].

There are many type of liquid electrode discharges reported so far. Our thesis has just summarized some typical ones. The other can be found in some review articles reported by Jamoz [3], He [7], Karanassios [39], Miclea [40], and Franzke [41].

Future prospect

Liquid electrode discharge microplasma offers a low-cost, portable platform for fast and direct analysis of metals in aqueous samples because of no supportive gases required for plasma production. The integration of liquid electrode discharge onto microfluidics systems has been realized. The mechanism of atomization and excitation by the discharge plasmas has been under debate. It is required to explore these mechanisms in the future efforts.

Miniaturized and portable devices are likely the most fruitful applications of liquid plasma discharges. However, only liquid electrode plasma optical emission

spectrometry (LEP OES), which is introduced in later section, has been successfully developed in a form of a compact analyzer so far.

In general, the analytic performance of these liquid electrode discharge based systems cannot be well-compared with that of conventional ICP MS and ICP AES. Therefore, improving the analytical performance of these discharge plasma sources will be an interesting challenge in the future.

1.2. Introduction to Liquid Electrode Plasma Optical Emission Spectrometry

About ten years ago, Karanassios asked a question on his review article: "Microplasmas for chemical analysis: analytical tools or research toys?" [39].The invention and development of LEP would be a good answer since it might solve almost all of the above question. Firstly, LEP does not need a nebulizer that was considered as the Achilles' heel of microplasma. Moreover, LEP can generate a vapor bubble even when sample is stationary. Secondly, LEP consumes little power, thus it can be battery-operated. Finally, the microplasma can be generated in a microfluidic chip that is small and versatile to be modified its design and to be controlled. As a result, LEP can realize the expected portability of micro-plasma based analyzers. Fig. 1.10 shows a photo and basic features of an ultra-compact elemental analyzer MH-5000 that has been developed by Micro Emission Ltd.

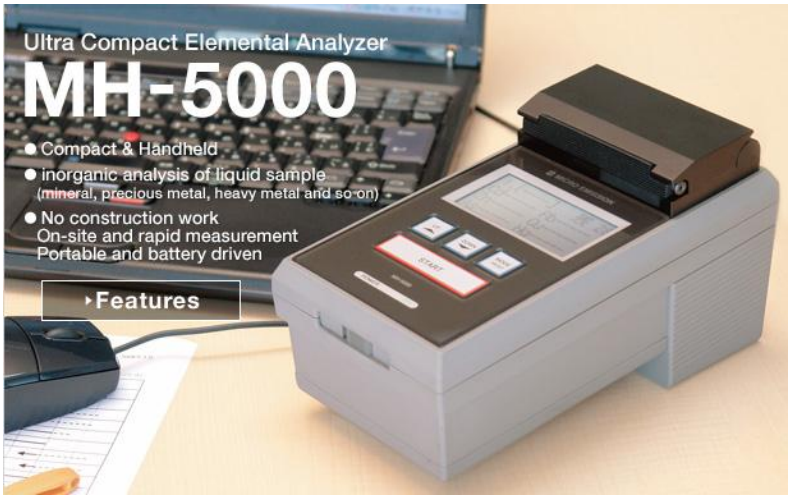

Figure 1.10 An ultra-compact elemental analyzer MH-5000. (Source: http://www.micro-emission.com/)

Compared with the other microplasma sources for elemental analysis, liquid electrode plasma (LEP) has a short history from its investigation to applications. It was accidentally invented when applying a too high voltage to separate ionic species in capillary electrophoresis. It was presented by Iiduka for the first time in 2004 [42]. This novel technique allows miniaturizing the plasma source, and requires neither plasma gas nor high power source. Thus, the LEP-based device can be made compact and portable.

The principle of LEP-AES is briefly shown in Fig. 1.11. It can be also found in our published papers [42-48]. If a high DC voltage is applied to Pt electrodes at both ends of a micro-channel which has a narrower part at the center, electrical field is concentrated at the narrow part. A water bubble generates at the center because of joule heating (a). Subsequently, plasma occurs in the bubble (b). Elements in sample solution enter the plasma and emit their characteristic emission wavelength

(c) that is acquired and analyzed by a detector (spectrometer). The plasma generation and the acquisition of emission signals could be done in milliseconds.

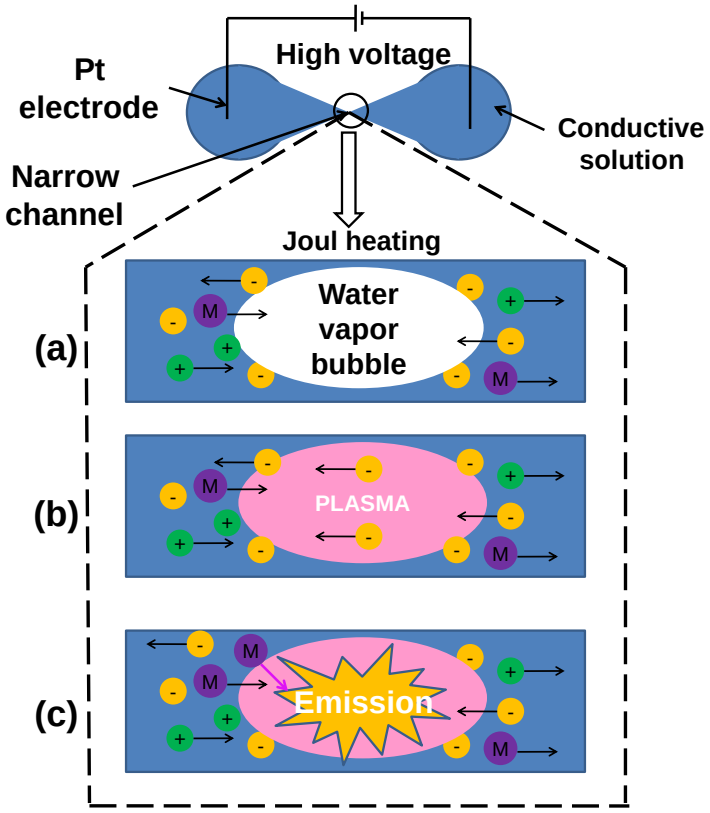

Figure 1.11 Principle of plasma generation at a narrow part of a fluidic channel.

Through recent reported studies, some advantages of the method are proven: high sensitivity, easy manipulation (no special skills required), ultralow background and small sample amount (20 μL for a single measurement). Importantly, LEP-AES does not require gas plasma or nebulizer and it can be battery-operated. The two latter features enable the LEP-based handheld device.

There are several works related to this method have been reported so far. Banno utilized the LEP OES to determine trace amounts of sodium and lithium in zirconium dioxide [43]. Detection limits (3SD) of the trace elements, Na and Li, in 4000 μg/g zirconium dioxide aqueous solution are found to be 0.02 and 0.133 μg/g, respectively. These values are comparable to LODs of Na and Li in ZrO_2 using ICP AEC because emission signals of Zr in LEP is very weak.

One of the advantages of LEP is that it uses a resin chip. The resin might be PDMS and thus micro-fabrication can be utilized. However plasma expansion may cause a severe deformation on resin channel, leading to high uncertainty of emission signals. To overcome this issue, Kitano made LEP chip by quartz glass, a harder material [44]. Also, he proposed a voltage pulse accumulation mode to generate a longer plasma and sample flowing technique to remove gas bubble in the microchannel after a measurement. It was reported that limits of detection for Cd and Pb were significantly improved, 0.52 μg/L for Cd and 19.0 μg/L for Pb with optimized conditions. The long accumulation mode using the quartz chip with sample flow was effective to improve the sensitivity [44].

Excitation temperature and the electron density of LEP, two of the most important parameters of a plasma source that is employed as a excitation source,

were measured by Kohara [45] and Kumai [46]. The estimated excitation temperature was about 8000 K, and the estimated electron density was $1x10^{15}$ cm^{-3} [45]. The limit of detection determined was 4.0 μg/L for Pb. In other research, Kumai [46] reported that excitation temperature was deduced using a Boltzmann plot. The temperature was determined to be 6200K with a plastic chip at an applied voltage of 800 V, and the temperature of plasma is strongly dependent on geometric dimension of the narrow channel but it seemed not to be dependent on voltage applied.

More recently, Tung developed a sensing technique of silver nanoparticles as labels for immunoassay using LEP. Schematic representation of the immunoassay system is shown in Fig. 1.12. Because LEP is remarkably suitable for metallic ion detection, the biological samples was supposed impossible to be detected. However, the presence of hCG antigens could be detected through labeling silver nanoparticles that were oxidized to sensitively detectable silver ions by a commercialized quartz chip [49].

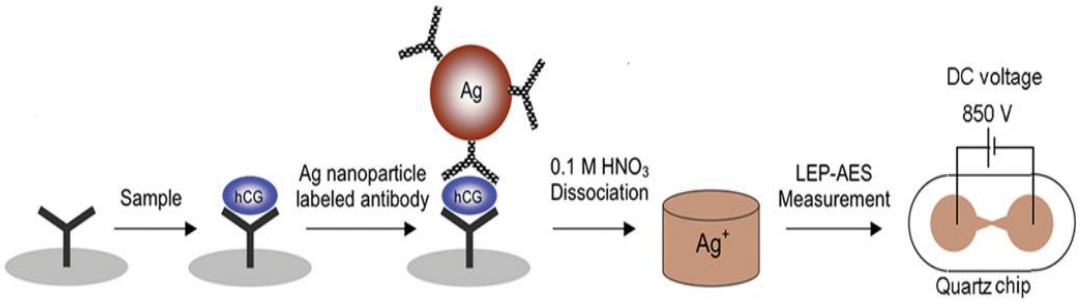

Figure 1.12 Schematic representation of the immunoassay system. hCG was sandwiched between two antibodies, of which one was immobilized onto the microwell and the other was conjugated to Ag nanoparticles. The Ag nanoparticles were dissociated oxidatively, and the silver ion concentration was measured. The work was done by Tung el al. [49].

Another approach to improve the sensitivity for LEP is the combination with a preconcentration technique. Solid phase extraction was chosen because of its advantages that are mentioned in the introduction part for solid phase extraction. Utilizing the idea, Kagaya [50] used chelate resin that was packed in a minicolumn for preconcentration to detect cadmium in certified waste water and ground water. Achieved LOD for Cd was 0.2 μg in 200 mL of sample solution, equivalent to a concentration of 1 μg/L. Nakayama [51] simultaneously determined metal ions in water using LEP OES combined with multi-element concentration using liquid organic ion associate extraction. The analytical performance is reported in Table 1.2.

Table 1.2 Detection limits of LEP OES (extracted from ref. [51])

Element	DL (100-fold enrichment) /mg.L^{-1}	DL without enrichment/ mg.L^{-1}	Magnification of sensitivity
Cu	**0.011**	13	1200
Mn	**0.012**	12	1000
Pd	**0.009**	6	700
Zn	**0.17**	14	80
Cd	**0.006**	1	200
Pb	**0.015**	1	70

In brief summary, LEP-OES is a novel liquid discharge based analytical method remarkably sensitive with metals. It possesses some considerable advantages such as: low power consumed, portable, highly versatile, etc. However the sensitivity of the method still needs to be improved. In the study, to improve the sensitivity of LEP, solid phase extraction was used as an on-chip preconcentrator. By this way the concentration of analyte of interest was sufficiently high to be detectable. Eventually the sensitivity of LEP was improved.

1.3. Introduction to pollution of heavy metals

One of the greatest problems that the world has been facing today is that of environmental pollution. A simple definition of pollution is an undesirable state of the environment caused by contamination by humans with harmful stuff, as a consequence of their actions. Nowadays, there has been increasing in concerns about such all types of pollutions, especially the water pollution by heavy metals.

Regarding the definition of heavy metal in the environment field, the term “heavy metal” is simply defined as a variety of toxic metallic substances including individual metals and metal compounds that impact on the environment and subsequently they take significantly harmful effects on human body. The most pollutant heavy metals are lead, mercury, cadmium, chromium, and copper. Heavy metal poisoning may cause some bad effects to human body. This is so popular that we can find it easily on the internet.

To prevent heavy metal pollution, the most important issue is to control the quality of drinking water, food, and further of surface and underground water, soil,

etc. [52]. It means that keeping heavy metal concentration under control. For reference, Table 1.3 shows United State Environmental Protection Agency (USEPA) maximum contamination levels for heavy metal concentration in air, soil and water [52]. Table 1.4 presents Guideline in drinking water by the World Health Organization (WHO) [52]. In order to quickly detect heavy metals at trace concentration that is lower than the regulatory limits, the duty of analytical scientists is to develop new devices or techniques that enable quick and on-site detection and lower detection limit.

Table 1.3 Maximum contamination levels for heavy metal concentration in air, soil and water in the United State [52].

Heavy metal	**Max conc. in air (mg/m^3)**	**Max conc. in sludge (soil) (ppm)**	**Max conc. in drinking water (ppm)**	**Max conc. in H_2O supporting aquatic life (pm)**
Cd	0.1-0.2	85	0.005	0.008
Pb	--	420	0.0-0.1	0.0058
Zn	1.5	7500	5.00	0.0766
Hg	--	<1	0.002	0.05
Ca	5	Tolerable	50	Tolerable >50
Ag	0.1	--	0.0	0.1
As	--	--	0.01	--

Table 1.4 Guideline in drinking water by the World Health Organization (WHO) [52]

Heavy metal	Max. acceptable conc. (WHO) (ppm)
Zinc	5
Arsenic	0.01
Magnesium	50
Calcium	50
Cadmium	0.003
Lead	0.01
Silver	0.0
Mercury	0.001

1.4. Introduction to solid phase extraction

Despite the selectivity and sensitivity of elemental analysis methods such as atomic absorption spectrometry (AAS), inductively coupled plasma atomic spectrometry (ICP AES) and inductively coupled plasma mass spectrometry (ICP MS), the need for the preconcentration of trace elements is crucial because the trace elements often exist at extremely low concentrations. Regarding the conventional technique, liquid–liquid extraction is, without doubt, the most popular method for pretreatment of analytical samples (preconcentrate and refine the samples). However some disadvantages of the method are [53]:

- Require much time, especially when performing several successive extraction processes;
- Require relatively large sample volumes.
- Use of large volumes of toxic organic solvents;

Solid phase extraction (SPE) is another approach for the sample pretreatment that offers **a number of important advantages**. With SPE solvent usage and exposure is minimized. In addition extraction time for sample preparation is reduced. Consequently, SPE has been more increasingly used for the enrichment, separation and determination of metal ions in aqueous samples [53]. Modern SPE is, therefore, a technique placed between the classical LSE and column liquid chromatography and is in full accord with the IUPAC definition of chromatography. Since SPE is versatile so it is utilized many purposes, such as purification, trace enrichment, and so on.

Basic principle of SPE

The principle of SPE is similar to that of LLE, however SPE involves partitioning between a liquid (mobile phase) and a solid (sorbent) stationary phase. When the sample is passed through the sorbent, the analyte in the sample is retained on the solid sorbent by high affinity of the functional group of the sorbent toward the analyte. The retained analytes are then recovered in elution with an appropriate solvent [54-56].

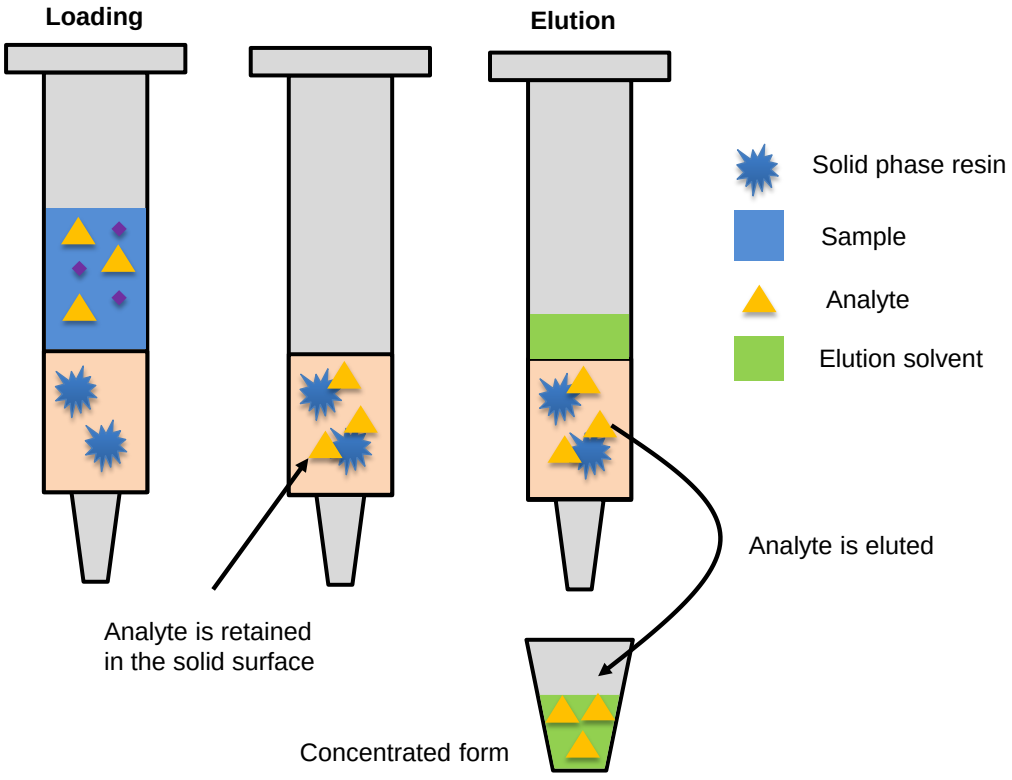

Figure 1.13 A typical working principle of solid phase extraction.

Figure 1.13 illustrates the operational principle of the SPE method. A typical SPE method consists of three to four steps: conditioning, sample loading, cleaning (optional), and eluting. First, the solid sorbent should be conditioned using an appropriate solvent, followed by the same solvent as the sample solvent. This step is crucial, as it enables the wetting of the packing material and removes possible impurities initially contained in the sorbent. In addition, this step helps ensure no air in the column. It is necessary to keep the sorbent completely surrounded by solvent. The sorbent must be reconditioned if it dries.

The second step is the loading of the sample through the sorbent. Sample volumes can range from 1 ml to 1 L depending on the system (amount of sorbent, column shape, etc.). The sample may be applied to the column by many types of forces such as pumping, aspirated by vacuum, gravity or by an automated system. The flow rate should be low enough to enable efficient retention of the analytes, and high enough to avoid excessive duration. During this step, the analytes are kept and thus concentrated on the sorbent.

The third step is the washing of the sorbent with an appropriate solvent that must have low elution strength, to eliminate matrix components, without removing the analytes. This step is optional. An additional drying step may be recommended, especially for aqueous matrices, to remove completely the water from the sorbent because in some cases the presence of water may hinder the elution and the subsequent analysis.

The final step is the elution of the analytes of interest by an appropriate eluent. The eluent volume should be adjusted so that quantitative recovery of the

analytes is achieved with minimized dilution. In addition, the flow rate should also be adjusted to ensure efficient elution. The principle of SPE was referred from ref. [53].

Adsorption of analytes on the sorbent is required for preconcentration. The mechanism of retention of analyte depends on the nature of the sorbent including physical adsorption, ion-exchange or chelation [53]. SPE can be easily automated, and coupled online to analysis techniques, in which it often involves with flow injection (FI) techniques. On-line procedures avoid sample manipulation between preconcentration and subsequent analysis, thus it reduces analyte loss and contamination risk, allowing high reproducibility [57-59]. In addition, the retained analyte is more engaged in analysis. As the result, the necessary sample volume is smaller. However, off-line SPE might be preferred for complex samples because it is more flexible.

On-line flow injection procedures have several advantages: higher sample throughput, smaller necessary amount of sample and reagent, greater precision, lower risk of analyte loss or contamination. However, the flow injection technique using column extraction has some disadvantages. In particular, insufficient adsorption and clogging of the column by insoluble ligands are two of the main issues [70]. Applications of SPE to FI on-line preconcentration systems were summarized in ref. [53].

The sorbent may be packaged in different formats: filled micro-columns, cartridges, syringe barrels and discs [60-62]. In which, on-line systems mainly use a micro-column. The size of the column may be adapted to the sample volume. In

particular, a bigger extraction column allows larger sample volumes, thus enabling the preconcentration of metal ions at very low concentration levels. However, such column must be reused because of quite expensive SPE materials. As the result, cross-contamination must be taken into account. In addition, columns with a narrow internal diameter limit usable sample flow rates to a range 1–10 ml/min that needs long time for large sample volumes [63]. SPE has high versatility so that it could be online coupled with liquid chromatography [64], atomic absorption spectrometry [65-67], ICP AES [68], ICP MS [69], etc.

In the study, a SPE column is integrated into a LEP chip to preconcentrate and detect lead (Pb) in pure liquid samples to employ the advantages of SPE that were mentioned above. The Pb-specialized SPE resin was commercialized and characterized analytical performance [71].

1.5. Purpose and scope

There are many variations of micro-plasma sources that are utilized for optical determination of elements. Although solution discharge plasma offers a low-cost, portable, small platform for fast and direct analysis of metal ions in liquid samples, this discharge plasma family remains some critical problems. In general the analytical methods based on these novel liquid plasmas are less sensitive than conventional ones such as ICP OES, ICP MS. Some may have reached the critical sensitivity. Mechanism of discharge plasmas is still under debate. Some methods require a large amount of sample. Some have been successfully downscaled to chip platform, however carrier gas for plasma is still required except LEP.

Among the micro-plasma sources, LEP is promising because it is capable of using the PDMS-made chips, thus, it might be highly capable of combining with other embedded elements such as SPE because the chip architecture can be easily modified. Compared with the other preconcentration methods, on-chip SPE has some interesting merits. First on-chip SPE enables a very small connection volume from the column to detection site (LEP element in this case). As a result, required sample volume and organic eluent released are minimized. Second, on-chip SPE consumes very little amount of SPE resin, thus the SPE column can be disposable, and reactivation and storage of the used resin is not needed.

The main purpose of this study is to improve the sensitivity for LEP OES by combining it with SPE. Accordingly, a SPE column is integrated into LEP chip so that the analyte is preconcentrated before the detection of it by LEP. To realize the idea, at first, the LEP is characterized to find the most suitable conditions for the combination of SPE. Subsequently, suitable matching components have been developed to connect SPE with LEP. The chip layouts, measurement protocols, data processing have been also developed suitable with the SPE-LEP combination. Finally, the developed methods have been applied to the detection of lead, an element that is known as a typical toxic metal having bad effect on environment and human life.

1.6. Dissertation organization

Chapter 1 presents a general introduction to plasma, current development of liquid discharge plasmas with versatile configurations and their applications to metal detection. In this chapter, most of the reports on LEP are also collected and

summarized. In addition, basic literature review of solid phase extraction including its working principle and applications is presented. Finally the objective of the research is pointed out.

Chapter 2 presents the characterization of the liquid electrode plasma in different conditions. The effect of flow rate on the plasma and effect of the high temperature plasma on PDMS-made channel is presented. In addition, the investigation of alternating current driven liquid electrode plasma (AC LEP) has been reported for the first time. The enhancement effect of organic substances on emission intensities of both DC LEP and AC LEP is tested and evaluated. From the investigation, the strategies of the SPE-LEP combination have been proposed.

Chapter 3 presents the development of a simply designed internal micropump, which is used for fluid actuation for the effective integration of SPE with DC LEP. Chip design, measurement protocol, data acquisition and processing are proposed to be suitable with the performance of the pump in the SPE-LEP combination platform. The application of the proposed method for the highly sensitive detection of lead is presented.

Chapter 4 reports a rapid and highly sensitive analysis method for lead based on the integration of SPE with AC LEP. Some parameters affecting the operation are characterized and data processing is discussed. Chip design, measurement protocol, data acquisition and processing are proposed to be suitable with the combination of the novel LEP with SPE. The chapter is also presenting the application of the novel integrated chip for the quantitative detection of lead.

Chapter 5 gives some general conclusions and notable points throughout the dissertation.

1.7. References

[1] A. Fridman, Plasma chemistry, Cambridge University Press, 2008.

[2] B. Chapman, Glow discharge process, John Wiley & Sons Press, 1980.

[3] P. Jamroz, K. Greda, and P. Pohl, Development of direct-current, atmospheric-pressure, glow discharges generated in contact with flowing electrolyte solutions for elemental analysis by optical emission spectrometry, TrAC, Trends Anal. Chem. 41 (2012) 105.

[4] P. Mezei and T. Cserfalvi, Electrolyte cathode atmospheric glow discharges for direct solution analysis. Appl. Spectrosc. Rev., 42 (6): 573–604.

[5] M. A. Mottaleb, J. S. Yang, and H. J. Kim, Electrolyte-as-cathode glow discharge (ELCAD)/glow discharge electrolysis at the gas–solution interface, Appl. Spectrosc. Rev. 37 (2002) 247.

[6] M. R. Webb, and G. M. Hieftje, Spectrochemical analysis by using discharge devices with solution electrodes, Anal. Chem., 81 (2009) 862.

[7] Q. He, Zh. Zhu, Sh. Hu, Flowing and Nonflowing Liquid Electrode Discharge Microplasma for Metal Ion Detection by Optical Emission Spectrometry, Applied Spectroscopy Reviews, 49:249–269, 2014.

[8] P. Mezei and T. Cserfalvi, Electrolyte cathode atmospheric glow discharges for direct solution analysis, Appl. Spectrosc. Rev., 42 (2007) 573.

[9] T. Cserfalvi, P. Mezei, and P. Apai, Emission studies on a glow discharge in atmospheric pressure air using water as a cathode, J. Phys. D: Appl. Phys. 26 (1993) 2184–2188.

[10] K. Gyorgy, L. Bencs, P. Mezei, and T. Cserfalvi, Novel application of the electrolyte cathode atmospheric glow discharge, Atomic absorption spectrometry studies. Spectrochim. Acta, Part B. 77 (2012) 52.

[11] R. Shekhar, D. Karunasagar, M. Ranjit, and J. Arunachalam, Determination of elemental constituents in different matrix materials and flow injection studies

by the electrolyte cathode glow discharge technique with a new design. Anal. Chem. 81 (2009) 8157.

[12] R. Shekhar, Improvement of sensitivity of electrolyte cathode discharge atomic emission spectrometry (ELCAD-AES) for mercury using acetic acid medium, Talanta 93 (2012) 32.

[13] T. Cserfalvi, P. Mezei, and P. Apai, Emission studies on a glow discharge in atmospheric pressure air using water as a cathode, J. Phys. D: Appl. Phys. 26 (1993) 2184.

[14] P. Mezei and T. Cserfalvi Direct solution analysis by glow discharge: Electrolyte–cathode discharge spectrometry, J. Anal. At. Spectrom. 9 (1994) 345.

[15] T. Cserfalvi, and P. Mezei, Operating mechanism of the electrolyte cathode atmospheric glow discharge, Fresenius J. Anal. Chem. 355 (1996) 813.

[16] Y. S. Park, S. H. Ku, S. H. Hong, H. J. Kim, and E. H. Piepmeier, Fundamental studies of electrolyte-as-cathode glow discharge–atomic emission spectrometry for the determination of trace metals in flowing water, Spectrochim. Acta, Part B 5(1998) 1167.

[17] H. J. Kim, J. H. Lee, M. Y. Kim, T. Cserfalvi, and P. Mezei, Development of open-air type electrolyte-as-cathode glow discharge–atomic emission spectrometry for determination of trace metals in water, Spectrochim. Acta, Part B 55 (2000) 823–831.

[18] M. A. Mottaleb, Y. A. Woo., and H. J. Kim, Evaluation of open-air type electrolyte-ascathode glow discharge–atomic emission spectrometry for determination of trace heavy metals in liquid samples, Microchem. J., 69 (2001) 219.

[19] T. Cserfalvi and P. Mezei, Subnanogram sensitive multimetal detector with atmospheric electrolyte cathode glow discharge, J. Anal. At. Spectrom., 18 (2003) 596.

[20] P. Mezei and T. Cserfalvi, The investigation of an abnormal electrolyte cathode atmospheric glow discharge (ELCAD), J. Phys. D: Appl. Phys., 39 (2006) 2534.

[21] Mezei, P., Cserfalvi, T., Kim, H.J., and Mottaleb, M.A. (2001) The influence of chlorine on the intensity of metal atomic lines emitted by an electrolyte cathode atmospheric glow discharge. Analyst, 126: 712–714.

[22] T. Cserfalvi and P. Mezei, Investigations on the element dependency of sputtering process in the electrolyte cathode atmospheric discharge. J. Anal. At. Spectrom., 20 (2005) 939.

[23] P. Mezei, T. Cserfalvi and L. Csillag, The spatial distribution of the temperatures and the emitted spectrum in the electrolyte cathode atmospheric glow discharge, J. Phys. D: Appl. Phys., 38 (2005) 2804.

[24] P. Mezei, T. Cserfalvi, P. Hartmann,, and L. Bencs, The effect of OH radicals on Cr–I spectral lines emitted by DC glow discharges, Spectrochim. Acta, Part B 65 (2010) 218–224.

[25] G. Jenkins and A. Manz, A miniaturized glow discharge applied for optical emission detection in aqueous analytes, J. Micromech. Microeng., 12 (2002) N19.

[26] G. Jenkins, J. Franzke, and A. Manz, Direct optical emission spectroscopy of liquid analytes using an electrolyte as a cathode discharge source (ELCAD) integrated on a microfluidic chip, Lab Chip 5 (2005) 711.

[27] M. R. Webb, F. J. Andrade, G. Gamez, R. McCrindle, and G. M. Hieftje, Spectroscopic and electrical studies of a solution-cathode glow discharge, J. Anal. At. Spectrom., 20 (2005) 1218.

[28] M. R. Webb, F. J. Andrade, and G. M. Hieftje, Compact glow discharge for the elemental analysis of aqueous samples, Anal. Chem., 79 (2007) 7899.

[29] M. R. Webb, F. J. Andrade, and G. M. Hieftje, High-throughput elemental analysis of small aqueous samples by emission spectrometry with a compact,

atmospheric-pressure solutioncathode glow discharge. Anal. Chem., 79 (2007) 7807.

[30] T.A. Doroski, A. M. King, M. P. Fritz, and M. R. Webb, Solution–cathode glow discharge–optical emission spectrometry of a new design and using a compact spectrograph, J. Anal. At. Spectrom., 28 (2013) 1090.

[31] Z. Zhu, G. C. –Y. Chan, S. J. Ray, X. Zhang, and G. M. Hieftje. Use of a solution cathode glow discharge for cold vapor generation of mercury with determination by ICP–atomic emission spectrometry, Anal. Chem., 80 (2008) 7043.

[32] Z. Zhu, Q. He, Q. Shuai, H. Zheng, and S. Hu Solution cathode glow discharge induced vapor generation of iodine for determination by inductively coupled plasma optical emission spectrometry, J. Anal. At. Spectrom., 25 (2010) 1390.

[33] Z. Zhu, C. Huang, Q. He, Q. Xiao, Z. Liu, S. Zhang and S. Hu, On line vapor generation of osmium based on solution cathode glow discharge for the determination by ICP-OES, Talanta 106 (2013) 133.

[34] R. K. Marcus, and W. C. Davis, An atmospheric pressure glow discharge optical emission source for the direct sampling of liquid media, Anal. Chem, 73 (2001) 2903.

[35] V. Samoilovich, V. Gibalov, and K. V. Kozlov, Physical chemistry of the barrier discharge, DVS-Verlag GmbH, Dusseldorf, 1997.

[36] S. Tombrink, S. Muller, R. Heming, A. Michels, P. Lampen, and J. Franzke, Liquid analysis dielectric capillary barrier discharge, Anal. Bioanal. Chem. 397 (2010) 2917.

[37] T. Krahling, S. Muller, C. Meyer, A. K. Stark, and F. Franzke, Liquid electrode dielectric barrier discharge for the analysis of solved metals, J. Anal. At. Spectrom. 26 (2011) 1974.

[38] R. Huang, Z. Zhu, H. Zheng, Z. Liu, S. Zhang, and S. Hu, Alternating current driven atmospheric-pressure liquid discharge for the determination of elements with optical emission spectrometry, J. Anal. At. Spectrom. 26 (2011) 1178.

[39] V. Karanassios, Microplasma for chemical analysis: analytical tools or research toys? Spectrochimica Acta Part B 59 (2004) 909.

[40] M. Miclea, J. Franzke, Analytical detectors based on microplasma spectrometry, Plasma Chem Plasma Process 27 (2007) 205.

[41] J. Franzke, K. Kunze, M. Miclea and K. Niemax, Microplasmas for analytical spectrometry, J. Anal. At. Spectrom.18 (2003) 802.

[42] A. Iiduka, Y. Morita, E. Tamiya, and Y. Takamura: Proc. μTAS, 2004, Vol. 1, p. 423.

[43] M. Banno, E. Tamiya and Y. Takamura, Determination of trace amounts of sodium and lithium in zirconium dioxide (ZrO2) using liquid electrode plasma optical emission spectrometry Anal. Chim. Acta. 634 (2009) 153.

[44] A. Kitano, A. Iiduka, T. Yamamoto, Y. Ukita, E. Tamiya, and Y. Takamura, Highly Sensitive Elemental Analysis for Cd and Pb by Liquid Electrode Plasma Atomic Emission Spectrometry with Quartz Glass Chip and Sample Flow, Anal. Chem. 83 (2011) 9424.

[45] Y. Kohara, Y. Terui, M. Ichikawa, T. Shirasaki, K. Yamamoto, T. Yamamoto, and Y. Takamura, Characteristics of liquid electrode plasma for atomic emission spectrometry, J. Anal. At. Spectrom. 27 (2012) 1457.

[46] M. Kumai and Y. Takamura, Excitation temperature measurement in liquid electrode plasma, Jpn. J. Appl. Phys. 50 (2011) 096001.

[47] D. V. Khoai, A. Kitano, T. Yamamoto, Y. Ukita, and Y. Takamura, Development of high sensitive liquid electrode plasma–Atomic emission spectrometry (LEP-AES) integrated with solid phase pre-concentration, Microelectron. Eng. 111 (2013) 343.

[48] D. V. Khoai, T. Yamamoto, Y. Ukita, and Y. Takamura, On-chip solid phase extraction–liquid electrode plasma atomic emission spectrometry for detection of trace lead, Jpn. J. Appl. Phys. 53 (2014) 05FS01.

[49] N. H. Tung, M. Chikae, Y. Ukita, P. H. Viet, Y. Takamura, Sensing Technique of Silver Nanoparticles as Labels for Immunoassay Using Liquid Electrode Plasma Atomic Emission Spectrometry, Anal. Chem. 2012, 84, 1210.

[50] S. Kagaya, E. Maeba, Y. Inoue, W. Kamichatani, T. Kajiwara, H. Yanai, M. Saito, T. Yamamoto, Y. Takamura and K. Tohda, determination of cadmium in Water Samples by Liquid electrode Plasma atomic emission Spectrometry after Solid Phase extraction using a mini cartridge Packed with chelate resin immobilizing carboxymethylated Pentaethylenehexamine, Analytical sciences, 26 (2010) 515.

[51] K. Nakayama, T. Yamamoto, N. Hata, S. Taguchi, and Y. Takamura, Liquid electrode plasma atomic emission spectrometry combined with multi-element concentration using liquid organic ion associate extraction for simultaneous determination of trace metals in water, Bunseki Kagaku [6] 60 (2011) 515.

[52] J. O. Duruibe, M. O. C. Ogwuegbu, and J. N. Egwurugwu, Heavy metal pollution and human biotoxic effects. Int J Phys Sci, 2 (2007) 112.

[53] V. Camel, Review Solid phase extraction of trace elements, Spectrochimica Acta Part B 58 (2003) 1177.

[54] A. Żwir-Ferenc, M. Biziuk, Polish J. of Environ. Stud.15 (2006) 677.

[55] Yau Ho Pan Michael, Doctoral dissertation, The University of Hong Kong, 2006.

[56] Zeev B. Alfassi, Determination of trace elements, VCH Balaban publisher, 1994, p. 129.

[57] D.T. Rossi, N. Zhang, Automating solid-phase extraction: current aspects and future prospects, J. Chromatogr. A 885 (2000) 97.

[58] O. Keil, J. Dahmen, D.A. Volmer, Automated matrix separation and preconcentration for the trace level determination of metal impurities in ultrapure inorganic salts by high-resolution ICP–MS, Fresenius J. Anal. Chem. 364 (1999) 694.

[59] J.F. Tyson, Flow injection atomic spectrometry, Spectrochim. Acta Rev. 14 (1991) 169.

[60] C.F. Poole, Solid-phase extraction, Encyclopedia of Separation Science, 3, Academic Press, 2000, p. 1405.

[61] E.M. Thurman, K. Snavely, Advances in solid-phase extraction disks for environmental chemistry, Trends Anal. Chem. 19 (2000) 18;

[62] C.F. Poole, Solid-phase extraction with disks, Encyclopedia of Separation Science, 9, Academic Press, 2000, p. 4141

[63] M. Kumar, D.P.S. Rathore, A.K. Singh, Quinalizarin anchored on Amberlite XAD-2. A new matrix for solidphase extraction of metal ions for flame atomic absorption spectrometric determination, Fresenius J. Anal. Chem. 370 (2001) 377.

[64] X. Yin, W. Frech, E. Hoffmann, C. Ludke, J. Skole, ¨ Mercury speciation by coupling cold vapour atomic absorption spectrometry with flow injection on-line preconcentration and liquid chromatographic separation, Fresenius J. Anal. Chem. 361 (1998) 761.

[65] S. Olsen, L.C.R. Pessenda, J. Ruzicka, E.H. Hansen, Combination of flow injection analysis with flame atomic absorption spectrophotometry: determination of trace amounts of heavy metals in polluted seawater, Analyst 108 (1983) 905;

[66] Z. Fang, J. Ruzicka, E.H. Hansen, An efficient flowinjection system with on-line ion-exchange preconcentration for the determination of trace amounts of heavy metals by atomic absorption spectrometry, Anal. Chim. Acta 164 (1984) 23;

[67] Z. Fang, Z. Zhu, S. Zhang, S. Xu, L. Guo, L. Sun, Online separation and preconcentration in flow injection analysis, Anal. Chim. Acta 214 (1988) 41.

[68] G.A. Zachariadis, A.N. Anthemidis, P.G. Bettas, J.A. Stratis, Determination of lead by on-line solid phase extraction using a PTFE micro-column and flame atomic absorption spectrometry, Talanta 57 (2002) 919.

[69] K. Benkhedda, H.G. Infante, F.C. Adams, E. Ivanova, Inductively coupled plasma mass spectrometry for trace analysis using flow injection on-line preconcentration and time-of-flight mass analyser, Trends Anal. Chem. 21 (2002) 332.

[70] J.N. King, J.S. Fritz, Concentration of metal ions by complexation with sodium bis(2-hydroxyethyl)dithiocarbamate and sorption on XAD-4 resin, Anal. Chem. 57 (1985) 1016.

[71] A. Sabarudin, N. Lenghor, Y. Liping, Y. Furusho, S. Motomizu, Automated Online Preconcentration System for the Determination of Trace Amounts of Lead Using Pb‐Selective Resin and Inductively Coupled Plasma‐Atomic Emission Spectrometry, Spectroscopy Letters 39 (2006) 669-682.

Chapter 2
Characterization of liquid electrode plasma

Abstract

The main purpose of the study is to improve sensitivity of LEP in metal detection with the integration of SPE. The effective SPE needs low flow rate, whereas LEP requires high flow rate to overcome the air bubble issue. Thus, the investigation of a condition to generate LEP that is suitable with the SPE combination is needed. In this chapter, conventional liquid electrode plasma driven by direct current (DC LEP) is characterized with different conditions. The DC LEP was produced with low flow rate to observe the effect of low flow rate LEP on emission intensity and on the destruction of PDMS channel. In addition, a novel liquid electrode plasma source powered by alternating current (AC LEP) has been developed for the first time. The condition to generate the AC LEP was found. Basic properties were characterized. Both of the two LEP sources were evaluated their performance of elemental determination. In addition, the enhancement effect of some organic additives on emission intensity was tested in order to improve sensitivity of the low flow rate LEP. Through the chapter, two strategies of the SPE-LEP combination have been proposed. They are presented in chapter 3 and 4 respectively in this thesis.

2.1. Introduction

As presented in the chapter 1, liquid electrode plasma optical emission spectrometry (LEP OES) is a novel analytical method, which employs the discharge plasma generated by liquid electrodes as an excitation source for optical emission spectrometric analysis. LEP OES offers a low-cost and portable method for rapid analysis of metal ions in solution samples. The mechanism of plasma generation by pulsed DC voltage is presented in the previous part. The plasma characteristics vary in regard to some factors that were briefly reported in earlier studies [2,3]. The electron density and excitation temperature were estimated, and these quantities is dependent upon the geometric dimension of LEP channel, especially strongly on the height and width of the micro channel [2]. The effect of accumulative expansion of the DC driven plasma results in expansion of PDMS channel was also reported [5]. The deformation of LEP channel may affect the reproducibility of emission intensity.

The conventional LEP measurement with a handy device is performed as follows. A 40 μL of a liquid sample is pipetted to a LEP chip. It is ensured that the liquid sample fills properly the entire channel without air bubble. A DC pulsed voltage is applied through two electrodes that is put at both ends of LEP channel. Kitano et al. reported a modified measurement protocol with sample flow during pulsed voltage application.

The integration of SPE to LEP chip results in a change in how LEP is generated. In particular, with SPE integration, plasma would be generated in different electrical process and more pulsed voltage applied. The chip is made by

PDMS, thus the effects mentioned above would be greater. Eventually, the property of LEP and how it is generated affect the performance of the resulting SPE-LEP. The effective SPE needs low flow rate, whereas LEP requires high flow rate to overcome the air bubble issue [5]. Therefore the characterization of LEP generated at low flow rate is necessary.

In this chapter, liquid electrode plasma is characterized with different conditions. The DC LEP was produced with low flow rate to observe the effect of low flow rate LEP on emission intensity and on the destruction of PDMS channel was discussed. In addition, a novel liquid electrode plasma source powered by alternating current (AC LEP) has been developed for the first time. The condition to generate the AC LEP was found. Basic parameters for the novel LEP generation were characterized. Both of the two LEP sources were evaluated their performance of elemental determination. In addition, the enhancement effect of some organic additives on emission intensity was tested in order to improve sensitivity of the low flow rate LEP.

2.2. Experimental section

2.2.1. Chip design and fabrication

Fig. 2.1 (a) shows a schematic illustration of a chip. The chip includes a PDMS layer containing a microchannel in between where the plasma is generated. The PDMS layer is attached onto a glass slide or a quartz slide that is a substrate for the chip. The channel is carved on the PDMS sheet by a photolithographic technique that is described in Fabrication section. The design of the LEP channel is shown below in the Fig. 1(a). The width of the narrowest channel is 100 μm. The

depth of the channel on PDMS sheet is also 100 µm and is determined by the height of photoresist patterned on silicon wafer. The PDMS layer and the substrate are bound together by oxygen plasma. Fig. 2.1(b) shows a ready-to-use LEP chip. The large size of PDMS sheet enhances bonding with the substrate, while the large size of substrate help fix the chip on the measurement system more easily.

The fabrication was carried out in a clean room environment for semiconductor processes. The PDMS layer was fabricated by lithographic and molding methods. The fabrication process is shown in Fig. 2.2. Accordingly, a four-inch silicon wafer was cleaned with deionized (DI) water and dehydrated at 200 °C for 5 min. Permanent epoxy negative photoresist SU-8 3050 was spin-coated onto the wafer at 1400 rpm for 30 s, soft baked at 95 °C for 30 min on a hotplate, exposed to UV light, and then baked at 95 °C for 5 min on a hotplate. The wafer was cooled to room temperature. Subsequently, the channel pattern was developed with the SU8 developer and rinsed with isopropanol. PDMS with 10% mass of curing agent (curing catalyst) was cast onto the mold and cured at 75 °C for 90 min. Then, the PDMS replica sheet was peeled off. Two 2-mm diameter holes were punched at each end of the LEP channel. The obtained PDMS sheet was bound with a glass substrate by oxygen plasma bonding (75 W for 10 s). Finally, the obtained chip was tubed and pinned with two platinum electrodes (0.3 mm diameter, 5 cm long).

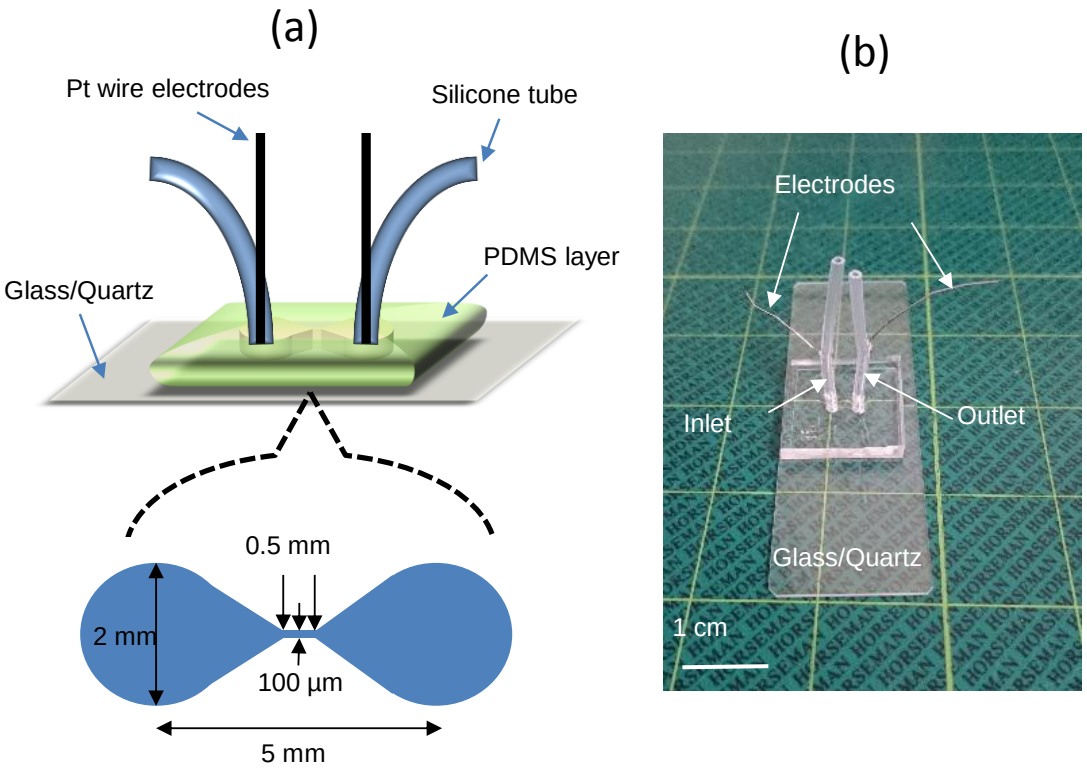

Figure 2.1 (a) Illustrative structure of a LEP chip. (b) A ready-to-use chip

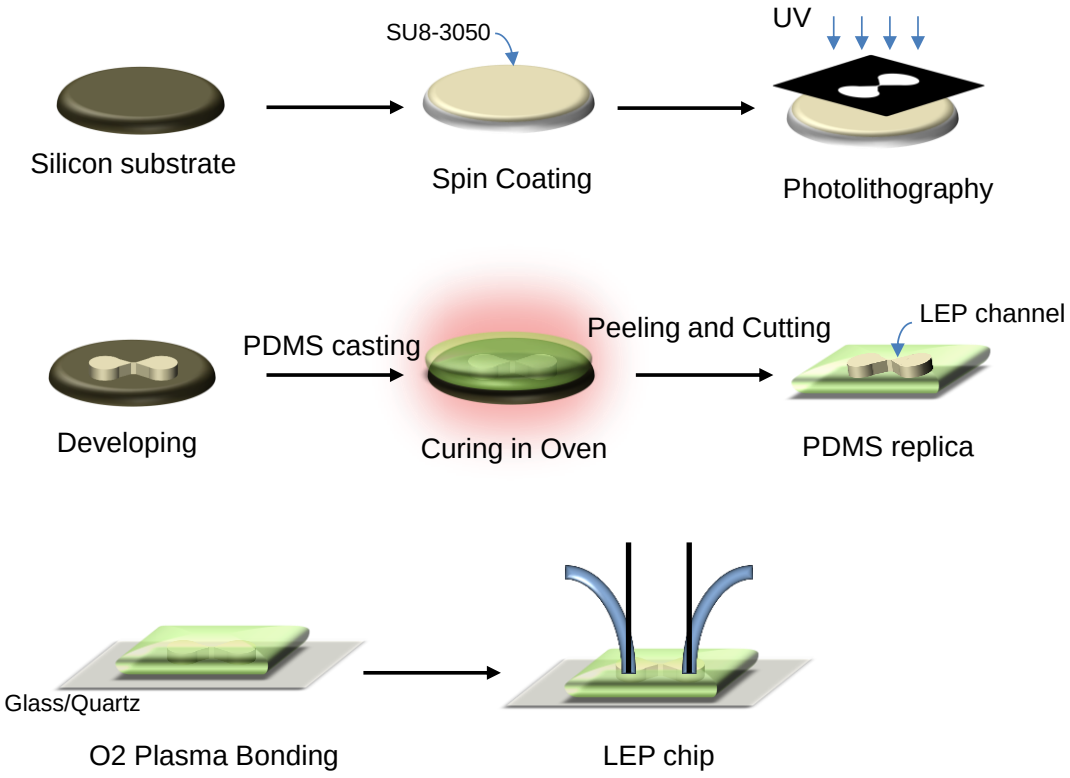

Figure 2.2 Schematic flow of a chip fabrication process

2.2.2. Reagents and chemicals

Photoresist SU8-3050 and developing solution were purchased from Nippon Kayaku, Japan, while PDMS and curing catalyst were purchased from Dow Corning Toray Silicone, Japan. Lead and cadmium standard solution (1000 mg/L, Kanto Chemical, Japan) were used as analyte of interest in our study because these elements are typical toxic metals that reportedly affect human life and environment. Sample solutions were prepared by diluting from the standard solutions with nitric acid (0.1 M; Kanto Chemical, Japan). Nitric acid (0.1 M) was also used as a blank sample. The other chemicals and materials used were of analytical grade. Mili-Q water (18.2 MΩ.cm at 25 ^{o}C) was obtained from an ultrapure water system (NANOpure Diamond, HANSEN, USA), which was used for the preparation of samples.

2.2.3. LEP measurement

For LEP measurement, the chip was fixed in a measurement system that is illustrated in Fig. 2.3. Two Pt electrodes were connected with an AC electric source (Voltage of 3 kV, frequency of 18.8 kV, Plasma Concept Tokyo, Inc). Before LEP-measured, the entire channel of the chip was cleaned by DI water flow for 10 min at a flow-rate of 100 µL/min. Sample solutions were introduced by a syringe pump. After each measurement, the electric power was turned off and the entire channel was washed by 1 mL of the upcoming sample with a flow-rate of 100 µL/min. Emission spectrums were acquired by a spectrometer (Andor Shamrock SR303i, focal length 0.303m, diffraction grating of lines 2400 lines/mm). We used Andor SOLIS software to manage the parameters of emission signal acquisition (ex. signal

acquisition time, readout rate, output amplifier, etc…). The obtained spectrums were processed with Igor software to calculate corresponding peak areas that were used for quantification of analytes.

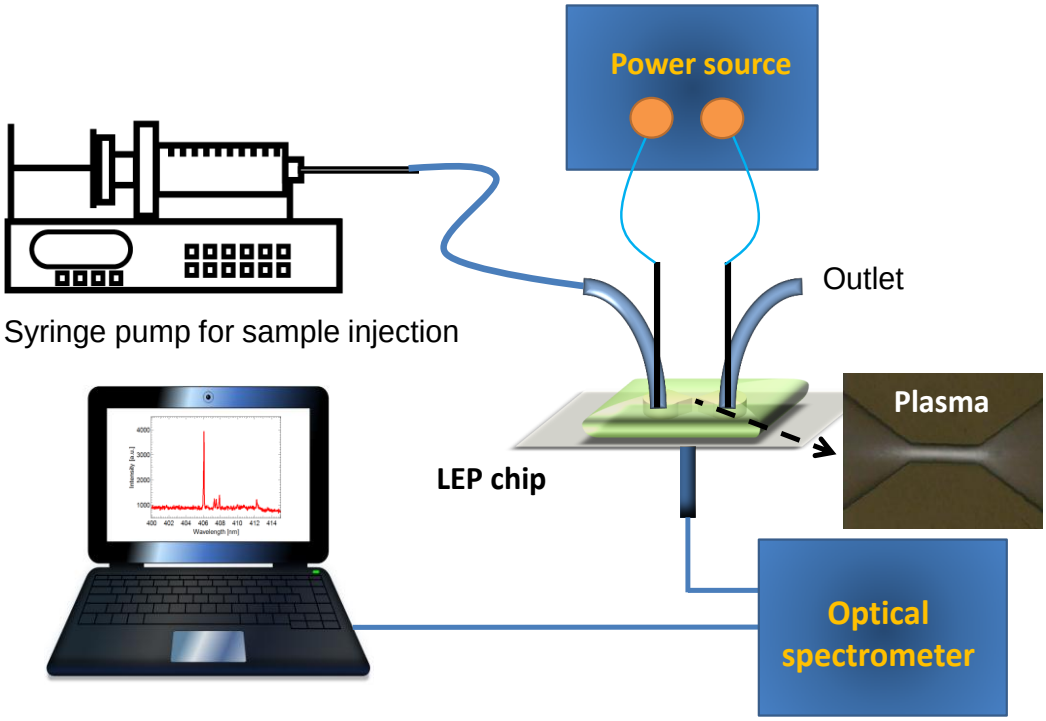

Figure 2.3 LEP measurement system.

2.3. Result and discussion

2.3.1. Characterization of direct current liquid electrode plasma generated at low flow rate

2.3.1.1. Effect of voltage

As mentioned in the introduction part, liquid electrode plasma is generated by an application of a DC voltage. Electrical field concentrated at narrow channel causes a water vapor bubble and plasma appears in such bubble. [1-6]. Thus, the voltage is a very important parameter when characterizing DC-LEP. The voltage applied affects strongly emission intensities of analytes that enter plasma.

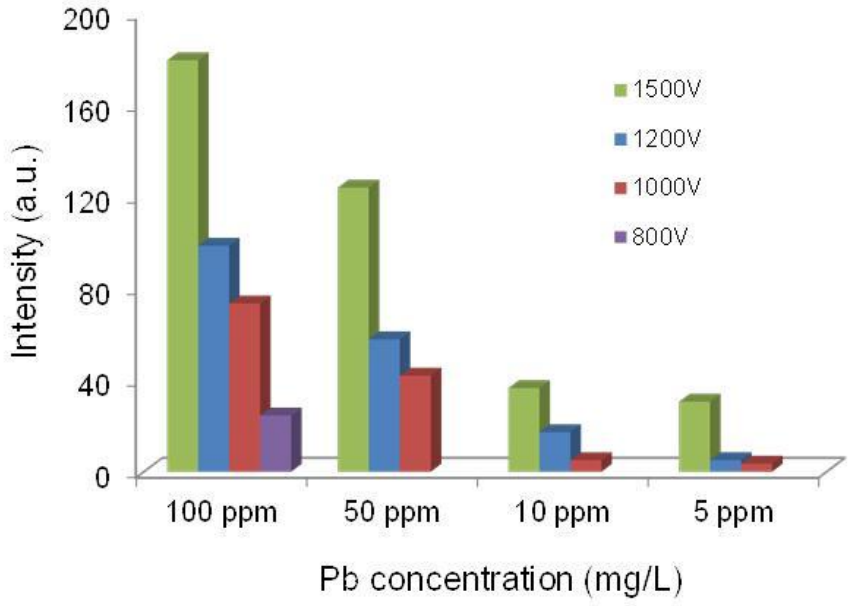

Figure 2.4 Effect of voltage applied on emission intensities. Signals were obtained with direct voltages (4 electrical pulses, one pulse includes pulse on-time of 3 ms, pulse off-time of 2 ms)[1]

Our result about the dependence of emission intensities on voltages applied is shown in Fig. 2.4. The characterization was done for lead (Pb) with different concentrations at various voltages. Signals were obtained with direct voltages (4 electrical pulses, one pulse includes pulse on-time of 3 ms, pulse off-time of 2 ms). Data points were obtained by five repeated measurements. The increase of intensity is attributed to the increase in discharge current [3] and the expansion of generated plasma volume [2]. Accordingly, Kohara et al presented a directly proportional relation between discharge current and emission intensity within one electrical pulse.

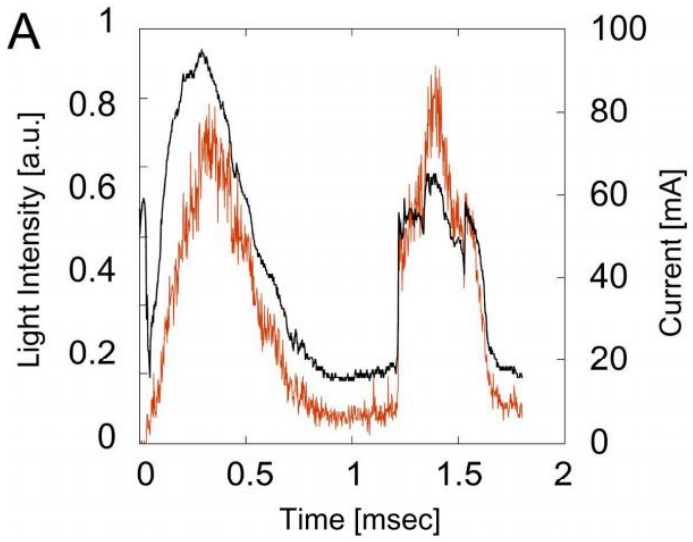

Figure 2.5 Time course of emission and current for one pulse experiment. PMT with 405-nm 10-nm-FWHM bandpass interference filter was used. Condition: 2.5 kV-1.8 msec. Sample: 100 mg/L Pb with 0.1 M nitric acid. [Fig. 6A in ref. 3]

Interestingly, the increase of voltage might not lead to increase in plasma temperature. However, the temperature of plasma is strongly affected by height of the narrow center channel [2]. According to characterization of plasma temperature by Kumai et al, The deduced excitation temperatures were 8600 K with narrower chip (h = 43 μm) and 7800 K with a broader chip (h = 77 μm). This result suggests that using a narrower chip is similar to the thermal pinch effect [2,7].

2.3.1.2. Channel destruction

The high temperature of plasma and expansion of plasma cause a damage of the narrow channel, leading to expansion of the channel and sometime. Kitano et al reported that the channel that was made by PDMS could be expanded about 1.5 times after 143 measurements (one measurement included 100 electrical pulses applied) [5]. Moreover, the emission intensity was significantly degraded after only 40 measurements. In our characterization, a significant amount of ash that was generated by burning PDMS by plasma was observed. The deformation of channel and generation of ash are further discussed in the chapter 3. Fig. 2.6 presents the channel destruction by DC LEP with different applied voltages. It is clear that the greater voltage applied is, the more the channel destruction is.

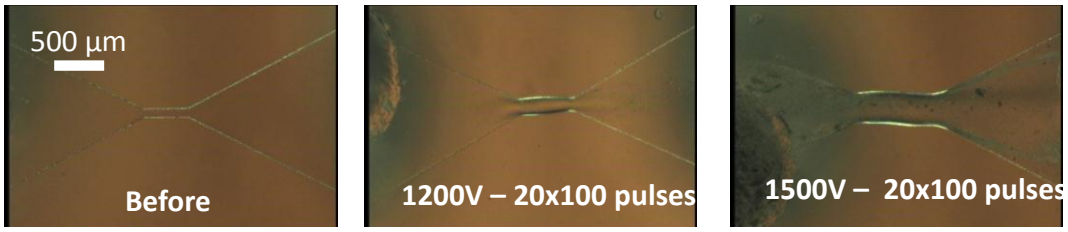

Figure 2.6 Deformation and ash generation in LEP channel with different voltages (20 cycles, one cycle includes 100 voltage pulses; 3 ms-ON and 2 ms-OFF)

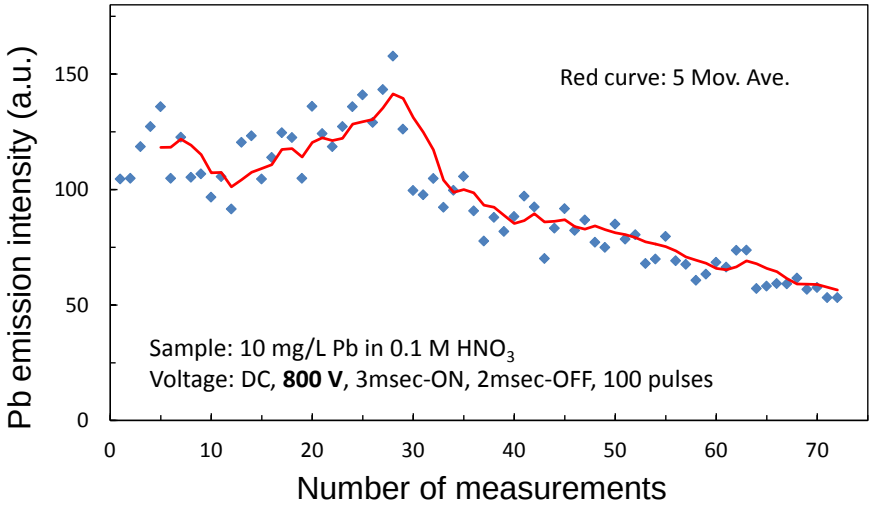

Figure 2.7 Variation of emission signal in low flow-rate DC plasma

2.3.1.3. Variation of emission signals

The figure 2.7 shows the variation of emission signal in low flow-rate DC plasma. The great variation of emission signals can be attributed to effect of air bubble still remaining in LEP channel. The decrease of emission signal is because of greater expansion of LEP channel because of poorer heat release capability due to low flow-rate. From the result, it is deduced that the repetition of LEP measurement with PDMS channel should be small in case of high voltage is utilized. Smaller voltage enables long life time of the LEP channel.

2.3.1.4. Analytical performance

In the section, the detection of Pb was performed in and without the presence of organic additive with optimized conditions. Figure 2.8 shows the calibration curve for Pb with wide concentration range. One measurement was done with 100 pulse accumulation and background subtraction. The voltage was 1500 V. The measurement was repeated 7 times at each concentration, and the average intensity, the SD, denoted by the error bars. Here, the coefficient of correlation (R^2) for the concentration range from 0.1 to 100 mg/L was 0.9995.

Figure 2.9 shows the calibration curve for Pb with concentration range from 0 to 1 mg/L. One measurement was done with 100 pulse accumulation and background subtraction. The voltage was 1200V. The measurement was repeated 7 times at each concentration, and the average intensity, the SD, denoted by the error bars. Here, the coefficient of correlation (R^2) for the concentration range from 0.1 to 100 mg/L was 0.9965. The SD for the blank solution (0.1 mol/L HNO_3) was calculated to be 2.2 au. The slope of the calibration curve of the Pb for the range

from 0.01 to 1 mg/L is 87.2 au. Thus, the LOD for Pb using PDMS chip was determined to be 52.0 µg/L (ppb).

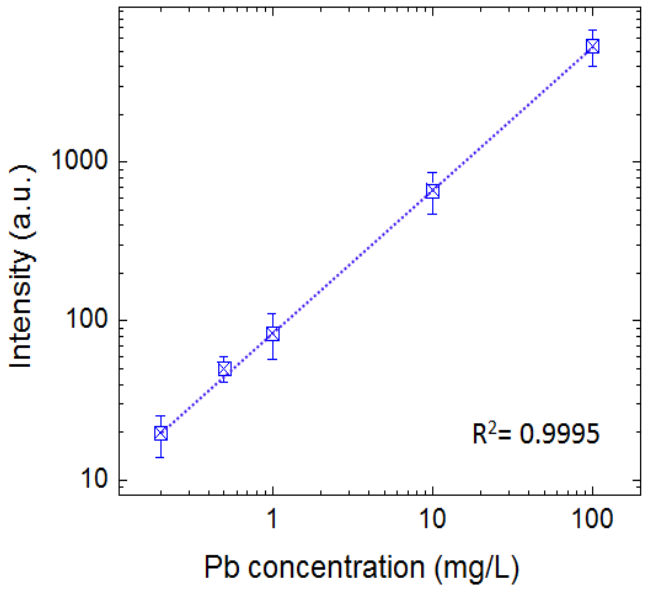

Figure 2.8 Calibration curves for Pb with wide concentration range. One measurement was done with 100 pulse accumulation. Voltage: 1500 V.

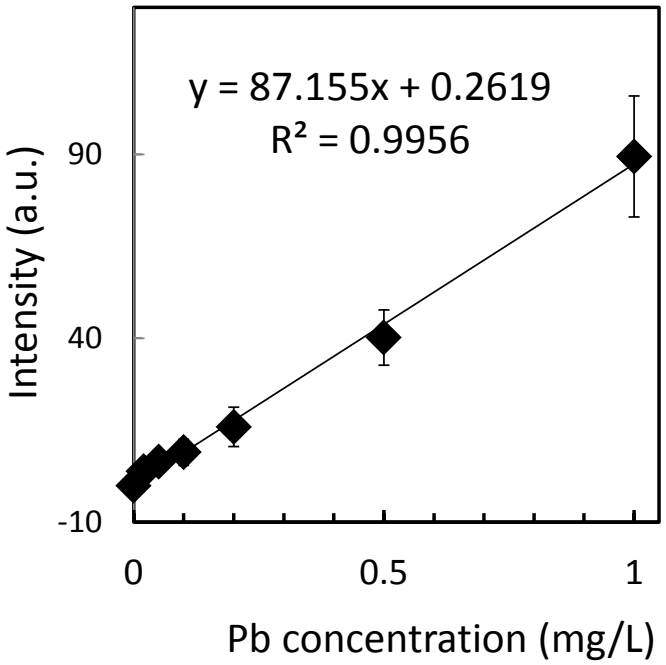

Figure 2.9 Calibration curve for Pb with concentration range from 0 to 1 mg/L. One measurement was done with 100 pulse accumulation. The voltage was 1200V.

2.3.2. Novel liquid electrode plasma driven by alternating current

2.3.2.1. Effect of flow rate and mechanism of AC LEP generation.

In the conventional DC LEP, plasma appears in a water vapor bubble that is generated by Joule heating when the voltage is applied. The water bubble is over-expanded, and then disturbs the electric flow, eventually extinguishes the plasma. As a result, plasma can occur for short time (about a few milliseconds). In the study, the AC LEP could be sustained for minutes with high stability in the liquid channel. In this study, to maintain the stable plasma in the liquid channel, flow-rate of liquid sample is crucial. The effect of flow rate on emission intensity is shown in Fig. 2.10.

Compared to DC LEP, suitable range of flow rate is narrow. The best flow rate was obtained at 30 µL/min. We chose a long integration time (10 seconds) to characterize more clearly the effect of flow-rates. The long integration time causes higher error in final results as can be seen in the Fig. 2.10.

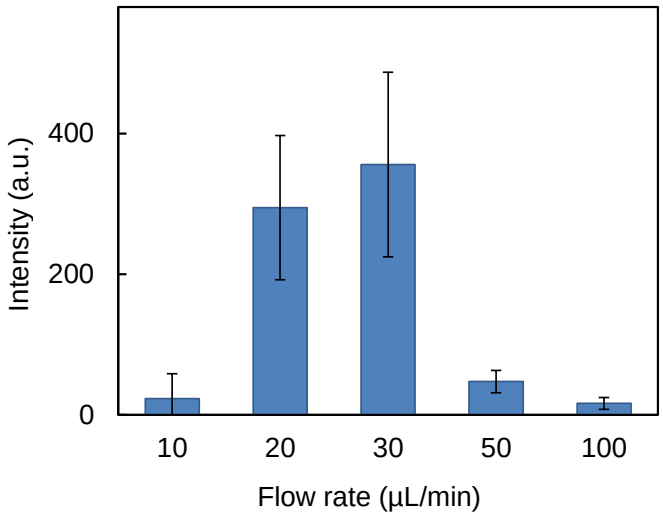

Figure 2.10 Effect of flow rate on emission signals. Sample was Pb (1 mg/L in 0.1 HNO_3). Integration time was 10 seconds. Error bar presents standard deviation (SD) of 7 replicates.

From the video recorded by high speed camera during plasma generation, we observed an air bubble remaining in the liquid channel. Because of applied voltage, the bubble is expanded and plasma appears in the bubble. Fig. 2.11 shows the states of the air bubble when it is shrunk and expanded. After that, the bubble returns the shrunk form but not disappeared. The expansion and shrinkage of the bubble follows the regulation of alternating voltage. It is deduced that an air bubble

with adequate size was always kept in the channel during plasma generation.

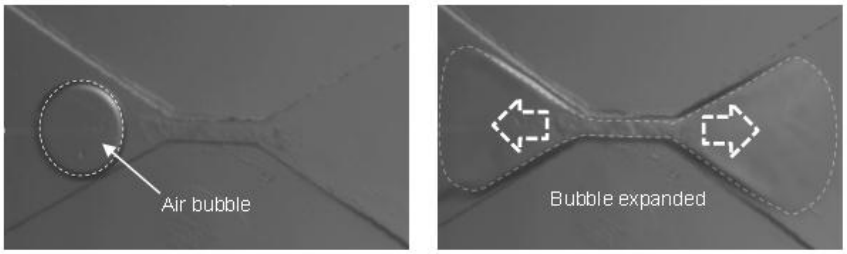

Figure 2.11 (a) An air bubble remains in the LEP channel during plasma generation. (b) Bubble expanded because of sufficiently high voltage application. The images were extracted from a video recorded by a high speed camera.

Regarding the effect of electric flow on electrolyte, when applying the voltage to the electrodes, electrolysis of water occurs at both electrodes with the simultaneous processes:

$$2H_2O \rightarrow O_2\,(g) + 4H^+ + 4e^-$$

$$2H_2O + 2e\text{-} \rightarrow H_2\,(g) + 2OH^-$$

As a result, the alternating current electrolysis of water produces a stoichiometric O_2/H_2 mixture as following combined electrolysis reaction.

$$2H_2O \rightarrow 2H_2\,(g) + O_2\,(g)$$

These electrolysis gas products (hydrogen and oxygen) generate at the two electrodes. A sample flow provided by a syringe pump drags the product gas from the upstream through the narrow channel. The gas product may contribute to the

existence of the stable air bubble in the channel. High flowrate may flush the air bubble off the channel, while low flow rate may increase the size of the air bubble. Both of the two cases lead to the instability of AC LEP. This is the reason why AC LEP generation is strongly dependent on the flow rate.

2.3.2.2. Channel destruction

Fig. 2.12 shows channel destruction before and after 10 minutes LEP generates. Interestingly the channel seems not to be changed in shape. There is only a small expansion at the narrow channel. The destruction of PDMS channel because of DC LEP has been reported. The destruction of the channel is more severe as can be clearly seen in Fig. 2.6. According to the calculation of the PDMS resin lost, channel damage by AC LEP is roughly 1/3000 less than that by DC LEP. This indicates that long life-time of device is enabled even with PDMS which is easily fabricated and integrated with other microTAS elements.

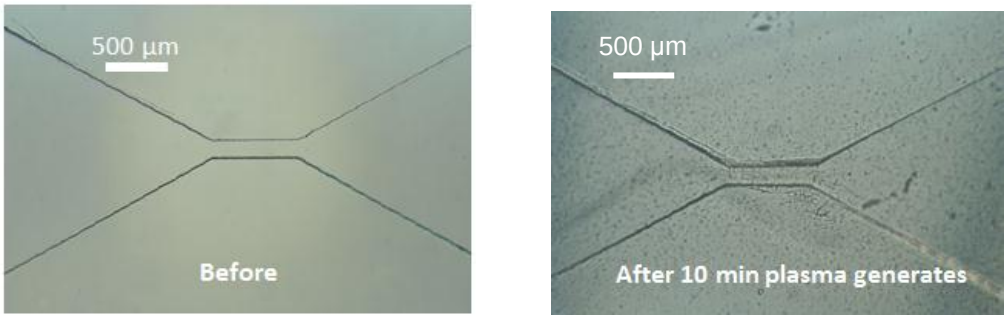

Figure 2.12 Channel destruction before and after 10 minutes LEP generates.

2.3.2.3. Emission spectra

Fig. 2.13 shows the blank emission spectra of AC LEP (red curve) and DC LEP (blue curve). The blank solution is 0.1 M HNO3. Emission spectra of DC LEP was obtained with the voltage of 900 V, 2 ms-ON, 23 ms-OFF, 20 pulses accumulated, while that of AC LEP was achieved with integration time of 2 s. Emission peaks attributed to Hβ (434.1 nm), Hγ (486.1 nm) can be seen in both cases. In addition, emission peaks corresponding with OH (262.2 nm, 343.2 nm, and 347.2 nm) can be also observed. The wide bands of OH group (260-270 nm, 280-290 nm and 306-320 nm) are clear. The results indicate that there is a similarity in emission spectra generated by LEP driven by AC and DC.

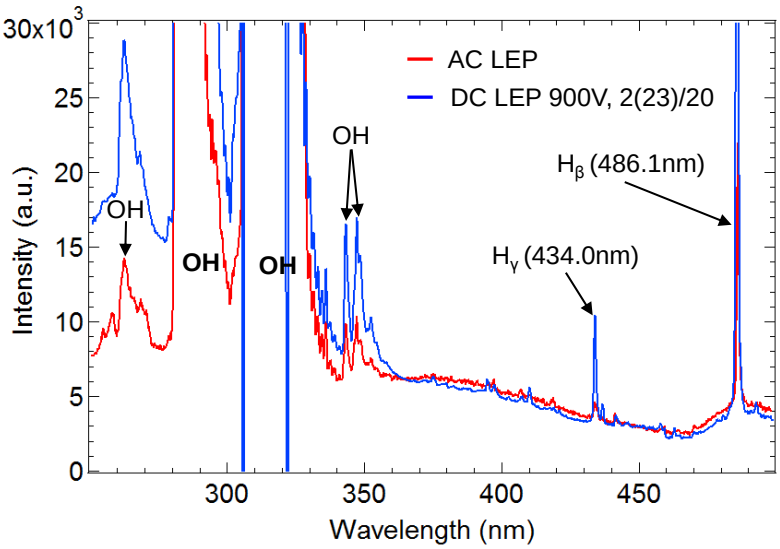

Figure 2.13 Emission spectra of 0.1 M nitric acid solution generated by AC LEP (red curve) and DC LEP (blue curve).

Fig. 2.14 shows the 20 consecutive emission spectra of Pb (1 mg/L). The sample was prepared in 0.1 M HNO3. Flow rate and integration time are 30 µL/min

and 2 seconds, respectively. The result indicates that the emission spectra are highly reproducible and the emission spectra can be used for quantitative analysis of lead.

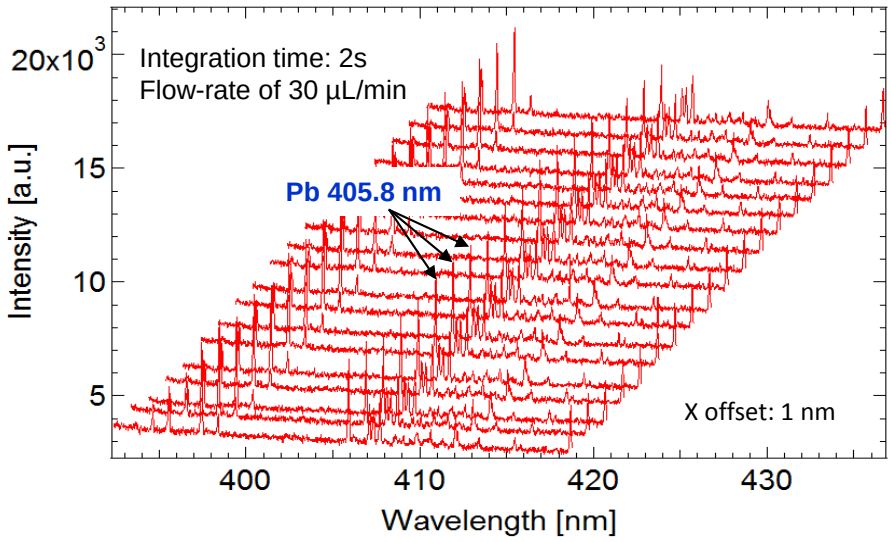

(b)

Figure 2.14 Consecutive emission spectra of 1 mg/L Pb in 0.1 M HNO_3 with optimized conditions.

2.3.2.4. Analysis performance

Lead and cadmium were chosen as analytes of interest in the study because these elements are typical toxic metals that reportedly affect human and environment. Fig. 2.15 shows the calibration curve for cadmium in the concentration range from 0.001 to 0.1 mg/L. Cd solution samples were prepared by diluting the standard solution (1000 mg/L) with 0.1 M nitric acid. The emission

signals at wavelength of 228 nm were used for quantification. Therefore, quartz substrate of the LEP chip must be used. Sample flow-rate was 30 µL/min. The integration time was one second. Data points present the mean of 9 replicates, and error bars present corresponding standard deviation from the mean. During plasma generation, liquid sample was flowing, and replications were done by internal triggering on the software (Andor SOLIS). The coefficient of correlation (R^2) for the concentration range from 0 to 0.1 mg/L was 0.9708. The SD for the blank solution (0.1 M HNO_3) was calculated to be 2.2 au. The slope of the calibration curve of the Cd for the range from 0.001 to 0.1 mg/L is 1444.9 au. From these values, the LOD for Cd with the novel plasma source using PDMS chip was determined to be 4.5 µg/L. The obtained limit of detection for Cd is about four times lower than the limit of detection for Cd using DC plasma with PDMS chip. However, the obtained value is still ten times larger than the limit of detection for Cd using DC plasma with quartz chip.

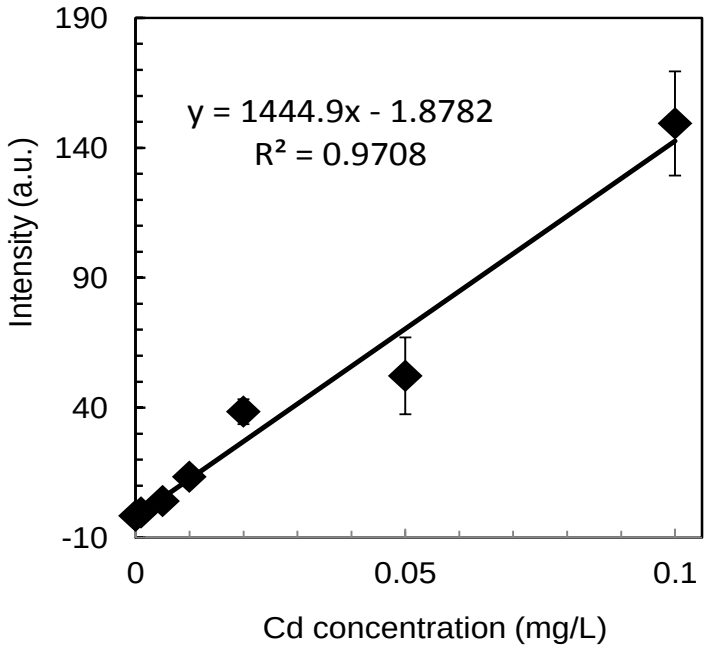

Figure 2.15 Calibration curve for cadmium. The samples were prepared in 0.1 M nitric acid. Sample flow rate was 30 µL/min.

The lead measurement was performed using the same setup. Fig. 2.16 shows the calibration curve for lead in the concentration range from 0.005 to 1 mg/L. Lead solution samples were prepared by diluting the standard solution (1000 mg/L) with 0.1 M nitric acid. The emission signals at wavelength of 405.8 nm were used for quantification. Therefore, we used a glass slide for the substrate of the LEP chip to detect Pb. Sample flow-rate was 30 µL/min. The integration time was two seconds. Data points present the mean of 11 replicates, and error bars present corresponding standard deviation from the mean. The coefficient of correlation (R2) for the concentration range from 0.005 to 1 mg/L was 0.9905. The SD for the blank solution (0.1 M HNO3) was calculated to be 2.2 au. The slope of the calibration

curve of the Cd for the range from 0.005 to 0.1 mg/L is 86.8 au, and the LOD for Pb was determined to be 75.0 µg/L. The value is the same order with limit of detection for Pb using DC LEP in quartz chips (19.02 µg/L).

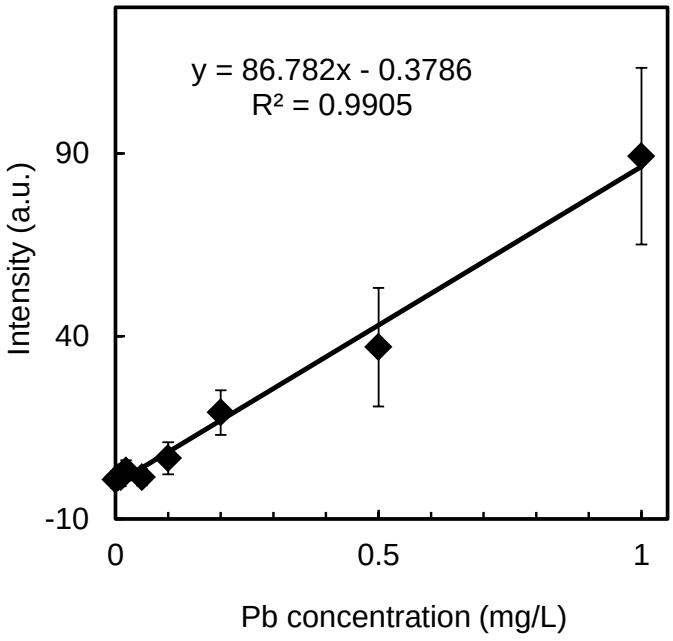

Figure 2.16 Calibration curve for lead. The samples were prepared in 0.1 M nitric acid. Sample flow rate was 30 µL/min.

2.3.3. Enhancement effect of organic additives on emission intensity

LEP is remarkably suitable with metal detection. Metal ions are often prepared in acid solutions with optimized concentrations (or pH). HCl, HNO_3 with different concentrations are often chosen as standard solution matrix for many metals. However, as reported by R. Shekhar [8] that that the ELCAD emission intensity of mercury could be enhanced by several low molecular weight organic substances. The characterization was done with different organic solvents mixed

with different nitric acid molarities. The results indicated that acetic acid results in five times improvement in the detection limit of ELCAD for mercury and thus increase in its sensitivity.

Further developing the R. Shekhar's study, Xiao et al. [9] demonstrated the significant improvement of sensitivity of ac-electrolyte atmospheric liquid discharge (ac-EALD) emission spectrometry in the presence of organic substances (formic acid, acetic acid and ethanol). With the addition of these reagents, the detection limits for Cd, Ag and Pb obtained from this method were also improved to a great extent.

In this study, I investigated that the additions of these organic reagents with different concentrations could enhance the sensitivity of LEP for lead. Formic acid, acetic acid, ethanol and methanol were selected for the characterization based on the previous studies [8,9]. The result is presented in Fig. 2.17. Each data point was repeated 7 measurements with a DC voltage of 1200 V, 100 pulses, on-time: 3 ms, off-time: 2 ms. 1 mg/L lead was used as sample and flow was kept constant at 0.1 mL/min. According to the result, all the selected additives have enhancement effect to emission intensities but with different extents. In the tested concentration range, the additions of ethanol and methanol gave a great improvement at the same levels; however, ethanol addition is better at reproducibility of emission signals (lower SD) than methanol addition. The simple addition resulted in a great improvement in performance of LEP.

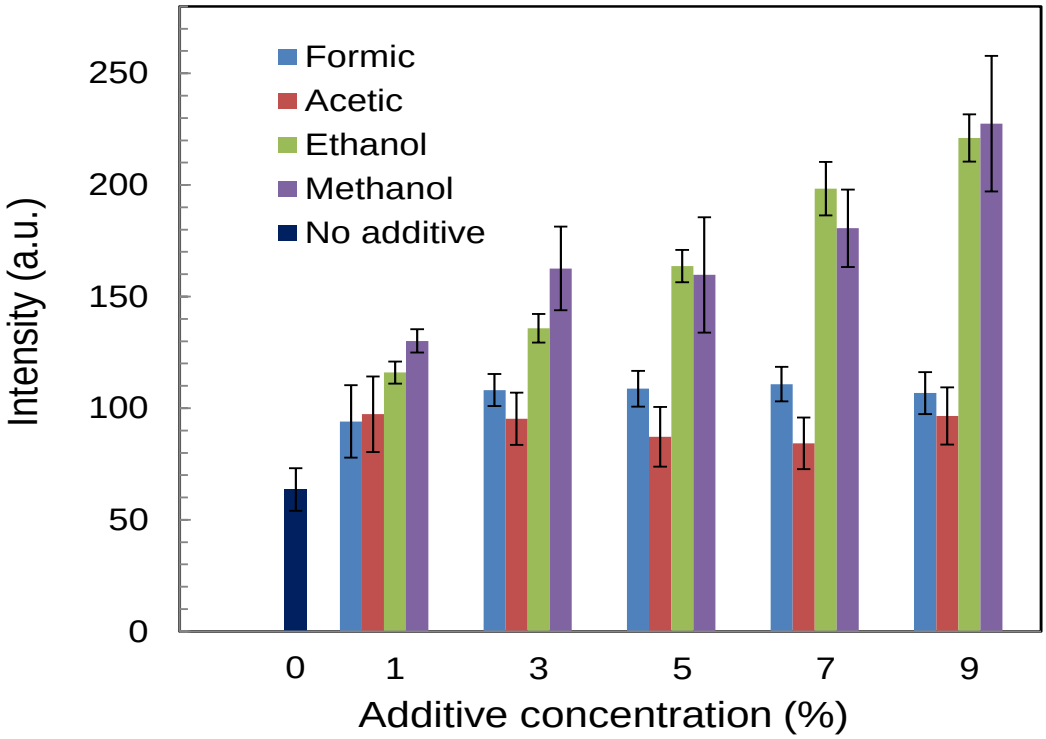

Figure 2.17 Enhancement effect of different organic substances (formic acid, acetic acid, ethanol and methanol) on the emission intensity of Pb. (HNO_3 molarity of 0.1 M, flow rate: 0.1 mL/min, voltage: 1200 V, 100 pulses, on-time: 3 ms, off-time: 2 ms) Error bars in the figure represent standard deviations of seven replicates.

Figure 2.18 shows the calibration curves for Pb with concentration range from 0 to 1 mg/L in the presence of 10 % ethanol. One measurement was done with 100 pulse accumulation and background subtraction. The voltage was 1200V. The measurement was repeated 7 times at each concentration, and the average intensity, the SD, denoted by the error bars. Here, the coefficient of correlation (R^2) for the concentration range from 0.1 to 100 mg/L was 0.9922. The SD for the blank solution (0.1 mol/L HNO_3) was calculated to be 2.1 au. The slope of the calibration curve of the Pb for the range from 0.01 to 1 mg/L is 258.3 au. Thus, the LOD for Pb using PDMS chip was determined to be 24.4 μg/L. The result indicated that the addition of 10 % ethanol enhanced slope of calibration about 2 times, whereas the SD was similar, thus LOD was improved about two times. The LOD is with the same order of magnitude with LOD for Pb using quartz chip [5]. The simple addition of organic substances resulted in a great improvement in performance of LEP.

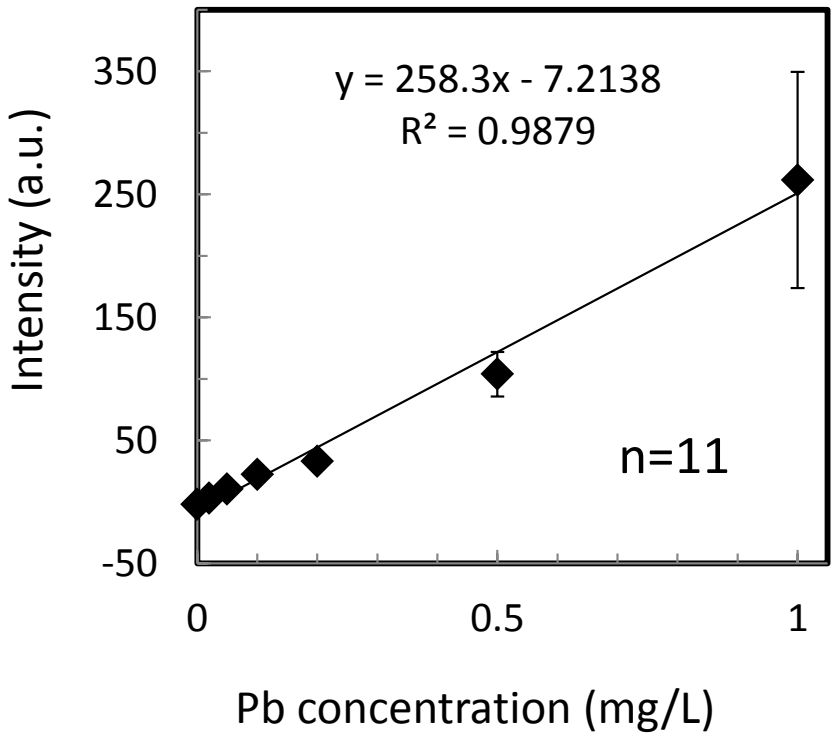

Figure 2.18 Calibration curve for Pb with concentration range from 0 to 1 mg/L in the presence of 10 % ethanol. One measurement was done with 100 pulse accumulation. Voltage: 1200V.

To characterize the effect of organic substances on the AC LEP source, we prepared sample solutions with different percentages of acetic acid, formic acid, and ethanol. Then the samples were performed AC LEP measurement. We investigated that acetic acid and formic acid helped enhance the emission intensities as shown in Fig. 2.19. The measurement was done with Pb samples with constant concentration of 1 mg/L in 0.1 M HNO_3. Additives were mixed into samples with different percentages (form 1% to 9%). We also investigated that ethanol caused instability in

plasma generation, thus did not support to signal enhancement.

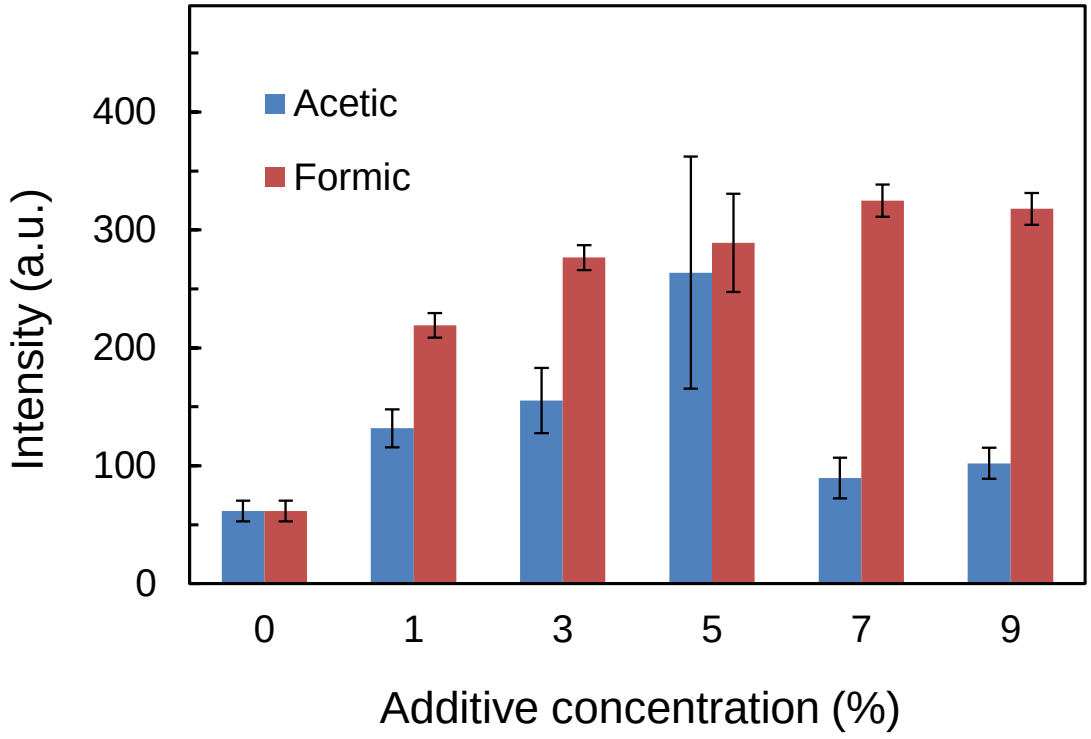

Figure 2.19 Enhancement effect of different organic substances (formic acid and acetic acid) on the emission intensity of Pb (1 mg/L). HNO_3 molarity of 0.1 M. Error bars in the figure represent standard deviations of seven replicates.

The enhancement effect of formic acid addition was investigated, thus we applied for Pb detection. Fig. 2.20 shows calibration for Pb in the presence of 3% (v/v) formic acid. The presence of formic acid enhanced the emission intensity, so that the slope of the calibration is about three times greater. The presence of the organic substance could improve plasma stability resulting in low standard deviation in general. As a final result, the LOD was improved. It was computed to be 19.1 μL/min.

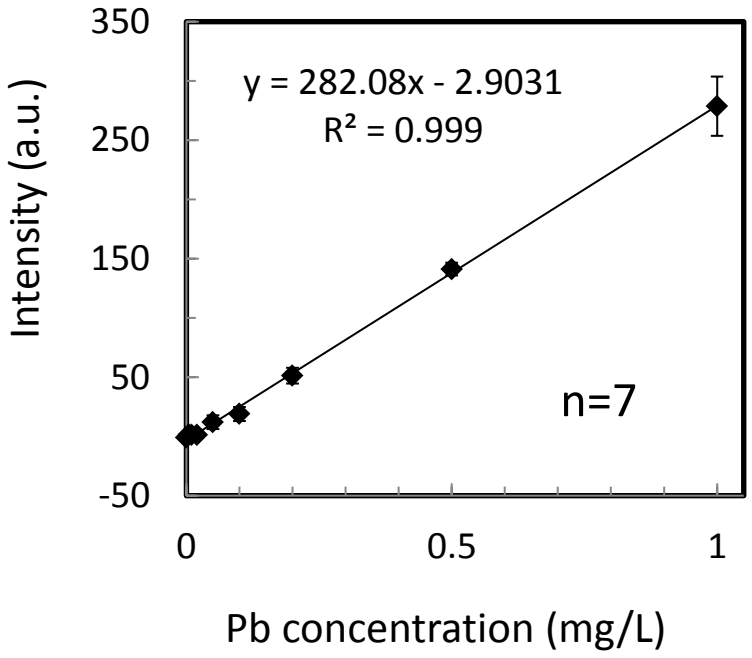

Figure 2.20 Calibration curve for Pb in 0.1 M nitric acid with 3 % v/v formic acid. Exposure time was 2 sec. Sample flow-rate was 30 μL/min.

2.3.3. Discussion

DC LEP is a conventional method with more than a decade of development and optimization. A pulsed direct voltage and high flow rate were applied increase reproducibility of emission signals. After each measurement, the LEP channel must be washed up and filled up by the fresh sample. This is ensured no air gap or air bubbles between two electrodes that may disturb the plasma generation. Low flow rate may cause the problem on the ineffective air bubble removal leading to highly variant emission intensity. Moreover, low flow-rate DC plasma causes more damage of LEP channel because heat release is not effective with low flow rate. For the integration with SPE, the channel destruction should be taken into great care.

In the attempt to find the condition to generate LEP that is suitable with SPE integration, I have tested LEP powered by alternating current resulting in a novel plasma source (AC LEP). The best condition was found to produce AC LEP in liquid channel with continuous mode. The hypothesized mechanism of AC LEP has been explained with the aid of graphic results. The interesting point of the novel plasma source is that it does not cause severe channel destruction. In addition, it is capable of generating at the flow rate as low as 30 µL/min. These two characteristics may enable a more simple combination with SPE.

Both DC LEP and AC LEP can be generated within microfluidic chip platforms. It is advantageous because the chip design has high capability of being easily modified to integrate other elements into the chip. In the next chapters, we present the integration of SPE column for preconcentration and other elements as

well. According to the investigated characteristics of two types of plasma, the suitable chip design for integration can be deduced.

In comparison to other liquid discharge systems as shown in table 2.1, the developed method is as sensitive as the others, but simply fabricated and performed. All the listed methods have sensitivity at the same level with ICP-AES reported by Hill [13].

Table 2.1 Analytical characteristics of AC-LEP and DC-LEP using PDMS and other liquid discharge systems.

	λ (nm)	ac-EALD LOD (μg/L) [9]	ac-EALD with formic LOD (μg/L) [9]	ELCAD LOD (μg/L) [12]	SCGD LOD (μg/L) [11]	DC-LEP Quartz chip LOD (μg/L) [5]	DC-LEP PDMS chip LOD (μg/L)*	AC-LEP PDMS chip*
Pb	405.8	281	45	45	6	19.0	52[a], 24[b]	75[a], 19[c]
Cd	228.8	163	17	5	2	0.52	-	4.5[a]

(*) This work

(a) Without additives

(b) With 10% ethanol

(c) With 3% formic acid

2.4. Conclusion

In this chapter, the basic parameters of LEP generated in PDMS platform were characterized in different conditions. Low flow rate LEP causes highly variable emission intensity leading to worse analytical performance. Low flow rate also causes greater destruction in channel.

A novel plasma source using alternating current has been developed for the first time (AC LEP). The AC-LEP could be maintained for long time in PDMS channel with the same chip layout with DC LEP. The best condition was found to generate the novel. The hypothesized mechanism of plasma generation was discussed.

Both types of plasma sources have been evaluated their sensitivity in detection of metals. The obtained sensitivities were generally lower than conventional high flow rate LEP.

The enhancement effect by the addition of organic substances on analytical performances of both AC and DC LEP was investigated. The addition of the suitable organic substances is helpful to improve sensitivity of both DC LEP and AC LEP.

Finally, based on the results of the characterization, the strategies of the combination with SPE were adopted. The developments of the combination are presented in chapter 3 and chapter 4 of the thesis.

2.5. References

[1] D. V. Khoai, A. Kitano, T. Yamamoto, Y. Ukita, and Y. Takamura, **Microelectron. Eng.** 111 (2013) 43–347.

[2] M. Kumai and Y. Takamura, **Jpn. J. Appl. Phys**. 50 (2011) 096001.

[3] Y. Kohara, Y. Terui, M. Ichikawa, T. Shirasaki, K. Yamamoto, T. Yamamoto, and Y. Takamura, **J. Anal. At. Spectrom**. 27 (2012) 1457-1464.

[4] M. Banno, E. Tamiya, and Y. Takamura, **Anal. Chim. Acta**, 634 (2009) 153-157.

[5] A. Kitano, A. Iiduka, T. Yamamoto, Y. Ukita, E. Tamiya, and Y. Takamura, **Anal. Chem.** 83 (2011) 9424–9430.

[6] D. V. Khoai, T. Yamamoto, Y. Ukita, and Y. Takamura, **Jpn. J. Appl. Phys**. 53 (2014) 05FS01.

[7] S. Greenfield, IL Jones, CT Berry, **Analyst**, 89 (1964) 713–720.

[8] R. Shekhar, **Talanta**, 93 (2012) 32-36.

[9] Qing Xiao, Zhenli Zhu, Hongtao Zheng, Haiyang He, Chunying Huang, Shenghong Hu, **Talanta** 106 (2013) 144-149.

[10] L. A. Currie and G. Svehla, **Pure Appl. Chem.** 66 (1994) 595-608.

[11] Michael R. Webb, Francisco J. Andrade, and Gary M. Hieftje, **Anal. Chem.** 79 (2007) 7899-7905.

[12] R. Shekhar, D. Karunasagar, Manjusha Ranjit, and J. Arunachalam, **Anal. Chem.** 2009, 81, 8157–8166.

[13] Hill, S. J.; Fisher, A.; Foulkes, M., Inductively Coupled Plasma Spectrometry and Its Applications, 2nd ed.; Hill, S. J., Ed.; Blackwell Publishing Ltd.: Oxford, 2007; pp 61-97.

Chapter 3

Integration of solid phase extraction with direct current driven liquid electrode plasma using an pneumatic micropump

Abstract

In this chapter, a simply designed internal pneumatic injection pump was developed and employed as a fluid actuator for direct current driven liquid electrode plasma integrated with solid phase extraction. The internal pump can be easily operated by an automated pneumatic pressure controller and is capable of injecting a reproducible amount of eluent for each measurement cycle of SPE-LEP. Additionally, the pump acted as a valve to stop the backflow caused by the high pressure created by plasma generation. More precise flow control by the internal pump helped improve the precision of the measurements. For data processing, exponentially modified Gaussian model was utilized to describe the elution peaks. The limit of detection for lead (0.4 ng/mL) was 50 times improved in comparison with conventional LEP. The proposed method and data processing model can be used to develop on-chip detection applications for methods that utilize pulsed micro-plasma sources.

3.1. Introduction

Nowadays, elemental analysis is commonly used to detect the contamination of water by heavy metals. The most popular and powerful tools for elemental analysis are inductively coupled plasma atomic emission spectrometry (ICP-AES) [1], inductively coupled plasma mass spectrometry (ICP-MS) [2], and atomic absorption spectrometry (AAS) [3]. These methods are highly sensitive and accurate; however, they are expensive and not suitable for on-site applications owing to their size and bulky support instruments. To develop miniaturized devices portable enough for on-site analysis, liquid-electrode dielectric barrier discharge (LEDBD) [4-6], electrolyte cathode discharge (ELCAD) [7,8], liquid-electrode spectral emission chip (Led-SpEC) [9], liquid-electrode plasma (LEP) [10,11]) microplasmas, among others, have been developed. Among them, LEP possesses some advantages. Accordingly, an LEP channel was completely miniaturized on a compact microfluidic chip so that the design could be easily modified for various purposes; for example, the LEP-based chip can be integrated into microvalves and micropumps for fluid control. This integration enables the potential development of LEP-based lab-on-a-chip devices. Additionally, LEP is comparable with conventional ICP in terms of excitation temperature and electron density [12,13].

Regarding the mechanism of LEP, the microplasma is formed by the electrical discharge when a DC pulsed voltage is applied to both ends of a microchannel that has a narrower channel (LEP channel) at the center. The principle of LEP-OES is illustrated in chapter 1. The LEP channel is first filled with an electroconductive liquid sample. When the voltage is applied, the electric field

concentrates at the LEP channel and the solution is subjected to localized Joule heating. Subsequently, water is evaporated, which forms a water-vapor bubble. The plasma appears in the bubble. The elements in the liquid sample enter the plasma and emit light with element-specific wavelengths, which is then analyzed with an optical spectrometer for qualitative and quantitative determination of elements [14-19,24,25].

The critical issue with LEP-OES is its insufficient sensitivity. To resolve this issue, Kitano et al. fabricated the chip from quartz glass, a harder material than polydimethylsiloxane PDMS; this significantly improved the sensitivity. However, the method is time consuming and laborious, and produces toxic wastes [15].

Another approach for improving the sensitivity is the integration of a solid-phase extraction (SPE) column with LEP-OES to preconcentrate the sample [24,25]. In this approach, the analyte of interest is retained by the solid-phase resin and is subsequently eluted in a more-concentrated form. Because of the liquid-handling capabilities of microchip devices, an SPE column can be easily integrated into microfluidic systems [21-23]. This approach exploits the easily modified structure of PDMS-based microchips. Because LEP is a pulsed excitation source, the plasma is generated on a millisecond timescale; therefore, elution cannot be performed continuously. Instead, the eluent is divided into small aliquots, each corresponding to a measurement cycle, and an external syringe pump is used to introduce the aliquots into the device. However, the presence of the resin-packed SPE column and the elasticity of the PDMS narrow channel delay pumping and lead to unpredictable response times.

In this study, we realized an internal pneumatic micropump with a simple structure and a simple operation method for more precise control of fluids, which is suitable for use with the highly sensitive SPE-LEP technique. The pneumatic micropump functioned as a fluid injector for introducing the aliquots of the eluent to the LEP channel without causing any delay; it also functioned as a valve to prevent backflow from the LEP channel during plasma generation. The pumping performance was examined to ensure these functions. The pump structure has been reported previously [26,27]; in this study, the pump structure is modified for more effective performance when integrated with the SPE-LEP chip. After characterization and optimization, the SPE-LEP chip with the internal pump was applied for lead detection. For data processing, an exponentially modified Gaussian (EMG) model was utilized to describe the elution peaks, which resulted in a better fit than the previous averaging model. The measurement protocol is proved to be suitable with pulsed DC LEP.

3.2. Experimental

3.2.1. Chip design

The pneumatic membrane-based micropump was developed by using a pump formed by two pneumatic valves for constant volume injection, an idea proposed by Shimomura et al. [26]. The pump consists of normally closed active valve and a normally-closed passive valve. Accordingly, the pump has two air chambers in the pneumatic layer, two floating block structures in the fluid channel (flow layer), and a 50-µm-thick PDMS intermembrane (Fig. 3.1 (a) and Fig. 3.1 (b)). The membrane can be deflected up and down to actuate the pumping when negative

and positive pneumatic pressures are cyclically applied. The working principle is illustrated in Fig. 2(a). When compressed air is applied to the active valve, the resulting flow pressure is transmitted to the passive valve, leading to rise in the membrane and opening the passive valve so that the liquid flows toward the LEP channel. On the contrary, if vacuum is applied, an instant drop in flow pressure closes the membrane at the passive valve and stops the backflow. Moreover, the pressure drop can drag the liquid from the SPE column into the pump chamber. The passive valve of the pump suppresses this backflow, thus preventing the deterioration of the general pump performance. The pumping structure also enables a more simple pumping operation than other reported pneumatic pump structures [28-30].

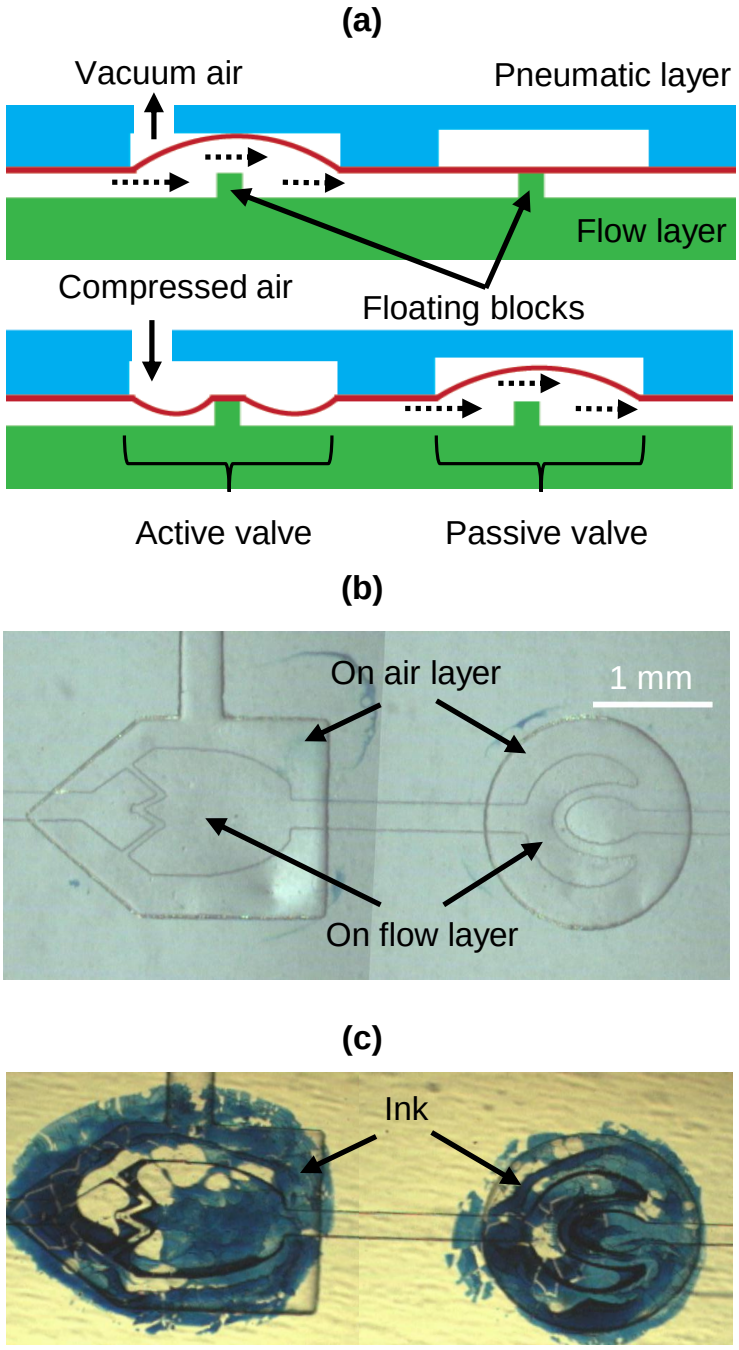

Figure 3.1 Schematic illustration of design and working principle of micropump. (a) Side view with working principle of micropump, dashed arrows present the fluid direction; (b) Top view of the pump region after cleaned. (c) Pump region with ink.

The original pump design catered to droplet formation in a microchannel; therefore, some modifications had to be made to the pump design for the SPE-LEP application in order to deal with high back pressure, more flow resistance from the SPE column, and sticking issues between the membrane and the floating blocks. The plasma treatment for bonding the PDMS layers caused the sticking problem; as a result, the membrane could not deflect properly. Hence, we applied marker-pen ink to the floating blocks and the corresponding region on the membrane to prevent the formation of the sticky deposit during the bonding treatment, as shown in Fig. 3.1 (c). The ink can be easily washed out by ethanol (100%). The final pump pattern used in our work was obtained from several designs under the consideration of the mentioned issues.

The SPE-LEP chip consists of five layers: a glass substrate (bottom layer), an LEP layer, an SPE layer, a PDMS membrane, and a pneumatic top layer. Fig. 3.2 (a) illustrates the plan views of the four layers: the LEP layer, the flow layer, the PDMS membrane, and the pneumatic layer; Fig. 3.2 (b) shows a schematic side view of the entire SPE-LEP chip. The dimensions of the SPE chamber are as follows: width, 2 mm; length, 10 mm; and depth, 350 μm; these dimensions correspond with a compact resin volume of 7 μL (the same as our previous work [25]). Two comb-like filters fixed the resin beads in the SPE chamber. The two pneumatic chambers had the same depth as the connecting flow channel (100 μm). The shape and size of the LEP channel are the same as those reported in our previous work [25] (200 μm wide, 500 μm long and 100 μm deep). The open angle of the LEP channel is 45°. The distance between the two electrodes is 4 mm. All

holes for the inlets and outlets had a diameter of 2 mm. Fig. 3.2 (c) shows an integrated SPE-LEP chip before the addition of the tubing.

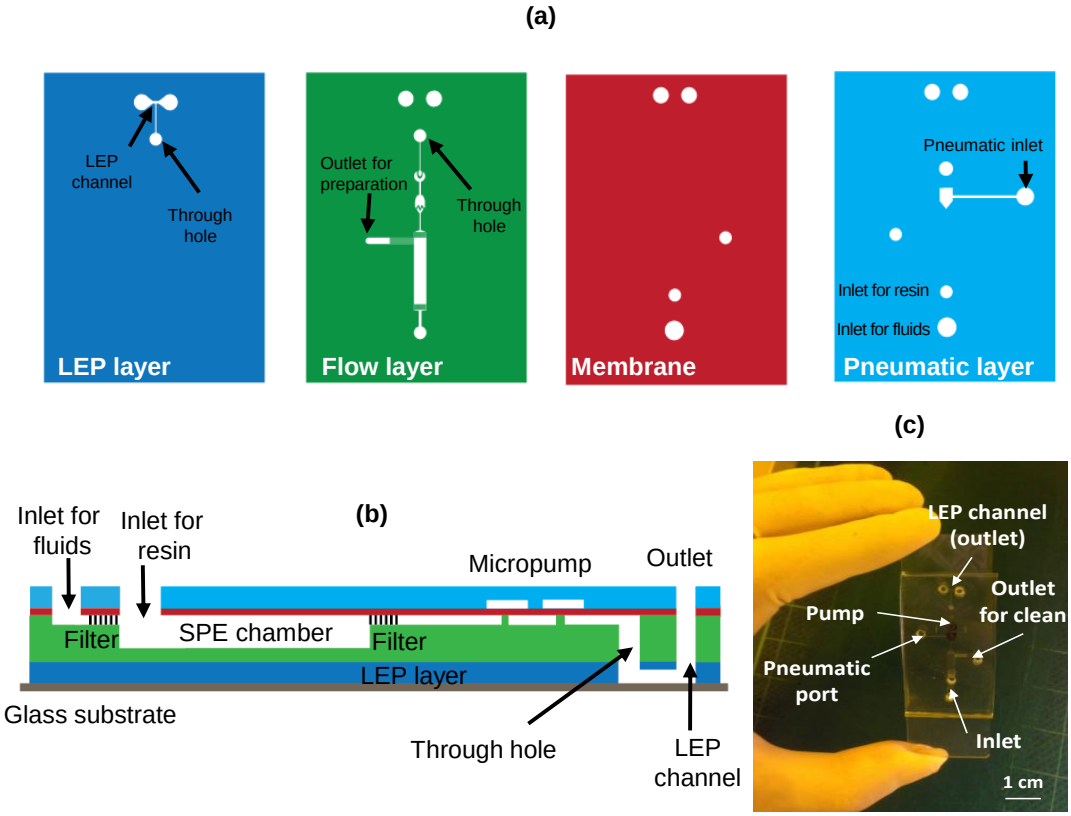

Figure 3.2 Schematic structure of SPE-LEP chip.
(a) Plan view of layers. (b) Side view. Five layers were attached by oxygen plasma bonding. (c) LEP-SPE chip before tubing.

3.2.2. Chip fabrication

The fabrication was carried out in a clean room environment for semiconductor processes. The PDMS layers were fabricated by lithographic and molding methods. The fabrication process for the flow layer is shown in Fig. 3.3. Accordingly, a four-inch silicon wafer was cleaned with deionized (DI) water and dehydrated at 200 °C for 5 min. Permanent epoxy negative photoresist SU-8 3050 (Nippon Kayaku, Japan) was spin coated onto the wafer at 1400 rpm for 30 s, soft baked at 95 °C for 30 min on a hotplate, exposed to UV light (first exposure), and then baked at 95 °C for 5 min on a hotplate. The wafer was cooled to room temperature, spin coated with SU-8 2100 (Nippon Kayaku, Japan) at 1000 rpm for 30 s, soft baked at 65 °C for 6 min and 95 °C for 60 min on a hotplate, exposed to UV light (second exposure), and then baked at 65 °C for 2 min and 95 °C for 15 min on a hotplate. The patterns were aligned with a mask aligner (PEM-800, Union Optical, Japan). Subsequently, the wafer was treated with the SU8 developer and rinsed with isopropanol. The obtained master mold has different height channels: 350 µm for the SPE chamber and 100 µm for the LEP channel. PDMS (Dow Corning Toray Silicone, Japan) with 10% mass of curing agent (curing catalyst) was cast onto the mold and cured at 75 °C for 90 min. Then, the PDMS replica sheet was peeled off. The through hole was punched with a 1.2-mm diameter needle. Two 2-mm diameter holes were punched at each end of the LEP channel. The fabrication of the LEP layer and the pneumatic layer was similarly carried out. A 50-µm-thick PDMS membrane was prepared by spin coating the PDMS gel (mixed with a curing agent in a 1:10 mass ratio) onto the surface of a Petri dish with a spin rate of 1400 rpm for 30 s, and then the dish was baked at 75 °C for 90 min. The

thickness of the membrane was controlled by the spin rate. After a separate fabrication, the layers were attached, and then bound with a glass substrate by oxygen plasma bonding (75 W for 10 s). Notably, the floating blocks were covered by marker-pen ink prior to oxygen plasma treatment so that they did not bind with the membrane. The ink was easily washed by ethanol, as shown above in Fig. 2. Finally, the obtained chip was tubed and pinned with two platinum electrodes (0.3 mm diameter, 5 cm long).

3.2.3. Chemicals and reagents

Lead-selective resin Analig Pb-01 (60–100 mesh; absorption capacity = 0.20 mmol/gram; GL Sciences Inc, Japan) is a proprietary polymeric organic material containing sequestering ligands that are highly selective for lead in acidic media with relatively high concentrations of other interfering ions. Lead sample solutions were prepared by diluting a standard solution (1000 mg/L; Kanto Chemical, Japan) with nitric acid (0.1 M; Kanto Chemical, Japan). Nitric acid (0.1 M) was used as a blank sample. The EDTA solution (0.03 M; pH 9) was prepared from an ammonium chloride buffer solution and ethylenediaminetetraacetic acid dihydrate (Dojindo, Japan) as follows: the buffer solution was prepared from ammonium chloride (5.64 g; Kanto Chemical, Japan) in a saturated aqueous solution of ammonia (48 mL; Wako, Japan) and the EDTA solution (0.03 M; 100 mL) was obtained by adding ethylenediaminetetraacetic acid dihydrate (0.88 g) and buffer solution (6 mL) to ultrapure water (94 mL). The EDTA solution (0.03 M) was also used as a cleaning buffer between the samples. The other chemicals and materials used were of analytical grade.

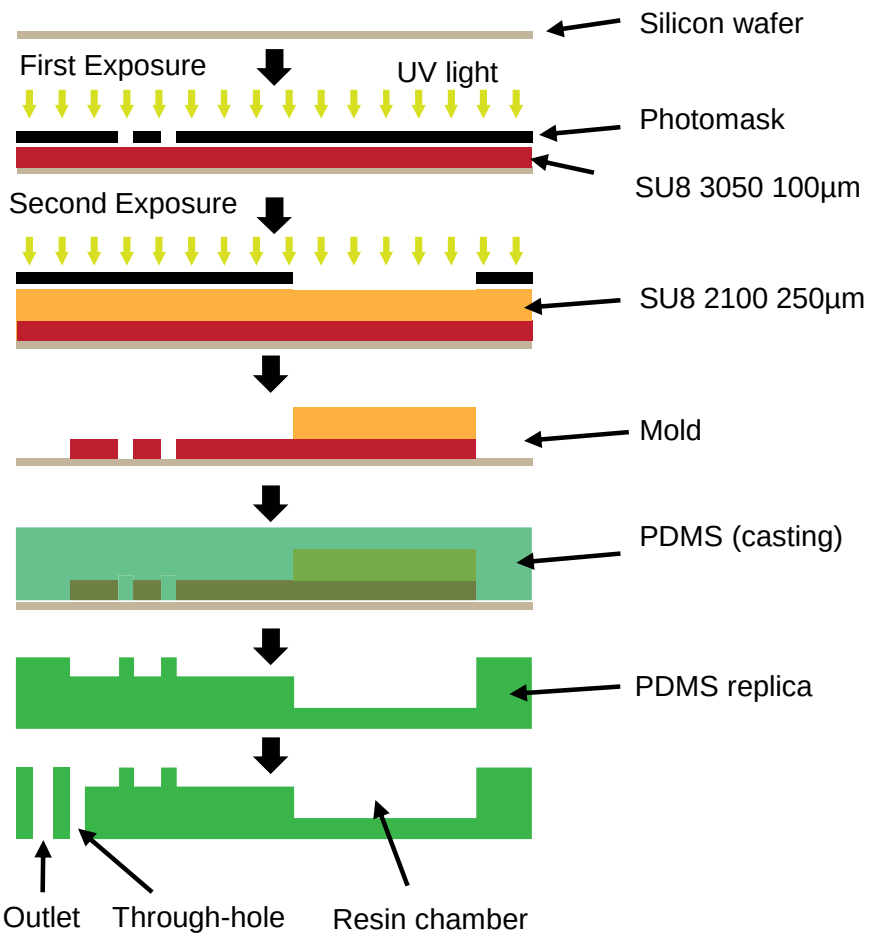

Figure 3.3 Schematic diagram of lithographic fabrication of flow layer.

3.2.4. Measurement procedure

3.2.4.1. Preconcentration

First, the entire microchannel was washed with ethanol (100%) and then with DI water. The SPE resin was packed into the column using a syringe, aided by a vacuum pump connected to the outlet, and the resin-loading inlet was closed. The resin was washed with EDTA solution (0.03 M) and DI water, and then the sample solution (1 mL; Pb in 0.1 M HNO_3) was introduced to the SPE column by a syringe pump at flow rate of 20 µL/min (the loading rate was optimized using the method described in a previous report with the same SPE chamber dimensions [25]). After cleaning with DI water (50 µL), the preparation outlet was closed, and the chip was set up in the measurement system. The entire channel, including the micropump and LEP channel, was filled with a saturated aqueous ammonia solution (50 µL, pH 9) at flow rate of 10 µL/min by using a syringe pump. The LEP channel was washed and prefilled with the EDTA solution (0.03 M). Finally, a 1-mL-pipette tip containing the EDTA solution (0.03 M) as an eluent was attached to the inlet. It was ensured that no air bubbles appeared in the channel.

The measurement setup is depicted in Fig. 3.4. The chip was fixed on the chip holder and connected to a DC-voltage supply (Nissei-Giken, Japan). An oscilloscope was connected to the power source to check the voltage and current. LEP-OES traces were acquired by a linked spectrometer (Andor Shamrock SR303i, Andor Technology, UK). Two syringe pumps were connected to enable the cleaning of the LEP channel by using the cleaning buffer after each measurement

cycle. The micropump was driven by a specifically built pneumatic pressure controller.

3.2.4.2. LEP Measurement

The LEP-OES measurement was performed during elution and was divided into “measurement cycles”. One measurement cycle started with cleaning the LEP channel with the cleaning buffer (15 µL) by using the two syringe pumps, as shown in Fig. 5. Then, an aliquot of the eluent was pumped into the LEP channel by 10 pumping cycles (eluent volume/measurement cycle was about 0.9 µL). Subsequently, a voltage of 1000 V with 20 electrical pulses was applied to the two electrodes to ignite microplasma, which was utilized as the atomization source for OES. Accordingly, for one measurement cycle, a small amount of eluent was consumed and an optical signal was obtained. The next measurement cycle was repeated from the injection of the cleaning buffer into the LEP channel. This ensured that the eluent engaged in LEP is renewed after each measurement cycle and minimized the influence of the previous cycle. The LEP measurement was performed until no emission signal could be observed. Generally, it takes about 40–50 measurement cycles for one analysis.

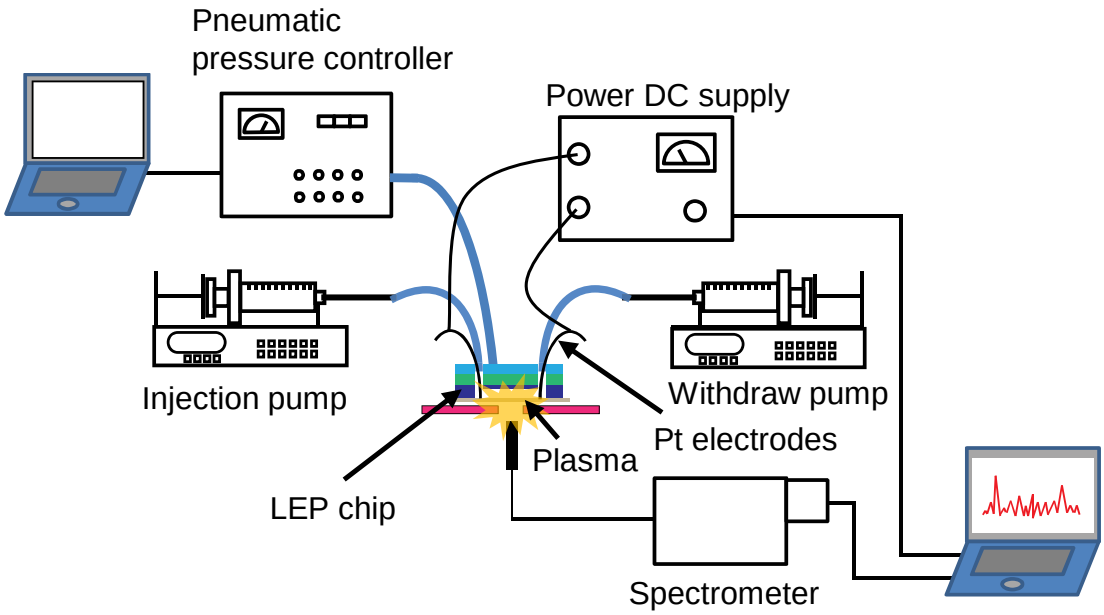

Figure 3.4 Measurement setup.

3. 3. Results and discussion

3.3.1. Characterization and optimization of the micropump

The performance of the micropump was characterized. Air pressures (±200 hPa) with a frequency of 0.25 Hz were applied to run the pump. The pressure was optimal to prevent the gas permeability of PDMS through the membrane to flow channel, and low frequency is more convenient to count the number of pumping cycles for subsequent SPE-LEP measurement.

The pumping performance was first characterized with the observation of the behavior of the eluent during pumping. Fig. 3.5(a) shows the time-lapse photos of one pumping cycle. The photos were extracted from a video captured at the T-junction of the channels. It can be seen from the time-lapse photos that the fluid started to flow about 0.2 seconds after it was actuated by the pump. The result showed that the proposed micropump could actuate the fluid with lower response time compared to syringe pump. The video attached in the Supplementary Information shows the fluid flow during the pump operation, which was captured at the channel between the pump and the LEP channel. The fluid was visualized by fluorescent beads. It can be seen that the liquid flow was well controlled by the pump as the flow movement was regulated by the pneumatic pressure sequence. The fluid flows for three seconds and immediately stops for one second, corresponding with pneumatic regulation (positive pressure for three seconds and negative pressure for one second). With the micropump, there is no delayed flow as referred in the introduction part. This delayed flow is the reason of low reproducibility in the SPE-LEP integration as we have reported when using syringe

pump [25]. The internal pump has overcome such delayed flow problem. These features of the pump (smaller response time and capability of delayed flow suppression) are essential to accurately actuate the eluent for SPE-LEP measurement.

The volume discharged by a pumping cycle was measured. A programmable pneumatic pressure dispenser was connected to a computer-controlled internal pump. Only one pneumatic control line was used to simplify the operation and avoid failure during the pneumatic programmed control. One up-down pulsation of the membrane denotes one pumping cycle. To determine the volume ejected by a pumping cycle, a zigzag channel (100 μm in depth and 400 μm in width) with fixed interval markers was located ahead of the pump as a scale system, and the volume pumped per cycle was calculated from the length of channel occupied by one pumping cycle, as shown in Fig. 3.5(b). The fluid was colored red by adding safranin (1%). The discharged volume of one cycle was 90 nL, with a relative standard deviation of 2%, as obtained by averaging the volumes of 10 consecutive pumping cycles. We have also characterized the volume with different back-pressures. The results indicated that the pump could produce high reproducible discharged volume with different back pressure.

Optimization of the number of pumping cycles was performed for effective use of the eluent. If the number of pumping cycles is insufficient, the cleaning buffer may dilute the eluent. On the contrary, too many pumping cycles cause wastage of the eluent, leading to excessive use of the sample. Dilution of the eluent by the cleaning buffer was observed in the early pumping cycles, but once the

amount of the eluent became sufficient, the dilution diminished. The observation of a colored fluids shows that five pumping cycles are sufficient. For other tests with LEP measurement, the eluent was introduced with different numbers of pumping cycles (1, 3, 5, 10, and 20); then, a voltage was applied to generate an emission signal. The result is shown in Fig. 3.5(c). Each measurement was repeated three times. The emission intensity increases as the number of pumping cycles increases up to 10. It implied a dilution when the number of pumping cycles was less than ten. Afterwards, the intensity is unchanged, because the dilution is effectively diminished. Therefore, ten pumping cycles for one measurement cycle was optimal. More pumping cycles did not increase the emission intensity; instead, it only caused wastage of the sample.

The forward leakage test was performed to check the performance of the internal pump as a valve. There is a possible flow that may leak from the SPE column to LEP channel due to the gravity of the eluent solution because the eluent was contained in a pipette tip placed at higher position than LEP channel. The lead sample (10 μg/mL, in 0.03M EDTA solution) was introduced from the SPE channel to the LEP channel by the pump. After the pump closed and cleaning by buffer solution (0.03 M EDTA solution) was carried out, the LEP measurement was performed. The results of lead intensity immediately after cleaning and 30 s after cleaning are shown in Fig. 3.5 (the inset). The emission intensity after 30 s was about 10% of that for lead with the concentration of 10 μg/mL. In addition, no clear leakage was observed with an optical microscope in the test with colored fluids. Thus, we supposed that the negligible lead signal was due to diffusion of high

concentration lead from the short channel between the pump and the LEP channel to the LEP channel and it increased over time. In case of no valve in between, the eluent flowed up through the chip with an estimated flow rate of about 50 μL/min. This indicated that the internal pump is an effective valve to suppress the leakage of the eluent.

The micropump also overcomes the back flow problem. The problem was observed when we used the zigzag channel to separate the LEP channel and the SPE column without the internal pump [25]. The backflow with high pressure during plasma generation affected the eluent flow. First, the backflow frequently push the ash that generated by burning of PDMS at LEP channel to the branch of SPE column, and probably hinder the eluent flow. Second, the backflow may bring air bubble to SPE resin, and then deteriorate the elution. With the internal pump, the backflow problem by LEP generation has been overcome. No effect of the backflow on SPE channel was observed. The backflow is suppressed not only by the close state of the pump but also the flow resistance and capacitance of the micropump.

In LEP, air bubbles are a serious issue, as mentioned in previous reports [15,25]. The plasma cannot be reproducible if the air bubble is present in the LEP channel. Air bubbles in the LEP channel mainly originated from the plasma generation and can be washed out of the channel by a flow of cleaning buffer from the side syringe pump [24,25,27]. Air bubbles dissolved in the eluent or generated by the gas permeability can be trapped in the dead space of the pump or in the through hole.

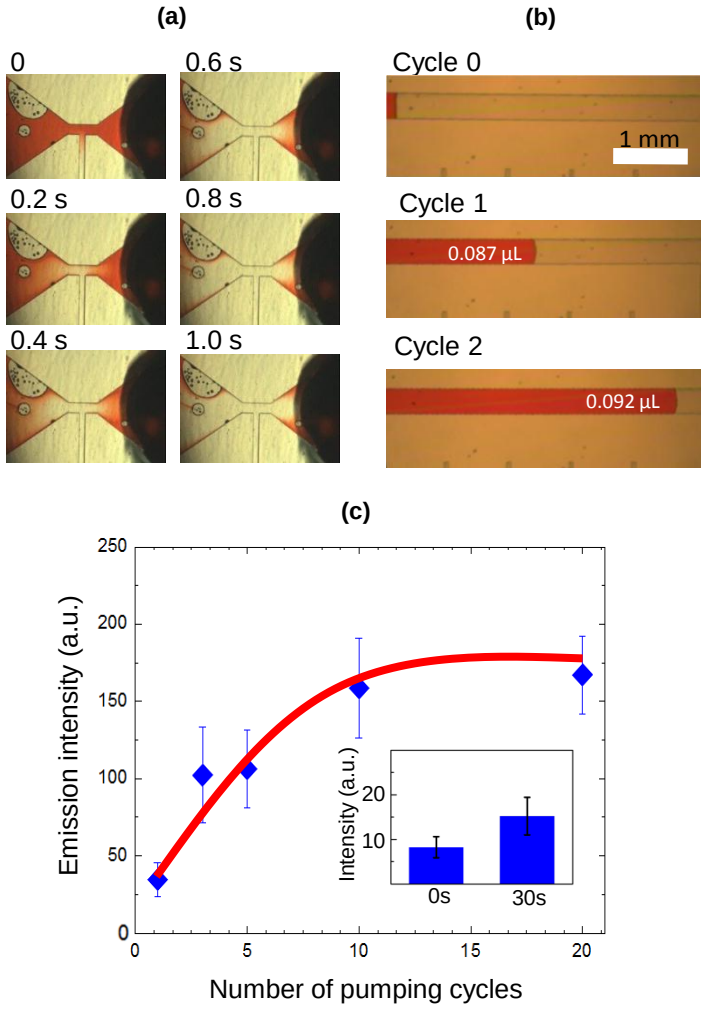

Figure 3.5 Characterization of the internal micropump. (a) Time course of one pumping cycle (1 s); (b) illustration of one cycle volume measurement; (c) optimization of the number of pumping cycles and leakage after 0 and 30 s (inset)

3.3.2. Optimization of parameters for plasma generation

3.3.2.1. Voltage

Voltage is the power source used to generate discharge plasma in the liquid microchannel. Because the SPE-LEP chip was made of PDMS, the original shape of the LEP channel was deformed because of the high-temperature plasma, which caused low reproducibility of the emission signals, as reported in earlier studies [15,25]. The ash generated by a significant amount of burnt PDMS adhered to the channel wall could cause higher back pressure, thus influencing the transport of fluids. Ash generation and channel deformation are dependent on the voltage applied and pulse accumulation (number of pulses per voltage application or measurement cycle). Moreover, ash build-up and channel deformation can accumulate due to repeated voltage application for the measurements. The ash issue is more critical when using an on-chip micropump, because the high flow-rate of the cleaning buffer could not be used to wash the ash. Thus, the voltage and pulse accumulation must be taken into greater consideration to minimize the amount of ash. Various voltages with different pulse accumulations were tested. The results showed that the amount of ash formed and the extent of LEP channel deformation were closely related to the voltage applied. When the voltage was 1200 V, the LEP channel notably expanded with a significant amount of ash after 50 cycles (Fig. 3.6 (a)). LEP channel deformation and ash generation were diminished if a voltage of 1000 V was used; in fact, the amount of ash was minimal, as shown in Fig. 3.6 (b). Thus, the voltage of 1000 V was deemed optimal for further experiments.

3.3.2.2. Electrical pulse accumulation

The effect of the number of pulses on the precision of the emission intensity was investigated. Without SPE preconcentration, lead (10 µg/mL) in EDTA solution (0.03 M) was introduced to the LEP channel by a syringe pump, and then a voltage of 1000 V was applied. The result is shown in Fig. 3.6 (c). The precision was evaluated by a reversed relative standard deviation of five responses; the LEP measurement accumulated from 20 electrical pulses showed the greatest precision. The optimized pulse accumulation depends on the architecture of the LEP element (distance between the two electrodes, dimension of the LEP channel, etc.). When the pulse accumulation was increased, the emission signal increased; however, precision decreased. Moreover, the increase in pulse accumulation boosted ash generation and channel deformation. Thus, a 20-pulse accumulation was optimal for lead detection.

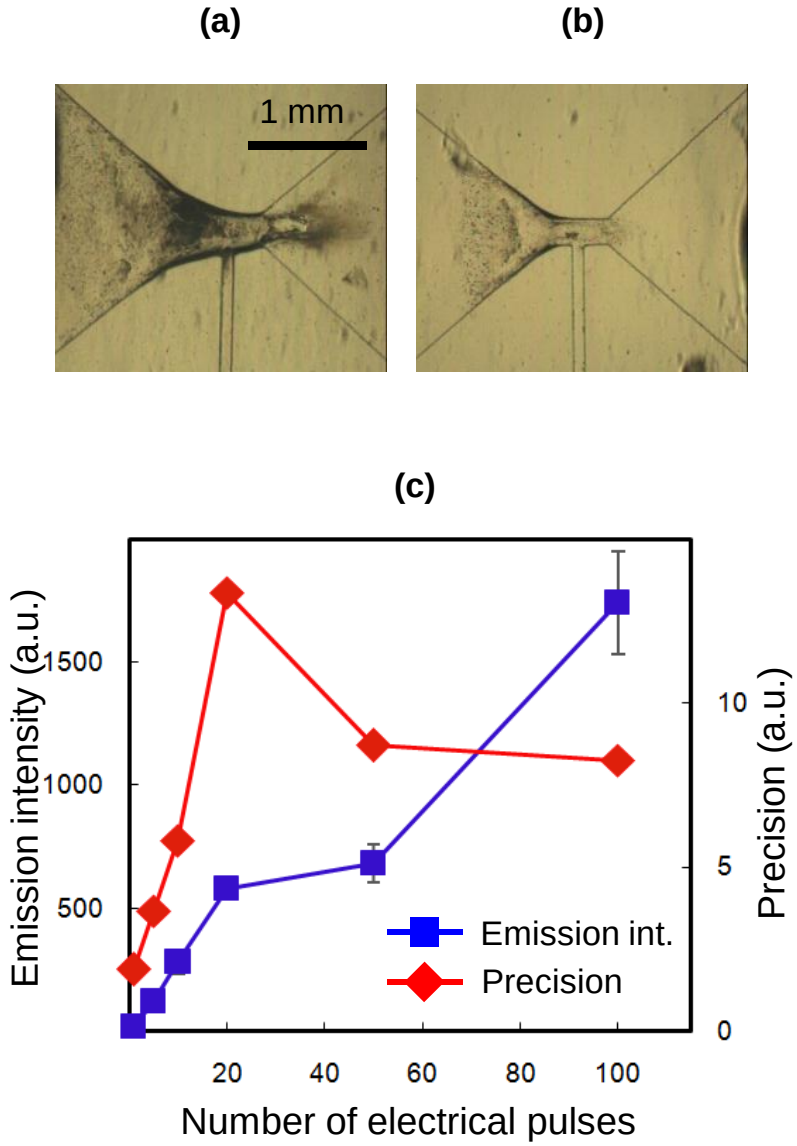

Figure 3.6 Optimization of the voltage. (a) LEP channel after application of 1200 V; (b) LEP channel after application of 1000 V; and (c) optimization of the number of electrical pulses. Blue: emission intensity; red: precision (reversed standard deviation of five responses).

3.3.3. Application to lead detection

After characterization and optimization, the integrated chip was applied for lead detection. Table 3.1 shows the optimized conditions for the analysis. Because the structures of the LEP channel and SPE column were kept the same, the sample volume and sample-loading rate were applied, as in our previous work [25]. The sample pH for SPE preparation was the same as that used in a previous study with the same SPE resin [34]. The voltage pulse on-time and off-time used by Kitano for lead detection by conventional LEP were applied [15]. SPE preparation and LEP measurement were performed as described in the Experimental section.

According to the proposed measurement protocol, a single emission peak was obtained after each measurement cycle. Thus, a set of emission peaks was obtained after a complete measurement. Fig. 3.7 (a) shows a typical single emission peak. The emission peak areas were calculated for each single emission peak (Igor 6.4, WaveMatrics Inc.). A series of emission peaks (Fig. 3.7 (b)) was obtained for a complete measurement, consequently, a series of emission peak areas was achieved. A plot of the emission peak areas versus measurement cycle is shown in Fig. 3.7 (c); the results indicate the change in the lead concentration during each measurement cycle (measurement-cycle-dependent intensity). The measurement-cycle-dependent intensity was fitted with an EMG model, as illustrated by the red curve in Fig. 8(b). The EMG model was in good agreement with the eluted peaks or chromatograms obtained by the SPE and chromatographic methods, respectively [31-33]. This model was used because it takes the tail of elution peak into consideration so that it can more precisely describe the elution. In our work, the

EMG curve is an elution peak; the elution peak area (the area under fitting curve) was obtained and used for quantization.

Table 3.1 Optimized parameters for lead detection by using the proposed method.

Preparation	
Sample volume	1 mL
pH of Sample	1 (in 0.1 M HNO_3)
Sample loading rate	20 µL/min
Elution	
Eluent	EDTA (0.03 M, pH 9)
Cleaning buffer	EDTA (0.03 M, pH 9)
Cleaning volume per cycle	15 µL
Pulsed DC voltage	
Voltage	1000 V
Voltage pulse on-time	3 ms
Voltage pulse off-time	2 ms
Electrical pulses per measurement cycle	20
Micropump	
Pneumatic program (pressure and frequency)	±200 hPa, 0.25 Hz
Number of pumping cycles	10

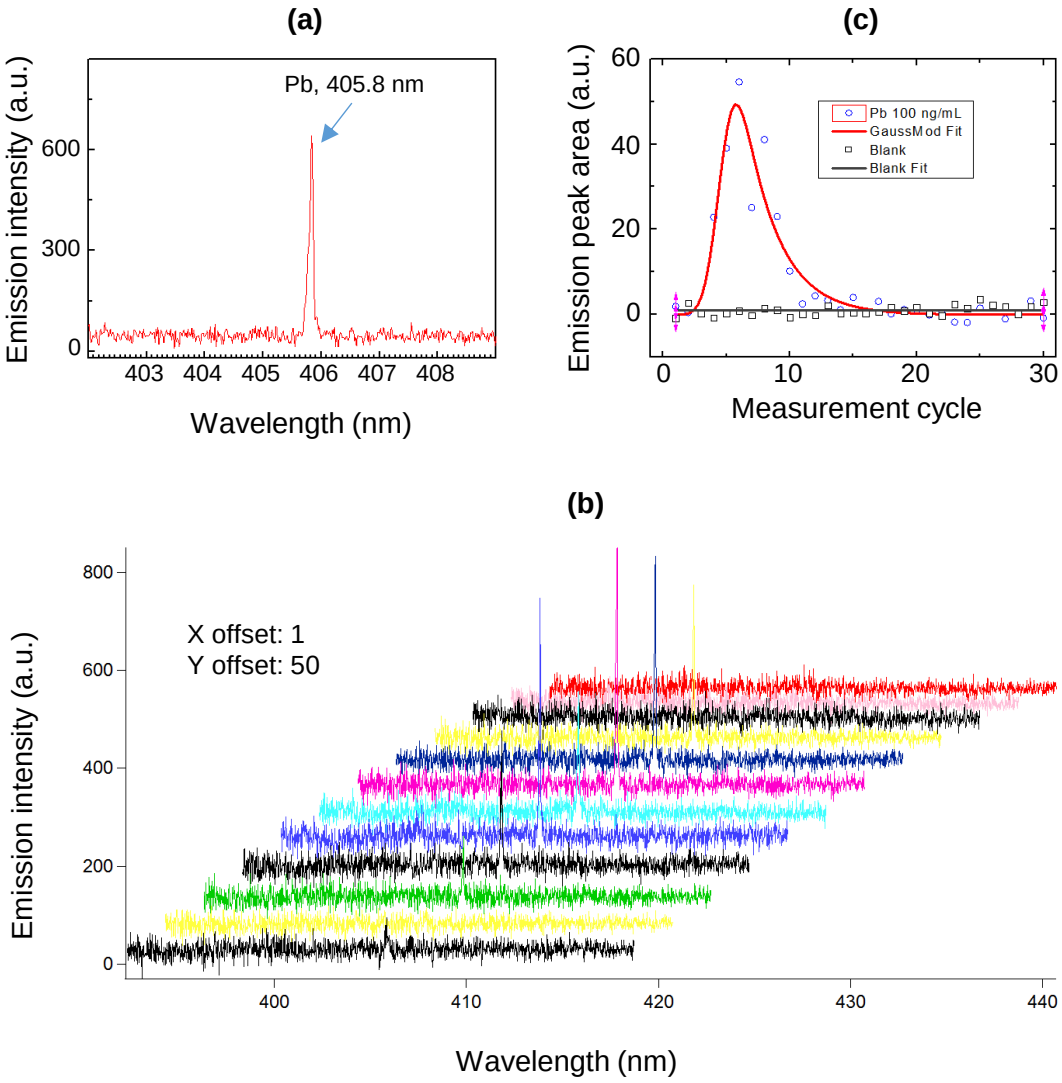

Figure 3.7 Illustration of data processing. (a) A typical single emission peak, (b) A series of emission peaks, (c) An elution peak; the red line is the EMG fit

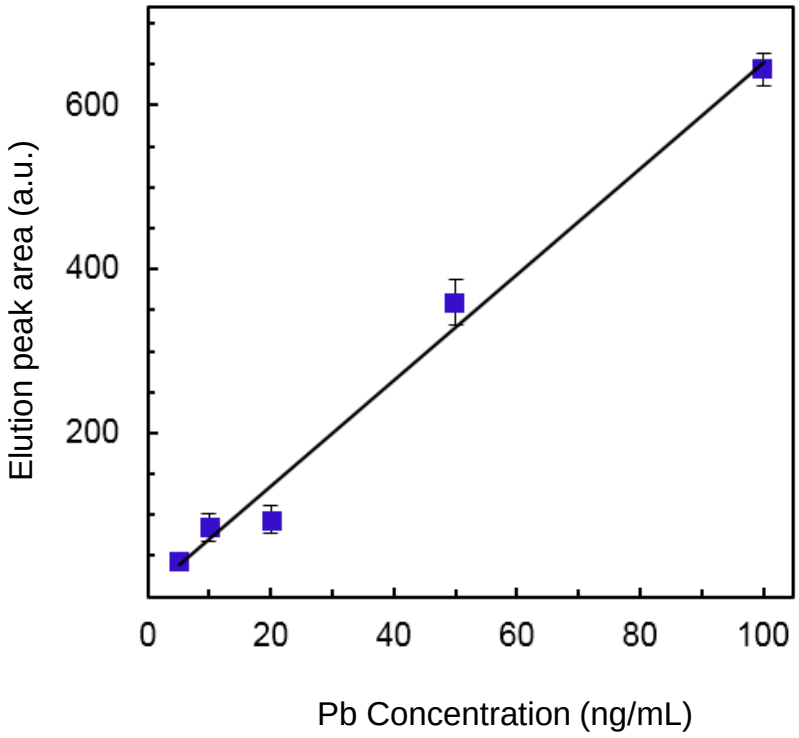

Figure 3.8 Calibration curve for lead using the proposed method.

Fig. 3.7 (c) shows elution curves for lead (100 ng/mL) in EDTA solution (red curve) and a blank (nitric acid, 0.1 M; black curve). The red curve was the result of EMG fitting for SPE elution. The calibration curve for lead analysis in the range 0–100 ng/mL is shown in Fig. 3.8. Each measurement was repeated three times. The correlation coefficient (R^2) for the concentration range is 0.989. The limit of detection (LOD) is defined as $3\sigma/a$, in which σ is the standard deviation of the blank sample and a is the slope of the calibration curve [35]. The LOD for lead

detection was calculated to be 0.4 ng/mL. The results indicated that the internal micropump improved the analysis performance because it was more precise than a syringe pump at transporting small volumes. For a lead concentration of 50 ng/mL, the precision (calculated by the reversed relative standard deviation of three measurements) was improved fourfold (12.8 with the internal micropump versus 3.7 with an external syringe pump). The EMG model is effective for describing the elution peak and it allows high reproducibility of the elution peak areas under fitting curve. Therefore, EMG could also be a reason for the improved precision.

Table 3.2 shows the comparison of this work with some related studies. The internal micropump helps improve the precision and LOD by about 3 and 1.5 times, respectively, relative to use of the external pump. Compared to conventional LEP [15], the LOD was improved about 50 times. Notably, our chip was made with PDMS; therefore, it is expected that the sensitivity would be further improved if quartz glass was used as the chip material. Moreover, on-chip SPE could significantly reduce the eluent and sample volumes required.

Table 3.2 Comparison of this work with some related studies

	Online SPE with ICP-AES [34]	**LEP-OES [15]**	**Off-line SPE LEP-OES [18]**	**On-chip SPE LEP with syringe pump [25]**	**On-chip SPE LEP with internal pump (this work)**
Sample volume (mL)	5–10	2–5	40	1	1
Eluent volume (μL)	25	-	400	40	20
Ratio of sample and eluent	200–400	-	100	25	50
LOD (ng/mL)	0.03	19	15	0.64	0.4
Precision (Reversed RSD)	-	-	-	3.7	12.8

3.4. Conclusion

A simple pneumatic pump for highly sensitive SPE integrated with DC LEP was realized. Three elements - the excitation source (DC LEP), sample preconcentrator (SPE), and fluid actuator (micropump) - were successfully integrated into a microfluidic chip. The design, fabrication process, and operation of the internal pump were redeveloped and optimized for high-pressure proof and more reproducibility for SPE–LEP. The micropump was aimed at a more precise actuation of the eluent. The internal pump performed two tasks: 1) it introduced the eluent in highly reproducible amounts without delay, and 2) it acted as a valve, which could close to protect the SPE channel from high back pressure during plasma generation. Moreover, the internal micropump had only one pneumatic control line and is thus operationally simpler and avoided failure in pneumatic programmed control. The pumping cycle volume was 90 nL with a deviation of 2%, which indicated high reproducibility of the pumping system. The internal pump helped improve the precision because the pump response time was decreased, resulting in a more precise flow control. An EMG model was used to describe the elution peaks with good agreement. The EMG model might contribute to the improvement of precision. With the internal micropump, precision and LOD were improved. The use of a micropump for LEP is highly prospective because it enables more effective use of the sample. In our opinion, the proposed use of an internal micropump with our measurement protocol and data processing procedures would be suitable not only for LEP but also for other methods that utilize pulsed

microplasma sources (such as LEDBD and ELCAD) to develop micro total analysis systems.

3.5 References

[1] R. A. Meyers, Encyclopedia of Analytical Chemistry, edited by R.A. Meyers, John Wiley and Sons (2000) 9468-9485.

[2] R. S. Houk, V. A. Fassel, G. D. Flesch, and H. J. Svec, Inductively coupled argon plasma as an ion source for mass spectrometric determination of trace elements, Anal. Chem. 52 (1980) 2283-2289.

[3] A. Walsh, The application of atomic absorption spectra to chemical analysis, Spectrochim. Acta 7 (1956) 108-117.

[4] M. Miclea, K. Kunze, G. Musa, J. Franzke, and K. Niemax, The dielectric barrier discharge—a powerful microchip plasma for diode laser spectrometry, Spectrochim. Acta, Part B 56 (2001) 37-43.

[5] S. Tombrink, S. Müller, R. Heming, A. Michels, P. Lampen, and J. Franzke, Liquid analysis dielectric capillary barrier discharge, Anal. Bioanal. Chem. 397(7) (2010) 2917-2922.

[6] T. Krähling, S. Müller, C. Meyer, A. K. Stark, and J. Franzke, Liquid electrode dielectric barrier discharge for the analysis of solved metals, J. Anal. At. Spectrom. 26(10) (2011) 1974-1978.

[7] T. Cserfalvi, P. Mezei, and P. Apai, Emission studies on a glow discharge in atmospheric pressure air using water as a cathode, J. Phys. D: Appl. Phys. 26 (1993) 2184-2188.

[8] G. Jenkins, J. Franzke, and A. Manz, Direct optical emission spectroscopy of liquid analytes using an electrolyte as a cathode discharge source (ELCAD) integrated on a micro-fluidic chip, Lab Chip 5(7) (2005) 711-718.

[9] C. G. Wilson and Y.B. Gianchandani, Spectral detection of metal contaminants in water using an on-chip microglow discharge, IEEE Trans. Electron Devices 49 (2002) 2317-2322.

[10] A. Iiduka, Y. Morita, E. Tamiya, and Y. Takamura, Optical emission spectrometer of aqueous solution samples employing liquid electrode plasma, Proc. MicroTAS (2004) 423-425.

[11] H. Matsumoto, A. Iiduka, T. Yamamoto, E. Tamiya, and Y. Takamura, Heavy metal measurement in microfluidic channel by confined liquid electrode plasma optical emission spectrometry, Proc. μTAS (2005) 427-429.

[12] M. Kumai and Y. Takamura, Excitation temperature measurement in liquid electrode plasma, Jpn. J. Appl. Phys. 50 (2011) 096001.

[13] Y. Kohara, Y. Terui, M. Ichikawa, T. Shirasaki, K. Yamamoto, T. Yamamoto, and Y. Takamura, Characteristics of liquid electrode plasma for atomic emission spectrometry, J. Anal. At. Spectrom. 27 (2012) 1457-1464.

[14] M. Banno, E. Tamiya, and Y. Takamura, Determination of trace amounts of sodium and lithium in zirconium dioxide (ZrO_2) using liquid electrode plasma optical emission spectrometry, Anal. Chim. Acta, 634 (2009) 153-157.

[15] A. Kitano, A. Iiduka, T. Yamamoto, Y. Ukita, E. Tamiya, and Y. Takamura, Highly sensitive elemental analysis for Cd and Pb by liquid electrode plasma atomic emission spectrometry with quartz glass chip and sample flow, Anal. Chem. 83 (2011) 9424–9430.

[16] M. Kumai, K. Nakayama, Y. Furusho, T. Yamamoto, and Y. Takamura, Quantitative determination of lead in soil by solid-phase extraction/liquid

electrode plasma atomic emission spectrometry, Bunseki Kagaku 58 (2010) 561-567 (in Japanese).

[17] S. Kagaya, S. Nakada, Y. Inoue, W. Kamichatani, H. Yanai, M. Saito, T. Yamamoto, Y. Takamura, and K. Tohda, Characteristics of liquid electrode plasma for atomic emission spectrometry, Analytical Sciences 26 (2010) 515-518.

[18] K. Nakayama, T. Yamamoto, N. Hata, S. Taguchi, and Y. Takamura, Liquid electrode plasma atomic emission spectrometry combined with multi-element concentration using liquid organic ion associate extraction for simultaneous determination of trace metals in water, Bunseki Kagaku, 60(6) (2011) 515-520.

[19] N. H. Tung, M. Chikae, Y. Ukita, P. H. Viet, and Y. Takamura, Sensing technique of silver nanoparticles as labels for immunoassay using liquid electrode plasma atomic emission spectrometry, Anal. Chem. 84 (2012) 1210-1213.

[20] V. Camel, Review: Solid phase extraction of trace elements, Spectrochim. Acta Part B, 58 (2003) 1177-1233.

[21] C. Yu, M. H. Davey, F. Svec, and J. M. Fréchet, Monolithic porous polymer for on-chip solid-phase extraction and preconcentration prepared by photoinitiated in situ polymerization within a microfluidic device, Anal. Chem. 73(21) (2001) 5088-5096.

[22] J. P. Kutter, S. C. Jacobson, and J. M. Ramsey, Solid phase extraction on microfluidic devices, J. Microcolumn Separations, 12(2) (2000) 93-97.

[23] Y. Yang, C. Li, K. H. Lee, and H. G. Craighead, Isoelectric focusing in cyclic olefin copolymer microfluidic channels coated by polyacrylamide using a UV photografting method, Electrophoresis 26(19) (2005) 3622-3630.

[24] D. Van Khoai, A. Kitano, T. Yamamoto, Y. Ukita, and Y. Takamura, Development of high sensitive liquid electrode plasma–Atomic emission

spectrometry (LEP-AES) integrated with solid phase pre-concentration, Microelectron. Eng. 111 (2013) 343–347.

[25] D. Van Khoai, T. Yamamoto, Y. Ukita, and Y. Takamura, On-chip solid phase extraction–liquid electrode plasma atomic emission spectrometry for detection of trace lead, Jpn. J. Appl. Phys. 53 (2014) 05FS01.

[26] T. Shimomura, E. Tamya, and Y. Takamura, Simple constant volume injection pump for droplet separation in massively parallel microfluidic devices, Proc. microTAS (2005) 866-868.

[27] D. V. Khoai, T. Yamamoto, Y. Ukita, and Y. Takamura, Development of on-chip solid phase extraction (SPE) with precise flow-control by micropump for highly sensitive liquid electrode plasma, Proc. MicroTAS (2013) 233-235.

[28] Y.-N. Yang, S.-K. Hsiung, and G.-B. Lee, A pneumatic micropump incorporated with a normally closed valve capable of generating a high pumping rate and a high back pressure, Microfluid Nanofluid 6 (2009) 823-833.

[29] W. Inman, K. Domansky, J. Serdy, B. Owens, D. Trumper, and L. G. Griffith, Design, modeling and fabrication of a constant flow pneumatic micropump, J. Micromech. Microeng. 17 (2007) 891-899.

[30] C.-W. Huang, S.-B. Huang, and G.-B. Lee, Pneumatic micropumps with serially connected actuation chambers J. Micromech. Microeng. 16, (2006) 2265-2272.

[31] G. Hendriks, D. R. A. Uges, and J. P. Pranke, New practical algorithm for modelling analyte recovery in bioanalytical reversed phase and mixed-mode solid phase extraction, J. Pharm. Biomed. Anal. 48 (2008) 158-170.

[32] R. E. Pauls and L. B. Rogers, Band broadening studies using parameters for an exponentially modified Gaussian, Anal. Chem. 49(4) (1997) 625-628.

[33] P. J. Naish and S. Hartwell, Exponentially modified Gaussian functions - a good model for chromatographic peaks in isocratic HPLC, Chromatographia, 16 (1988) 285-296.

[34] A. Sabarudin, N. Lenghor, Y. Liping, Y. Furusho, and S. Motomizu, Automated Online Preconcentration System for the Determination of Trace Amounts of Lead Using Pb-Selective Resin and Inductively Coupled Plasma–Atomic Emission Spectrometry, Spectrosc. Lett. 39 (2006) 669-682.

[35] L. A. Currie and G. Svehla, Nomenclature for the presentation of results of chemical analysis, Pure Appl. Chem. 66 (1994) 595-608.

Chapter 4
Integration of solid phase extraction with alternating voltage driven liquid electrode plasma

Abstract

In this chapter, a sensitive analytical method based on the integration of solid phase extraction with liquid electrode plasma powered by alternating current source was developed. The T-shaped channel with a zigzag portion to separate LEP channel and SPE chamber was proposed. AC LEP was sustained by a buffer flow. Meanwhile, the eluent was introduced to the plasma so that the analyte can be detected. The procedure enabled a simple method without the necessity of internal pump or valve. The developed method was applied to lead detection with obtained limit of detection for lead of 0.5 µg/L. The used volume of sample was 2 mL. The preconcentration time was 50 min, while the measurement time/elution time was 8 minute. The consumed eluent was about 40 µL. The limit of detection was about 20 times lower than maximum acceptable concentration of lead in drinking water.

4.1. Introduction

In chapter 3, we presented the integration of SPE column onto LEP chip, in which the plasma was generated by pulsed direct voltage. The combination resulted in a control technique with an internal pump that is capable of working at high back pressure. The elution was divided into measurement cycle because the plasma is in pulsed form. The micropump provided an equally small amount of sample for one cycle of LEP measurement. After a measurement cycle, syringe pumps from the side channel injected the buffer solution to rinse the channel and to eliminate the remaining air bubbles. It took at least one minute to wait until the buffer flow stops. Then the next cycle was start again. This procedure is suitable with pulsed direct current driven LEP combined with SPE; however, it would complicate the general performance of the SPE-LEP measurement. In addition, the measurement took quite long time (about 40-50 min).

In chapter 2, a novel LEP powered by alternating current (AC LEP) was reported. The method exhibits some interesting features. Accordingly, it can be maintained in a liquid channel with high stability at an appropriate flow rate. In addition, it causes no significant damage on PDMS channel. However, its sensitivity seems still insufficient for direct assessment of trace metals in water.

In this chapter, we present a new approach to the integration of the SPE into AC LEP chip. The alternating current driven liquid electrode plasma was characterized in the chapter 2. It is shown that the novel plasma can be continuously generated in the LEP channel for quite long without severe deformation of the

PDMS channel. This interesting characteristic inspired the integration of SPE because the performance of SPE-LEP measurement is more easily. Neither internal pump nor valve is needed for flow control. Instead, a zigzag channel was put between LEP channel and SPE column to prevent the high pressure due to plasma generation during measurement.

4.2. Experimental section

4.2.1. Chip description and fabrication

The integrated chip consists of two layers: PDMS (flow layer) and glass substrate that are attached together by oxygen plasma. Figure 4.1 shows illustration of the chip and its side view. The SPE chamber is 2 mm wide, 10 mm long, and 0.4 mm deep, corresponding with 8 µL of total resin volume. The LEP channel includes the narrow bottleneck and two large chambers for connecting electrodes. The narrow channel size is 200 µm wide, 500 µm long and 100 µm deep. Between LEP channel and SPE chamber is a zigzag channel with total length of about 60 mm, width of 400 µm, and depth of 100 µm. The zigzag channel is to prevent the back flow by expansion due to plasma generation. A filter is set at one end of SPE chamber to fix the resin beads. There are a main inlet for sample, cleaning solution and eluent, and a side inlet for the buffer.

Chip fabrication Photolithography was employed for mold fabrication. This process was similarly described in chapter 2. The mold consists of two parts with different thickness corresponding with LEP channel and resin chamber that were made by SU8 photoresists (permanent epoxy negative photoresist, Nippon Kayaku Co. Ltd., Japan). Therefore, mold fabrication process includes two times of

spin-coating, exposure, post-baking, respectively for each of such patterns before developing by SU8 developer solution (Kayaku Microchem Co., Ltd., Japan). The thickness of photoresist layers was controlled by spin-coating rate being recommended by producer. The patterns were aligned by a mask aligner (PEM-800, Union Optical Co., Ltd., Japan). PDMS (Dow Corning Toray Silicone Co., Ltd., Japan) were used as chip material and cured in the convection oven at 75 ^{o}C for 90 min. After that, PDMS replica sheet was peeled off and attached with a glass substrate by oxygen plasma cleaner (Yamato – PDC210; 100 W for 10 seconds). Silicon tubes (2 mm in outer diameter) were connected to all ports, and two Pt wires (0.3 mm in diameter) were applied to the two ends of LEP channel. Finally, all connecting spots were sealed by PDMS and cured at a temperature of 90 ^{o}C for 1.5 hours.

4.2.3. Reagents and materials

Pb solutions (concentrations from 0.01 mg/L to 100 mg/L) were prepared by dilution of 1000 mg/L standard solutions (Pb 1000, Kanto Chemical Co., Inc., Japan.), with 0.1 mol/L nitric acid (Kanto Chemical Co., Inc., Japan). The 0.1 mol/L nitric acid was also used as a blank sample. EDTA solution 0.03 M (pH 9) was prepared from a buffer solution and EDTA dihydrate (Dojindo - Japan). The buffer solution was prepared by dissolution of 5.64 g ammonium chloride (Kanto Chemical Co., Inc., Japan) and 48 mL saturated ammonia solution (Wako - Japan). 100 mL EDTA solution 0.03 M was obtained by adding 0.88 g EDTA and 6 mL buffer solution into pure water. The other chemicals and materials used are analytical grade.

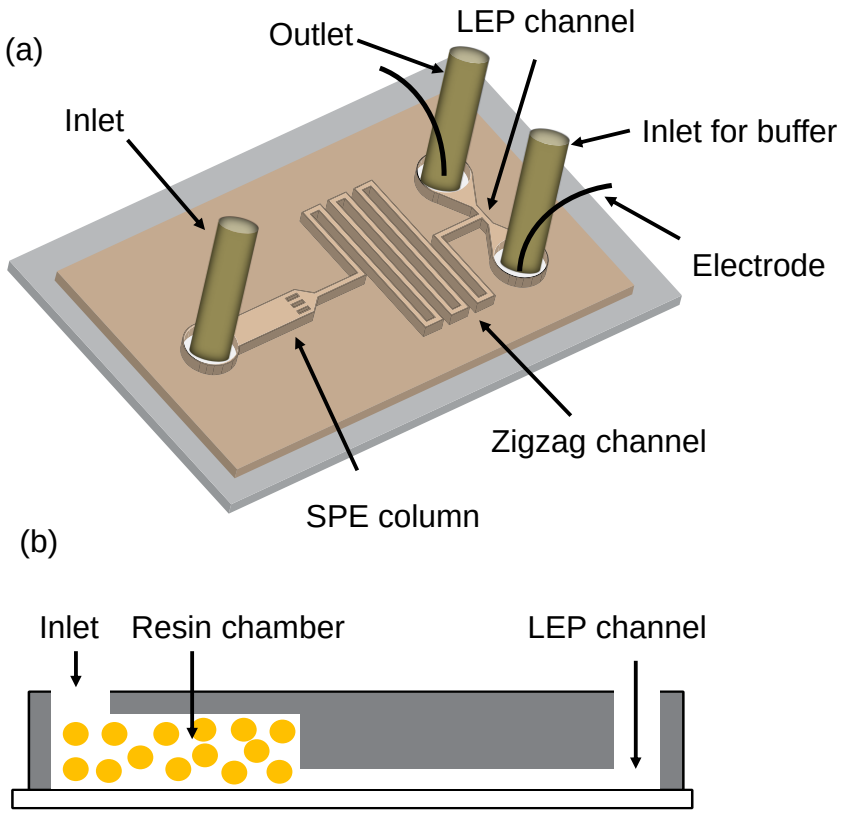

Figure 4.1 (a) Schematic illustration of SPE-LEP chip. (b) Illustration of side view.

4.2.4. Measurement setup

Figure 4.2 shows the diagram of measurement setup. The chip was fixed on the holder Emission light was acquired by a spectrometer (Andor Shamrock SR303i, focal length 0.303 m, diffraction grating of lines 2400 lines/mm). Voltage was in range of 800 - 1500V and provided by an AC voltage supplier (Plasma Concept Inc., Japan. Two syringe pumps (kdScientific - USA) were used to apply eluent and buffer.

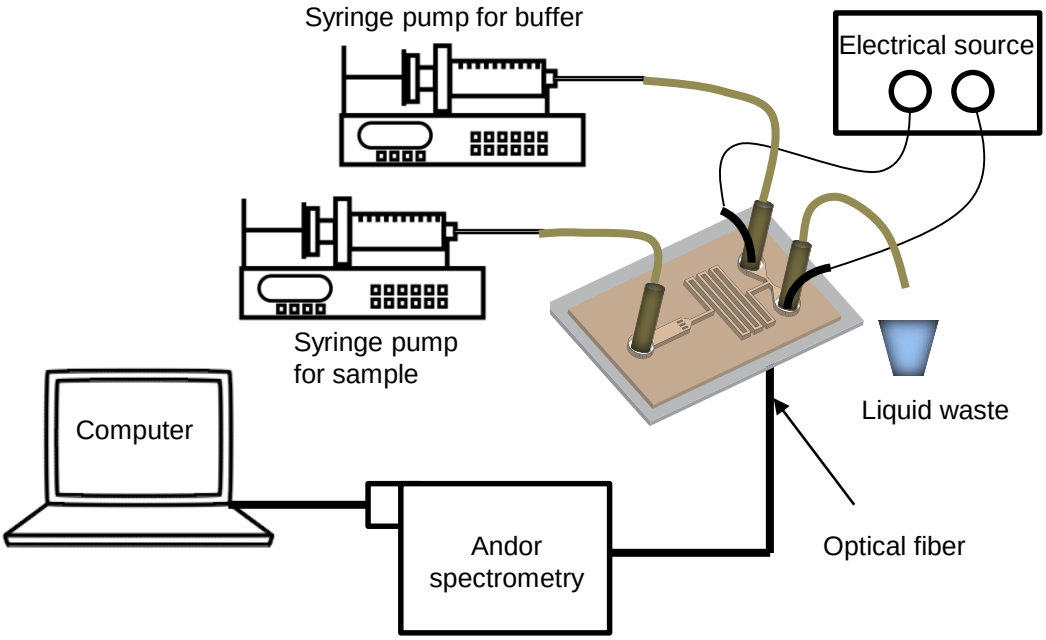

Figure 4.2 Setup of SPE-AC LEP measurement.

4.2.5. Analytical procedure

At first the whole chip was cleaned with pure water (20 µL/min for 5 min) by a syringe pump. Then, ion exchange resin stored in DI water (Analig Pb-01) was loaded into resin chamber by using a syringe and washed again by 0.03 M EDTA (1 mL, 200 µL/min) and then DI water (1 mL, 200 µL/min). The resin was activated by 0.1 M HNO_3 (0.5 mL, 100 µL/min). After this step, sample Pb in 0.1 M HNO_3 was introduced through the resin with a flow-rate of 50 µL/min. Preconcentration was independently carried out prior to LEP measurement.

After preconcentration, the entire channel of the chip was dried up. Then the chip was fixed on the measurement system as shown in Fig. 4.2. Fig. 4.3 shows the illustration of liquid flows during LEP measurement. A 30µL/min buffer flow containing 0.1 M nitric acid and 5 % formic acid was pumped from one side tube of LEP channel for few minutes to clean the LEP element. Then voltage supplier was turned on. Plasma was generated in the channel for 1 min until being stable. Once plasma was stable, eluent was introduced through SPE column to LEP channel. The flow-rate of the eluent flow is 5 µL/min. During this time, emission spectrums were acquired by manual internal trigger. The integration time is 2 sec. The elution process took about 8 minutes. It is ensured that all lead in the resin was eluted out.

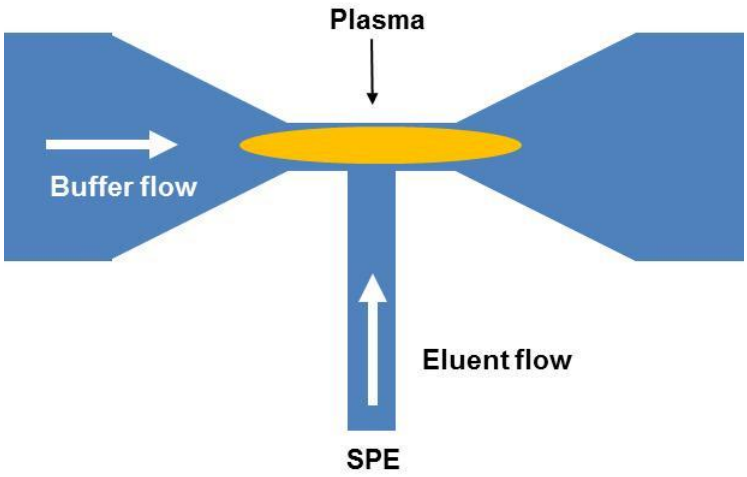

Figure 4.3 Illustration of liquid flows during LEP measurement.

4.3. Result and discussion

4.3.1. Choice of integration time for emission spectrum acquisition

The integration time (or exposure time) is the duration time that the optical fiber tip is exposed to acquire the emission light. Increase in the integration time leads to increase in intensity and background noise as well. The reverse is also true. With AC LEP that can generate continuous plasma for long time, we characterized the integration time in the range from 1 sec to 10 sec. And based on the results we chose the integration time of 2 sec for SPE-LEP measurement.

4.3.2. Effect of buffer constituents on plasma stability and emission spectrum background.

As discussed in the chapter 2, organic compounds have an interesting enhancement effect on emission intensity of LEP for not only DC LEP but also AC

LEP. We investigated the effects in the chapter 2. According to the results, acetic acid and formic acid helps enhance the emission intensities because we suppose they make the plasma more stable. Ethanol is very effective with DC LEP but does not show the same effect on AC LEP. The presence of ethanol, on the contrary, makes plasma not stable, causing lower intensity and lower reproducibility. The enhancement extents of the two acids are similar each other. However the spectral backgrounds generated by them are different. From these backgrounds, we obviously see that acid formic is better than acetic acid because formic acid enables a lower background noise. Moreover the emission signals of 1 mg/L Pb in 5 % HCOOH is higher than those in 10 % CH_3COOH. Thus, the mixture of 0.1 M HNO_3 and 5% HCOOH was the buffer to sustain the stable plasma during SPE-LEP measurement.

4.3.3. Choice of parameters for preconcentration and analysis

The table 4.1 shows the parameters for preconcentration step and SPE-LEP measurement. For preconcentration step the sample flow rate was applied the result that was optimized with DC plasma. Since the preconcentration performance is dependent upon the plasma sources, then the optimization of DC plasma can be deduced for AC plasma. The pH was referred to the optimization of the other study in which the same SPE resin was used.

Table 4.1 Parameters for SPE-LEP measurement

Preconcentration	
pH of samples	1 (prepared in 0.1 HNO_3)
Sample volume	2.5 mL
Sample loading flow-rate	50 µL/min
LEP measurement	
Voltage	AC, max 3 kV, 18.8 kHz.
Integration time	2 seconds
Buffer	0.1 M HNO_3 + 5 % HCOOH
Buffer flow-rate	30 µL/min
Eluent	0.03 EDTA (pH 11)
Eluent flow-rate	5 µL/min
Measurement time/ elution time	8 min

4.3.4. Data process and analytical performance

After SPE-LEP measurement whose procedure was presented in the experimental section, the raw experimental data were a series of emission spectrums. The data process is similar as we presented in chapter 3. All elution plots are exponentially modified Gaussian (EMG) fitted. Fig. 4.4 shows a series of emission peaks corresponding with the elution of Pb (2.5 mL, 100 µg/L). Fig. 4.5 (a) shows a raw elution peak profile (without EMG fitting) and Fig. 4.5 (b) shows the corresponding EMG curve. The adjusted correlation coefficient of the fitting is 0.971. This number indicated that the EMG curve is quite fit with the elution curve.

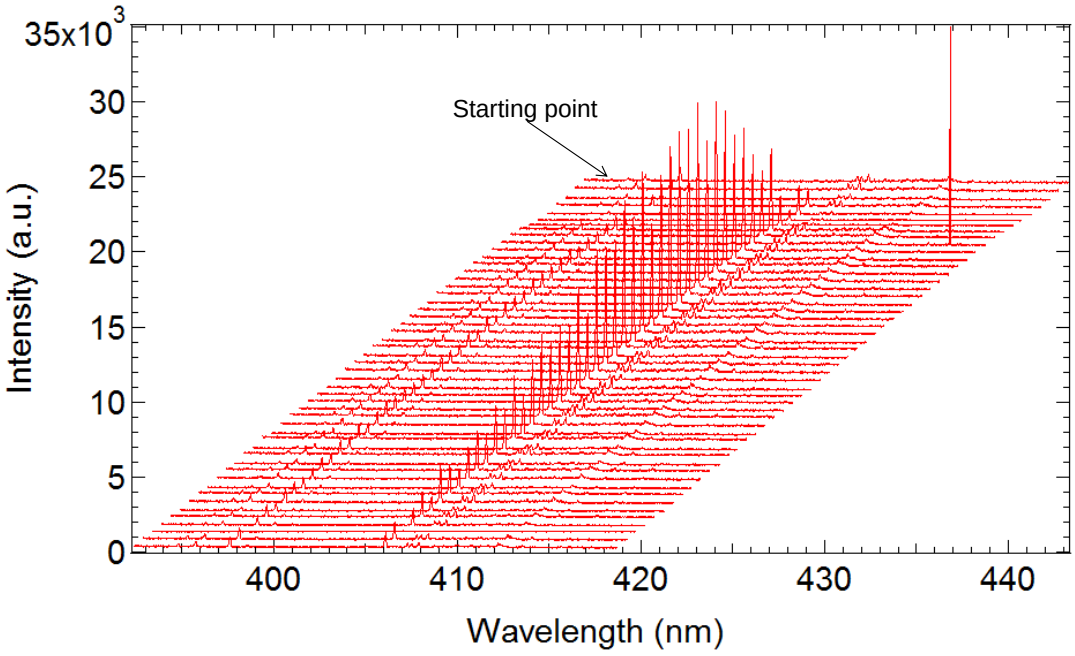

Figure 4.4 Emission spectra of Pb (2.5 mL, 100 µL/min). Buffer (0.1 M HNO_3 + 5% HCOOH) flow-rate was 30 µL/min. Elution flow-rate was 5 µL/min.

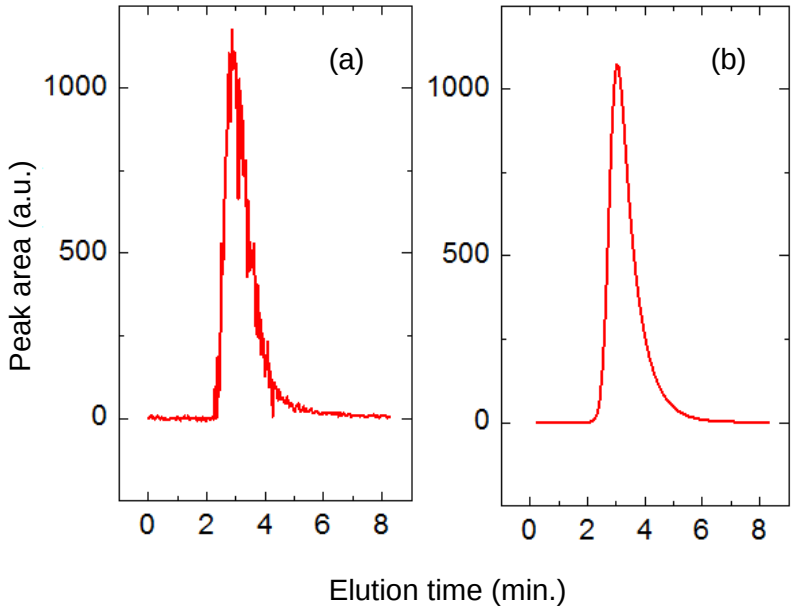

Figure 4.5 Elution peak of 100 ng/mL lead.

(a) Before EMG fitting and (b) After EMG fitting

Sample volume: 2.5 mL. Sample flow-rate: 50 µL/min. Elution flow-rate: 5 µL/min

Fig. 4.6 presents elution peak profiles of the elution of 100 µg/L, 50 µg/L, and 5 µg/L. Sample volume was 2.5 mL, sample flow-rate was 50 µL/min. The adjusted correlation coefficients were about 0.9 and above. This indicated good fit of EMG with the elution. The EMG curves even fit with elution curve with adjusted correlation coefficient of greater than 0.99. It is found that the fit of EMG for the elution in AC-LEP is better than that for DC-LEP. This is because there are about 40 – 60 data points (corresponding with the same numbers of measurement cycles) obtained for one elution curve. Consequently, adj. R^2 in DC-LEP is only around 0.8. For more clearly, the elution peak of Pb of µg/L was re-presented in Fig. 4.7.

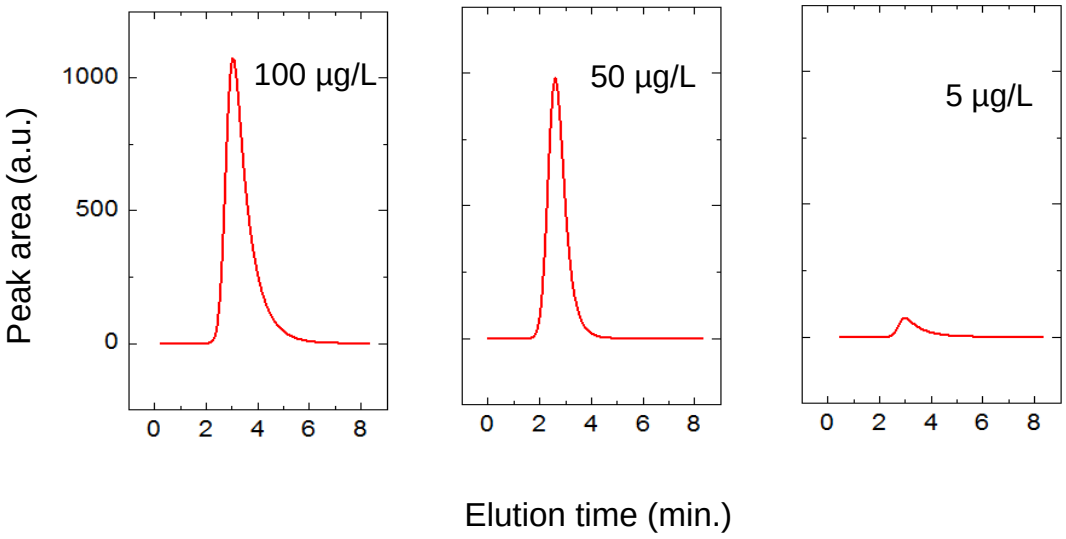

Figure 4.6 Elution peaks of 100 Pb with concentrations of 100 µg/L, 50 µg/L, and 5 µg/L.

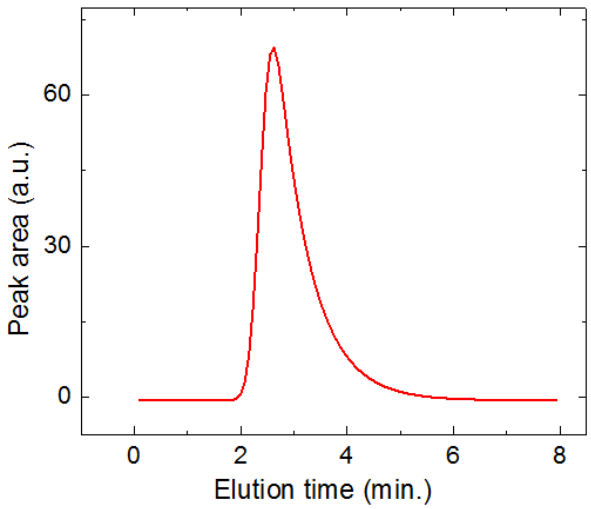

Figure 4.7 Elution peak of 5 µg/L lead.

The peak areas of elution peak were calculated by Igor. Those values are proportional with the lead captured by resin, thus can be used for quantitative determination.

Table 4.2 shows the quantitative results of elution peak areas with various concentrations. Herein, intensity 1, 2 and 3 are intensities calculated from raw emission peak areas, 5-point moving average of raw emission peak areas, and EMG fitting curve of raw emission peak areas, respectively.

Table 4.2 Quantitative results of lead employing the proposed method.

Concentration (ppb)	Intensity 1 (a.u)	Intensity 2 (a.u.)	Intensity 3 (a.u.)
0	3.1	3.0	-
0	-0.3	-0.1	-
0	2.7	2.8	-
5	71.7	72.0	70.3
5	71.7	72.4	73.4
5	77.1	77.7	83.4
50	795.3	795.6	802.1
50	485.9	486.1	742.1
100	1094.6	1094.8	1117.8
100	1103.8	1103.7	1135.3

Fig. 4.8 shows sketched calibration curve with data set that is shown in Table 4.2 for Pb employing the proposed method. Here, elution peak areas are obtained from EMG fitting curve of the elution peaks.

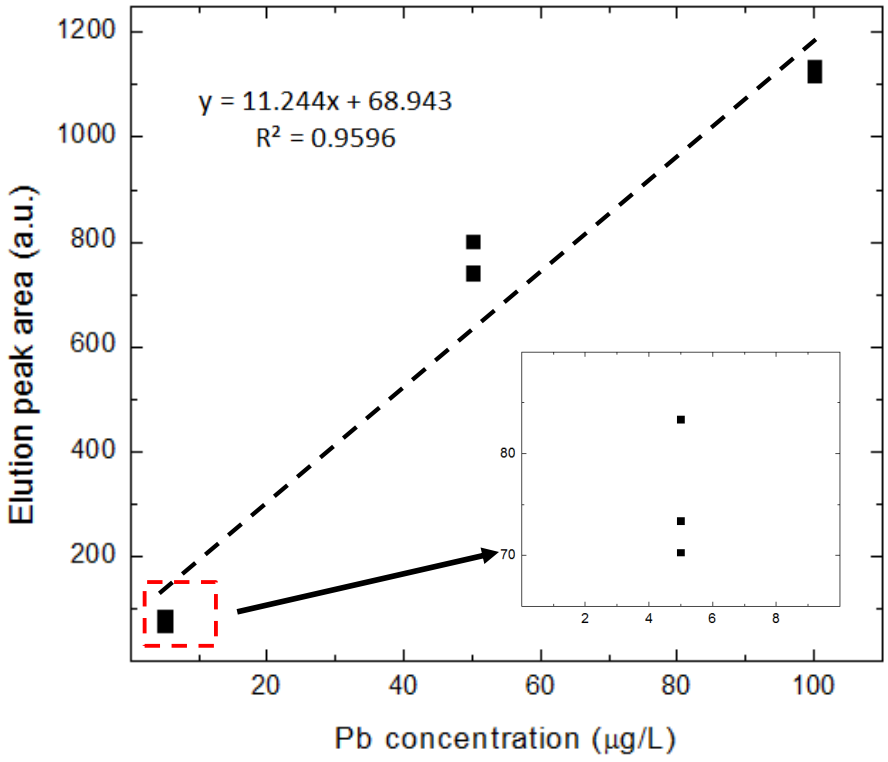

Figure 4.8 Calibration curve for Pb. Sample volume: 2.5 mL. Sample flow-rate: 50 µL/min. Elution flow-rate: 5 µL/min

The correlation coefficients of fitting are larger than 0.9 with almost the concentration. The EMG fitting cannot be used for blank samples, therefore we used 5-point moving average curve of the raw time-dependent intensity to calculate the emission peak area for blanks. The result is presented in column ‘intensity 2’ of blank samples. As a result, standard deviation of blank samples is 1.7 a.u.. The limit of detection for lead is determined according to ref. [6] to be about 0.5 μg/L.

In the extreme test, we performed the proposed method to detect Pb (0.5 μg/L, 10 mL, and sample loading rate of 100 μL/min). Since the loading rate is quite high, a small vacuum was needed to support the preconcentration step. Without the vacuum pump, the liquid sample may leak out at tube connecting points. The data was processed as mentioned above. The elution peak is shown in Fig. 4.9. The result indicated that the method would be more sensitive if the volume of sample increases.

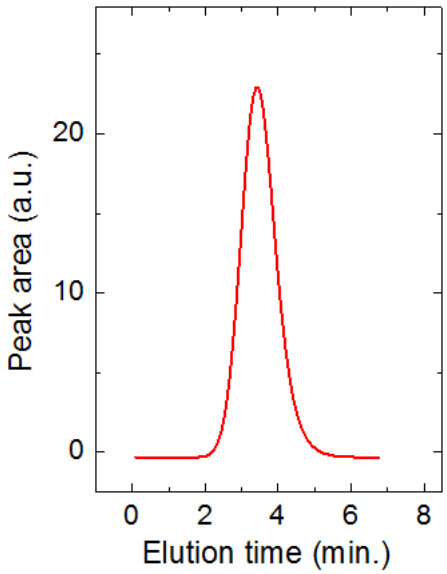

Figure 4.9 Elution peak of Pb (concentration of 0.5 μg/L, sample volume of 10 mL, and sample loading rate of 100 μL/min).

4.4. Conclusion

In this chapter, we have successfully developed a novel alternating current driven liquid electrode plasma integrated with solid phase extraction. The proposed method uses a more simply designed chip. A 8-mm^3 SPE chamber was integrated onto LEP channel for preconcentration prior to LEP measurement. Neither internal pump nor valve is needed. The small amount of SPE resin enables a low cost analytical method. Compared with DC LEP, AC LEP is more suitable for SPE integration because SPE- AC LEP does not require flow controller (micropump).

Thus SPE-LEP measurement is simpler and more rapid. The LOD of the proposed method for lead detection was about 0.5 μg/L, 40 times improved in comparison with conventional LEP using quartz glass chip. Sample volume was 2 mL, whereas

4.5. References

[1] D. V. Khoai, T. Yamamoto, Y. Ukita, Y. Takamura, Improvement of pneumatic micropump for high performance LEP-OES with preconcentrator, 27th International Microprocesses and Nanotechnology, Japan, 2014.

[2] D. V. Khoai, H. Miyahara, P. Ruengpirasiri, O. Chailapakul, S. Chuanuwatanakul, T. Yamamoto, P. T. Tue, A. Okino, Y. Takamura, Alternating Voltage Liquid Electrode Plasma (AC-LEP) for Highly Sensitive Detection of Lead, 7th International Symposium on Microchemistry and Microsystems, Japan, 2015.

[3] D. Van Khoai, T. Yamamoto, Y. Ukita, and Y. Takamura, On-chip solid phase extraction–liquid electrode plasma atomic emission spectrometry for detection of trace lead, Jpn. J. Appl. Phys. 53 (2014) 05FS01

[4] A. Sabarudin, N. Lenghor, Y. Liping, Y. Furusho, S. Motomizu: Spectroscopy Letters 39 (2006) 669-682.

[5] E. Grushka, Characterization of exponentially modified Gaussian peaks in chromatography, Anal. Chem., 1972, 44, 1733-1735.

[6] L. A. Currie and G. Svehla, Nomenclature for the presentation of results of chemical analysis, Pure Appl. Chem. 66 (1994) 595-608.

Chapter 5
General conclusions

In this study, an elemental analysis based on liquid electrode plasma optical emission spectrometry (LEP OES) integrated with solid phase extraction (SPE) has been successfully realized for highly sensitive detection of metals. Flow control techniques have been developed for the compatibility of SPE and LEP. Chip design, chip fabrication, performance protocols, data acquisition and data processing were proposed based on the characterization of LEP and the proposed flow control techniques.

For conventional direct current driven LEP (DC LEP), a simply designed pneumatic micropump was successfully developed for fluid controlling for the integration. The pump is capable of working under high backpressure condition created by plasma generation. In addition, the internal pump could act as a valve to prevent a back flow due to plasma generation to SPE column. The internal micropump had only one pneumatic control line and is thus operationally simpler and avoided failure in pneumatic programmed control. Based on the pumping structure, a suitable multilayer chip, measurement protocol, data acquisition and processing were developed. With the developed structure, LOD for lead was achieved to be 0.4 μg/L (ppb), about 50 times better than that of conventional LEP.

A novel liquid electrode plasma powered by alternating current has been realized for the first time. It was named as AC LEP to distinguish from the conventional one (DC LEP). The same chip layout with the conventional LEP that made by PDMS was utilized. The conditions to produce and sustain the AC LEP were found. The generation mechanism of the AC LEP was discussed. Emission lines of the electrolyte (0.3 M nitric acid), lead (Pb) and Cadmium (Cd) were

obtained and compared with those of DC LEP. The method was developed for quantitative measurement of Pb and Cd by optical emission spectrometry. It is found that AC LEP can be applied for quantitative determination of lead and cadmium as well as DC LEP. The LOD for Pb and Cd using AC LEP OES were 75 µg/L and 4.5 µg/L, respectively. The AC LEP can be sustained at low flow rate with small channel destruction on PDMS-based platform. This is promising for a development of microTAS device based on combination and integration on AC LEP-based chip.

An elemental analysis based on on-chip SPE integration with AC LEP has been realized. A flow control technique based on T-shaped channel with an in-between zigzag element to suppress back-pressure for continuous extraction-measurement has been developed. We investigated a buffer flow with an optimized flow-rate could maintain more stable plasma and improve the intensity of plasma. The eluent flow was actuated by a syringe pump. The LEP measurement was within 8 minutes. LOD of AC LEP – SPE for lead was 0.5 µg/L (ppb), the same order of magnitude with DC LEP – SPE.

In conclusion, the dissertation presented a novel approach on sensitivity enhancement for LEP by on-chip integration with solid phase extraction. The obtained limits of detection for lead using these proposed methods were ten times lower than the required minimum concentration of lead in drinking water. Hence, we suppose the methods are applicable for drinking water test as targeted. The integrated chip was made by PDMS that is inexpensive and simple with photolithographic micro fabrication and design modification. Also, our approach exploited the merits of on-chip SPE about using less sample and eluent amount. The novel strategic approach is promising, especially for the development of microTAS devices based on liquid electrode plasma.

LIST OF PUBLICATIONS

Journals

1. **D. V. Khoai**, A. Kitano, T. Yamamoto, Y. Ukita, Y. Takamura, "Development of high sensitive liquid electrode plasma – atomic emission spectrometry (LEP-AES) integrated with solid phase pre-concentration", Microelectronic Engineering 111 (2013) 343–347.

2. **D. V. Khoai**, T. Yamamoto, Y. Ukita, and Y. Takamura, "On-chip solid phase extraction – liquid electrode plasma atomic emission spectrometry for detection of trace lead", Japanese Journal of Applied Physics, 53 (2014) 05FS01.

3. **D. V. Khoai**, T. Yamamoto, Y. Ukita, and Y. Takamura, Precise flow control with internal pneumatic micropump driven for highly sensitive solid phase extraction liquid electrode plasma, Sensors and Actuators B, online accepted, DOI: 10.1016/j.snb.2015.07.117.

4. **D. V. Khoai**, H. Miyahara, T. Yamamoto, P. T. Tue, A. Okino, and Y. Takamura, Development of alternating current driven liquid electrode plasma for sensitive detection of metals. (Revised and re-submitted to Japanese Journal of Applied Physics).

5. **D. V. Khoai** et al., Study on measurement of excitation temperature of alternating current driven liquid electrode plasma, in preparation.

6. **D. V. Khoai** et al., Development of simple and rapid liquid electrode plasma driven by alternating current integrated with solid phase extraction for detection of trace lead, in preparation.

International conferences

Oral presentation:

1. **D. V. Khoai**, H. Miyahara, P. Ruengpirasiri, O. Chailapakul, S. Chuanuwatanakul, T. Yamamoto, P. T. Tue, A. Okino, and Y. Takamura, Alternating Voltage Liquid Electrode Plasma (AC-LEP) for Highly Sensitive Detection of Lead, 7th International Symposium on Microchemistry and Microsystems, Kyoto, Japan, June 8-10, 2015**.**

2. **D. V. Khoai**, T. Yamamoto, Y. Ukita, Y. Takamura, Improvement of pneumatic micropump for high performance LEP-OES elemental analyzer with preconcentrator, The 27th International Microprocesses and Nanotechnology Conference (MNC 2014), Japan, 2014/11/03-07.

Poster presentations

1**. D. V. Khoai**, H. Miyahara, T. Yamamoto, P. T. Tue, A. Okino, and Y. Takamura, Sensitive Detection of Metals with Disposable PDMS Chips by Alternating Current Liquid Electrode Plasma (AC LEP), The 5th International Symposium on Organic and Inorganic Electronic Materials and Related Nanotechnologies (EM-NANO 2015), Niigata, Japan. June 16-19, 2015.

2. **D. V. Khoai**, T. Yamamoto, Y. Ukita, Y. Takamura; Development of on-chip solid phase extraction (SPE) with precise flow-control by micropump for highly sensitive liquid electrode plasma, The 17th International Conference on Miniaturized Systems for Chemistry and Life Sciences (MicroTAS 2013), Germany, 2013/10/27-31.

3. **D. V. Khoai**, A. Kitano, T. Yamamoto, Y. Ukita, Y. Takamura, Development of high sensitive liquid electrode plasma – atomic emission spectrometry (LEP-AES) integrated with solid phase pre-concentration, the 38th International Micro & Nano Engineering Conference (MNE 2012), France, 2012/09/12-16.

Domestic conferences

1. **D. V. Khoai**, T. Yamamoto, Y. Ukita, Y. Takamura; Development of high sensitive liquid electrode plasma (LEP) integrated with solid phase extraction (SPE), 2013 JSAP-MRS joint symposia, 2013/09/16-20. (**Poster presentation**)

2. **D. V. Khoai**, T. Yamamoto, Y. Ukita, Y. Takamura; Development of high sensitive liquid electrode plasma (LEP) integrated with solid phase extraction (SPE) for trace heavy metal detection, 27th CHEMINAS, Sendai, 2013/05/23-24. **(Poster presentation**)

3. **D. V. Khoai**, H. Miyahara, T. Yamamoto, P. T. Tue, A. Okino, and Y. Takamura, Study on Excitation Temperature of Alternating Current Liquid Electrode Plasma, 76th JSAP Autumn meeting, Nagoya, 2015/09/13-16. **(Poster presentation)**

Awards

Best poster award at the 5th International Symposium on Organic and Inorganic electronic Materials and Related Nanotechnologies (EM-NANO 2015), Niigata, Japan.